



DISSERTATION

Collision Recovery Receivers for RFIDs

Conducted for the purpose of receiving the academic title
"Doktor der technischen Wissenschaften"

Jelena Kaitović, MSc.
born in Loznica, Serbia, June 3rd, 1986
Matriculation number: 1028381
Landstrasser Hauptstrasse 45/1/10, 1030 Vienna

December 2, 2015

.....

Submitted to the TU Wien, Faculty of Electrical Engineering and Information
Technology

Advisor

Univ.Prof. Dipl.-Ing. Dr.techn. Markus Rupp
TU Wien, Austria
Institute of Telecommunications

Examiner

Assoc. Prof. Dr. Javier Vales Alonso
Polytechnic University of Cartagena, Spain
Telematics Engineering Group

to my family

ABSTRACT

Radio Frequency Identification (RFID) is a very fast emerging technology that wirelessly transmits the identity of a tag attached to an object or a person. It usually operates in a dense tag environment. My work is focused on passive Ultra High Frequency (UHF) tags whose transmission on the Medium Access Control (MAC) layer is scheduled by Framed Slotted Aloha (FSA).

In this thesis, I propose the use of multiple antennas at the reader side in order to recover from collision. By exploiting the fact that a tag signal is real-valued while all other components of a received signal are complex-valued, I have separated real and imaginary part and in that way I have achieved a recovery from a collision that contains a two times higher number of tags than the number of the receive antennas at the reader, under perfect channel knowledge.

Furthermore, I have recommended a modification of a tag signal by an additional part that is specially designed to facilitate channel estimation. The recommended method provides excellent results in comparison to perfect channel knowledge. However, due to the constrained set of the designed sequences, a new issue arised. I have investigated the distribution of the additional sequence set within a tag population and depending on that, I have studied different collision scenarios. I have proposed a two phase collision recovery method that takes out all tags with a unique sequence per slot and if there is just one pair of tags with a common sequence left, such collision is resolved by projecting the signal constellation into the orthogonal subspace of the interference. The proposed method improves collision recovery and further increases the system throughput.

Moreover, in this thesis I have studied the influence of several parameters on the system throughput, and I have found the maxima of the theoretically expected throughput for receivers with different collision recovery factors and for different receiver architectures. Furthermore, in order to approach to the theoretical maxima, I have proposed spatial filtering in postprocessing. The main intention is to focus separately on different groups of tags by applying different weights within sector postprocessing. In that way tag signals are attenuated or amplified depending on the angle of arrival. I have designed a simple beamformer with the weights modelled by an FFT algorithm and a more complex beamformer with an eigenfilter design. The obtained results show that the reader has become more robust.

Additionally, I have derived a semi-analytical formula for calculating the optimal frame size. This formula incorporates properties of the spatial filter and throughput characteristics. In this way, further optimization of frame lengths is achieved. Furthermore,

I have pointed out what modifications in the protocols are required in order to benefit from collision recovery and I have proposed two acknowledgement schemes, applicable for collision scenarios. I have calculated the time necessary to successfully read tags from the reader's area. In these calculations I have taken into account the complete read out process, and the modified slot durations. The obtained results demonstrate that the proposed multiantenna collision recovery reader identifies tags in significantly shorter time which is of a great importance for time-sensitive applications.

ZUSAMMENFASSUNG

Radio Frequency Identification (RFID) ist eine neue Technologie welche es erlaubt, die Identität eines Chips (Tag), das an einem Objekt oder einer Person befestigt ist, über Funk zu übertragen. In meiner Arbeit fokussiere ich mich auf Ultra High Frequency (UHF) Tags, deren Übertragung in der Medium Access Control Schicht (MAC) durch ein sogenanntes Frame Slotted Aloha (FSA) zugeordnet wird.

In dieser Dissertation schlage ich vor, mehrfache Antennen beim Lesegerät (Reader) zu verwenden, um Kollisionen aufzulösen. Durch Ausnutzen der Tatsache, dass ein Tagssignal reellwertig ist, während alle anderen Signalkomponenten komplexwertig sind, teile ich die Signale in ihren Real- und Imaginärteil auf, wodurch ich Kollisionen unter perfekter Kanalkennntnis auflösen kann, die zweimal so viele Tags enthalten wie Empfangsantennen am Reader vorhanden sind.

Weiters habe ich eine Modifikation der Tagssignale empfohlen, indem ein spezieller Anteil hinzugefügt wird, der die Kanalschätzung erleichtert. Die von mir empfohlene Methode weist exzellente Ergebnisse unter perfekter Kanalkennntnis auf. Allerdings entsteht durch die beschränkte Menge von erzeugten Sequenzen ein neues Problem. Ich habe die Verteilung der zusätzlichen Sequenzen in der Tagpopulation analysiert und darauf basierend habe ich unterschiedliche Kollisionssituationen untersucht. Ich habe eine zweistufige Kollisionsvermeidung vorgeschlagen, die zunächst alle Tags mit einfach auftretender Sequenz per Slot entfernt. Bei auftretenden Paaren von gleichen Sequenzen wird die Kollision durch Projektion in den orthogonalen Unterraum der Interferenz aufgelöst. Die vorgeschlagene Methode verbessert die Kollisionsvermeidung und erhöht weiterhin den Durchsatz des Systems.

Darüber hinaus habe ich in dieser Arbeit den Einfluss verschiedener Parameter auf den Durchsatz untersucht und fand das Maximum des theoretisch erwarteten Durchsatzes für Empfänger mit verschiedenen Kollisionsvermeidungsfaktoren und unterschiedlichen Empfängerarchitekturen. Weiters habe ich die Verwendung von zusätzlichen Ortsfiltern vorgeschlagen, um noch näher an die theoretisch vorausgesagten Maxima zu gelangen. Die wesentliche Idee besteht darin, sich auf verschiedene Taggruppen durch unterschiedliche sektorielle Antennengewichte zu fokussieren. Auf diese Weise werden Tagssignale verstärkt oder gedämpft, je nach Empfangswinkel. So habe ich einen einfachen Beamformer per FFT und einen aufwendigeren durch Eigenfilter entwickelt. Die dadurch erhaltenen Resultate zeigen, dass der Reader robuster wird.

Zusätzlich habe ich eine halb-analytische Formel hergeleitet mit der optimale Rahmenlängen berechnet werden können. Die Formel beinhaltet Eigenschaften der Raumfil-

ter und der Durchsatzcharakteristika. Auf diesem Wege konnten weitere Optimierungen erzielt werden. Darüber hinaus habe ich auf Modifikationen der Protokolle hingewiesen, die nötig sind, um die Kollisionsvermeidung zu nutzen und zwei Acknowledgement Schemata vorgeschlagen, die zur Kollisionsvermeidung Anwendung finden. Ich habe die Zeit vorausgesagt, die notwendig ist, die Tags erfolgreich im Readerbereich zu lesen. Dabei wurde der gesamte Leseprozess modelliert sowie auch die veränderten Slotlängen. Die erhaltenen Ergebnisse zeigen, dass die vorgeschlagenen Mehrfachantennensysteme zur Kollisionsvermeidung Tags in signifikant kürzerer Zeit identifizieren, was von großer Wichtigkeit bei zeitkritischen Anwendungen ist.

ACKNOWLEDGEMENT

First of all, I would like to express my gratitude to Prof. Markus Rupp, my advisor, for his guidance, support and encouragement in my research throughout the time I spent at the TU Wien, and for his supervision of my thesis. Likewise, I would like to thank Prof. Javier Vales Alonso for agreeing to review the thesis and to be an examiner in the defence of the thesis. Furthermore, I would like to thank Prof. Christoph Mecklenbräuer for his fruitful discussions and stimulative thoughts.

I greatly benefited from the discussions with my colleagues Robert Langwieser, Michal Šimko and Martin Mayer. They provided an atmosphere for profitable scientific exchange, and introduced me in related topics of this thesis.

This work has been funded by the Christian Doppler Laboratory for Wireless Technologies for Sustainable Mobility, and its industrial partner Infineon Technologies. The financial support by the Federal Ministry of Economy, Family and Youth and the National Foundation for Research, Technology and Development is gratefully acknowledged.

CONTENT

1	Introduction	1
1.1	History of RFID Systems	1
1.2	Standardization of UHF RFID Systems	1
1.3	RFID Systems	2
1.4	Motivation	2
1.5	Related Work	3
1.6	Outline of the Thesis	5
2	RFID Collision Recovery Reader	7
2.1	Reader	7
2.2	Channel	7
2.3	Received Signal	8
2.4	Receivers	9
2.4.1	Zero Forcing Receiver - ZF	9
2.4.2	Minimum Mean Square Error Receiver - MMSE	10
2.4.3	Performance Analysis	10
2.5	Channel Estimation	12
2.5.1	Tag Signal Modification	12
2.5.2	Design of the "Postpreamble"	14
2.5.3	Least Squares Estimator - LS	15
2.5.4	Performance Evaluation	16
2.6	Collision Scenarios	18
2.7	Tag Signal Recovery	23
2.7.1	Successive Interference Cancellation	23
2.7.2	Channel Estimation with Projections	26
2.7.3	Results	27
2.8	Discussion and Conclusion	30
3	Postprocessing Beamforming	33
3.1	Geometrical Channel Model	33
3.2	FFT Beamforming	34
3.2.1	FFT Weights	36
3.2.2	FFT Sectors	36
3.2.3	FFT Postprocessing	39

3.2.4	Frame Optimization for FFT Postprocessing	40
3.3	Eigenfilter Beamforming	44
3.3.1	Eigenfilter Weights	44
3.3.2	Eigenfilter Sectors	46
3.3.3	Frame Optimization for Eigenfilter Postprocessing	49
3.3.4	Eigenfilter Postprocessing	50
3.4	Discussion and Conclusion	55
4	FSA with Collision Recovery	57
4.1	FSA Overview	57
4.2	Modifications in FSA	59
4.3	Throughput Constraints	60
4.3.1	Receiver Structure Constraints	61
4.3.2	“Postpreamble” Constraints	66
4.3.3	Channel Estimation Constraints - Cyan Set Constraints	69
4.4	Tag Identifications	71
4.4.1	Perfect DFSA	72
4.4.2	DFSA= 2^Q	73
4.4.3	DFSA= 4^Q	74
4.4.4	Optimized Frame Size	74
4.5	Performance evaluation	78
4.5.1	For $J = 1$ Acknowledged Tag	78
4.5.2	For $J = 2$ Acknowledged Tags	78
4.5.3	For $J = M$ Acknowledged Tags	80
4.5.4	Tag Identifications (in slots)	84
4.5.5	Theoretical Maxima of T_{ps} in FSA	87
4.5.6	Time Spent for Tag Identifications	89
4.6	Discussion and Conclusion	93
5	Conclusions	95
5.1	Open Issues and Outlook	95
5.2	Conclusion	96
	Appendices	97
A	List of Terms and Symbols	99
B	List of Acronyms	101
C	Approximations	103
C.1	Approximation of T_{ps_M}	103
C.2	Approximation of T_{ps_C}	104
C.3	Approximation of T_{ps_f}	104

Content xiii

Bibliography 107

LIST OF FIGURES

1.1	RFID reader and tags.	2
2.1	Communication between a reader and tags.	8
2.2	BER vs. SNR for ZF/MMSE receiver with R tags.	11
2.3	NSRP for ZF/MMSE receiver with R tags.	13
2.4	Preamble	14
2.5	Tag response.	14
2.6	BER vs. SNR (perf/est. channel).	17
2.7	Set of “postpreambles” / colours.	18
2.8	Possible scenarios with $R = 5$ tags.	20
2.9	Block diagram - SIC.	24
2.10	IQ diagram - four tags.	25
2.11	IQ diagram - remained two tags.	25
2.12	IQ diagram of the received signal.	26
2.13	MMSE collision recovery with $R = 4$ - Scenario 2.	28
2.14	MMSE collision recovery with $R = 8$ - Scenario 2.	29
3.1	Communication between the RFID reader and tags.	35
3.2	Azimuth and elevation.	35
3.3	Sectors - omni.	37
3.4	Rectangular patch antenna ($h = 0.1588$ cm, $\epsilon_r = 2.2$).	37
3.5	Sectoras - patch.	38
3.6	Residual tags vs. slots without postprocessing.	40
3.7	Residual tags vs. slots with postprocessing $Q=1$	41
3.8	Residual tags vs. slots with postprocessing $Q = \{\sqrt{2}, 2\}$	42
3.9	Throughput vs. SNR - with/without postprocessing.	43
3.10	Slots for reading 95% vs. speed factor Q.	44
3.11	A desired filter characteristic with a “stopband” from $90^\circ - 120^\circ$	45
3.12	The normalized angular attenuation with four sectors.	47
3.13	The normalized angular attenuation with six sectors.	48

3.14	Throughput in LOS case vs. SNR and fitting by Gauss3.	50
3.15	Throughput vs. SNR - with/without four-sector postprocessing.	52
3.16	Throughput vs. SNR - with/without six-sectors postprocessing.	53
4.1	Slot durations in FSA.	58
4.2	Modified slot durations in FSA due to "postpreamble" PP.	59
4.3	Acknowledgements of the resolved tags - type one.	59
4.4	Acknowledgements of the resolved tags - type two.	60
4.5	Expected throughput for $J = 1$	62
4.6	Expected throughput for $J \leq 2$	63
4.7	Expected throughput vs. collision recovery factor M	64
4.8	Expected throughput for $J = M$	65
4.9	Tag population and partitioned population.	67
4.10	Expected throughput - "postpreamble" constrain.	68
4.11	Expected throughput - Cyan set.	70
4.12	Identification time with ACK type 1	75
4.13	Identification time with ACK type 2	76
4.14	Residual tags vs. time with the optimized frames	77
4.15	Expected throughput for $J=1$	79
4.16	Expected throughput for $J \leq 2$	81
4.17	Expected throughput for $J = M$ - Cyan set.	83
4.18	Number of residual tags vs. number of required slots.	85
4.19	Number of decoded tags vs. number of frames.	86
4.20	Residual tags vs. slots at theoretical maxima - perf/est. channel.	88
4.21	Residual tags vs. elapsed time in perfect DFSA.	89
4.22	Residual tags vs. elapsed time in quantized 2^Q DFSA.	91
4.23	Residual tags vs. elapsed time in quantized 4^Q DFSA.	92

LIST OF TABLES

2.1	A set of eight orthogonal sequences.	15
2.2	BER for MMSE receiver and $R=2$	16
2.3	BER for MMSE receiver and $R=4$	16
2.4	BER for MMSE receiver and $R=8$	18
2.5	Collision scenarios for up to eight colliding tags per slot.	22
3.1	Elapsed slots at $\text{SNR}=15$ dB.	42
3.2	Fitting coefficients	50
3.3	Successfully read tags per slot vs. averaged SNR.	54
3.4	Number of slots elapsed for successfully decoding at $\text{SNR} = 15$ dB. . .	54
3.5	Number of slots elapsed for successfully decoding at $\text{SNR} = 30$ dB. . .	54
4.1	Abbreviations.	58
4.2	Slot durations in collision scenarios.	60
4.3	Frame size and throughput for $J = 1$	61
4.4	Frame size and throughput for $J \leq 2$	64
4.5	Frame size and throughput for $J = M$	66
4.6	Frame size and throughput - "postpreamble" constrain.	69
4.7	Frame size and throughput - Cyan set.	71
4.8	Expected Id. time in perfect DFSA	73
4.9	Expected Id. time in quantized 2^Q DFSA	73
4.10	Expected Id. time in quantized 4^Q DFSA	74
4.11	Expected throughput of FSA ($J=1$).	78
4.12	Expected throughput of FSA ($J \leq 2$).	80
4.13	Number of decoded tags and frame duration at $\text{SNR} = 15$ dB.	85
4.14	Number of spent slots for decoding 95%, 98% and 99.5%	86
4.15	Elapsed slots at theoretical maxima.	87
4.16	Elapsed slots at theoretical maxima and perf. channel.	87
4.17	Identification time in perfect DFSA	90
4.18	Identification time in quantized 2^Q DFSA	91

4.19 Identification time in quantized 4^Q DFSA	93
--	----

1 INTRODUCTION

Radio Frequency Identification (RFID) is an identification technology that wirelessly transmits the identity of a tag that is attached to an object or a person.

1.1 History of RFID Systems

The origin of RFID can be found in late 1940's when radar technology was employed for identifying planes that were approaching. The first famous scholarly article about RFID technology was written by Harry Stockman in 1948 [1]. Further research in the combined field of radar and RF communication systems was continued in the following decades.

In 1973, the first RFID transponder system was created. The same year Mario W. Cardullo received the first U.S. patent for an active RFID tag with rewritable memory [2], and Charles Walton was granted a patent for a passive transponder for radio-operated door lock [3]. The first identification chips were created in 1979. In the late 1980's, RFID was introduced in toll road payment systems in Europe. Furthermore, RFID was applied to enhance industrial applications and to facilitate short-range animal control systems.

In the early 1990's an ultra-high frequency (UHF) RFID system was developed and patented by IBM engineers. With this, longer read ranges were feasible and a reading distance that was from 10 cm to 1 m got extended to up to 12 m. Furthermore, a higher data rate was achieved (up to 640 kbit/s).

1.2 Standardization of UHF RFID Systems

EPCglobal is an organization with the main focus on Electronic Product Code (EPC) technology standardization. It represents a consortium of GS1, Auto-ID Labs, European Article Number (EAN) international, Uniform Code Council (UCC), Cisco Systems, DHL/Exel Supply Chain, Haier Group Company, Johnson & Johnson, Kimberly-Clark Corporation, LG Electronics, Lockheed Martin Corporation, METRO AG, Novartis Pharma AG, Office of the Secretary of Defense, Procter & Gamble, Sony Corporation, The Dow Chemical Company and Wal-Mart Stores, Inc. Their main goal is to increase the efficiency of the supply chains and to enhance the information exchange between companies and their trade partners.

In 2004, they published the EPCglobal UHF Class-1 Gen-2 air interface protocol. This protocol defines the requirements for passive RFID systems operation in the frequency range from 860 MHz - 960 MHz. It contains specifications for the hardware of the passive tags and for hardware and software of the reader. Over the years this protocol has established itself as the standard for UHF RFID.

In 2008, a new version of the standard Gen-2 Version 1.2.0 was released. This version contains enhancements required in order to improve RFID performance for the item level tagging applications, e.g., inserting a “smart label” on price the tags [4].

1.3 RFID Systems

RFID reader usually operates in a multiple RFID tag environment. The interrogation of the tags is scheduled on the Medium Access Control (MAC) layer. One of the interrogation protocols for scheduling tag responses to the reader's *Query* command is Framed Slotted Aloha (FSA). My work is focused on FSA as defined in the EPC standard [5].

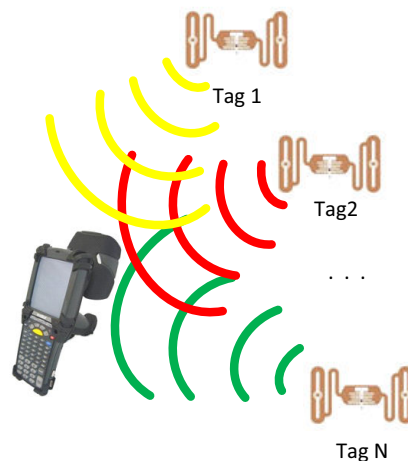


Figure 1.1: RFID reader and tags.

1.4 Motivation

At the beginning of an interrogation cycle, a reader announces the frame start and all tags that are in its read range, choose one of the slots within the frame for their transmission. If multiple tags respond simultaneously, a collision at the air interface occurs. The standard collision detection mechanism regards this as a destructive event and discards the information. Collided tags have to wait for the next frame and to choose a new slot for transmission. Thus, collisions decrease the system throughput and

prolong the interrogation time. It is important to find the optimal frame size in order to decrease the number of collisions and to increase the system throughput. Hence, only slots in which one tag is active can be decoded successfully [6]. This determines the maximal throughput per slot for an FSA system. The maximum throughput value of 0.368 is achieved when the inventory frame size F is equal to the tag population size N . To overcome such limitations, different research groups are working on collision arbitration protocols and collision recovery procedures.

In this thesis, I propose a method that resolves signals from collided tags. Thus, the information is used also from the collision slots and the time necessary for reading out the tag population is decreased. The shortened identification time is advantageous for numerous time-sensitive applications where a large tag population should be identified fast e.g., in production tracks where densely packed products should be identified as they are passing the reader gate or it could be used to save time during loading big shipments in busy ports. Furthermore, this could have a vast application in amusement parks, e.g., to track if all parts of a roller coaster are functioning correctly as a wagon is moving over the tracks. Moreover, the proposed approach could be employed during launching of a space shuttle to investigate if all screws (that would contain RFID tags) are staying fixed in their places. If some issues would be detected early enough, launching could be aborted and postponed for later and in that way a lot of money and possibly lives would be saved.

1.5 Related Work

Slots with colliding RFID tag signals were investigated in the following papers: Khasgiwale et al. [7] estimated the number of tags involved in collision by information from tag collisions on the physical layer. In that way they have achieved a more accurate estimation of the RFID tag population. They also showed that it is possible to recover from collisions and correctly read the data of the colliding tags. Shen et al. [8] analysed the signal constellations of responses from colliding tags. The authors proposed an algorithm for recovery from tag collisions. Furthermore, they simulated the error performance when multiple colliding tags were present. Mindikoglu et al. [9] developed a blind signal separation receiver for RFID collision recovery with multiple antennas based on the zero constant modulus algorithm.

Knerr et al. in [10] formulated a maximum likelihood estimator to yield the estimated number of tags on a slot-wise basis. Their method can be applied for an immediate update of the frame size, during the frame duration, according to the probability level of the current slot-by-slot estimate. In [11], Holzer et al. presented an improvement of the FSA. Their algorithm is suitable for the applications where the tag population size is known in advance. The authors are examining the first half of the frame and if they find an event with low probability, they restart the frame. In [12] the exact number of tags participating in a collision is extracted by employing the physical layer architecture of a reader. It is possible to increase the throughput by exploiting the information from collisions, not just to discard it. In that way, the optimal frame size is shorter and the tags that are in the reader range can be inventoried faster.

Yu et al. in [13] proposed an anti-collision algorithm based on smart antenna technology and implemented the space division multiple access in RFID systems. They divided the reader coverage area into several subspaces and applied an FSA or a binary tree search in each sector but they did not recover from collisions. Fyhn et al. showed that channel fading, the difference in delay and the tag frequency dispersion can be exploited for easier separation of colliding signals in a multipacket receiver in [14]. In [15], Ricciato et al. achieved a 20% to 25% gain in throughput by applying inter-frame successive interference cancellation (ISIC) with respect to traditional intra-frame SIC. Myung et al. elaborated frameless binary splitting methods in [16]. Their results show that adaptive binary splitting reduces delay and tag communication overhead for the tag reading process. In [17], a theoretical study on a collision recovery binary tree algorithm is proposed, and a closed form for calculating system efficiency is derived.

If readers with Collision Recovery (CR) features are available, slots with colliding tags can also be decoded successfully, and the throughput increases further. Knowing the maximum number of collisions that can be resolved by a certain receiver architecture, the frames can be reduced which results in further throughput enhancement and smaller inventory times. A practically working CR on a physical layer with a single antenna reader receiver with two colliding tags in one slot is demonstrated in [18]. With such reader, Angerer et al. obtained an expected throughput increase of approximately 60%. In [19,20], the authors derived a single antenna detection scheme for the simultaneous transmission of two tags with a memory-assisted detection of collided FMO signals. Furthermore, they calculated an inventory time reduction of 8% to 17% when a two-tag detection and collision recovery is applied. In [21], De Donno et al. showed, by experiments, that performances of conventional RFID systems can be considerably enhanced by employing collision recovery in case of two colliding tags. The authors achieved an inventory time reduction of 26% in actual measurements taken with a software-defined RFID reader and off-the-shelf programmable tags. In [22], Kim et al. presented an improved binary tree collision arbitration protocol that decreases the number of retransmissions and reduces the identification delay by exploiting multiple antennas at the reader.

Theoretical calculations of the FSA system throughput for the reader with physical layer collision recovery were performed in [23], and a significant increase is shown. Additionally, the authors proved a single antenna receiver with a channel estimation procedure for recovering from a two-tag collision to work in practice. Moreover, they have shown that multiple antenna receivers with perfect channel knowledge are capable of recovering from a collision of $R \leq M$ tags. Here, M denotes the so-called collision recovery factor, that is the maximum number of colliding tags a reader can resolve under best circumstances. It is directly related to the number of receive antennas N_{RA} . In [23], it was conjectured that $M = N_{RA}$.

Mayer et al. in [24] identified a large gain of throughput by introducing a novel tag identification scheme with the computationally efficient Approximate Message Passing (AMP) algorithm. They have shown that the proposed method works quite reliably even in the low SNR regime. In [25] Khelladi et al. proposed a method for channel estimation based on hidden pilots and they identified an incremental improvement of the channel estimation accuracy compared to the conventional pilot estimation method. In [26],

Vales et al. analytically computed the mean number of identifications in a given time interval. The authors point out that the performance description in terms of time-slots is not optimal since the slot durations can vary significantly.

1.6 Outline of the Thesis

This thesis is based on the following publications, which will be referred to in the overview of the chapters at the end of this section.

- J. Kaitovic, R. Langwieser, M. Rupp, "RFID Reader with Multi Antenna Physical Layer Collision Recovery Receivers", in Proc. of the 2011 IEEE International Conference on RFID-Technologies and Applications (RFID-TA), Sitges, Spain, September, 2011.
- J. Kaitovic, M. Šimko, R. Langwieser, M. Rupp, "Channel Estimation in Tag Collision Scenarios", in Proc. of the 2012 IEEE International Conference on RFID, Orlando, Florida (USA), April, 2012.
- J. Kaitovic, R. Langwieser, M. Rupp, "Advanced Collision Recovery Receiver for RFID", in Proc. of the 4th international EURASIP workshop on RFID technology, Torino, Italy, September, 2012.
- J. Kaitovic, R. Langwieser, M. Rupp, "A smart collision recovery receiver for RFIDs", EURASIP Journal on Embedded Systems, 7, pages 1 - 19, 2013.
- J. Kaitovic, M. Rupp, "Improved Physical Layer Collision Recovery Receivers for RFID Readers", in Proc. of the 2014 IEEE International Conference on RFID, Orlando, Florida (USA), April, 2014
- J. Kaitovic, M. Rupp, "RFID Physical Layer Collision Recovery Receivers with Spatial Filtering", in Proc. of the 2015 IEEE International Conference on RFID-Technologies and Applications (RFID-TA), Tokyo, Japan, September, 2015
- J. Kaitovic, M. Rupp, "Tag Identification Time in Multiantenna Collision Scenarios", in Proc. of the 5th international EURASIP workshop on RFID technology, Rosenheim, Germany, October, 2015

The content of the individual chapters and the main contributions of the thesis are briefly described in the following:

Chapter 1 introduces RFID and gives a brief overview of the history and standards. Furthermore, it lists the related work and explains the motivation that inspired this thesis. The last section of the chapter provides the outline of the thesis and summarises the content of the individual chapters.

Chapter 2 describes the setup and proposes a ZF and an MMSE receiver which allow separation of up to $M=2N_{RA}$ tags, where N_{RA} is the number of receive antennas on

the reader [27]. In more details, it explains the received signal and suggests necessary changes for channel estimation [28]. It suggests a method for channel estimation in collision scenarios with the modified tag response to the *Query* command of the reader. Furthermore, it explains the design of a set of mutually orthogonal sequences for channel estimation, called “postpreambles”. Based on the designed set, it defines collision scenarios [29] and evaluates performances of the reader in different scenarios [30]. In addition, it recommends a collision recovery method through successive interference cancellation and projection of the constellation into the orthogonal subspace of the interference. In that way “cyan” set collisions are recovered and all tags with a unique “postpreamble” are resolved as well as the remaining pair of tags with the same “postpreamble”.

Chapter 3 proposes a novel physical layer collision recovery mechanism with postprocessing of the received signal. It defines a geometrical channel model and proposes two different beamforming methods. In the first method, a simple postprocessing is employed with FFT weights and fixed beams are generated with a modified FFT algorithm [31]. In the second method, a more precise spatial filter is employed with an eigenfilter design for spatial filtering in 2D [32]. Additionally, a semi-analytical formula for calculating the optimal frame size by taking into account throughput and spatial filter properties is derived. The proposed methods are evaluated by means of Monte Carlo simulations. The obtained results show that the proposed methods resolve more colliding tags by making collisions less destructive.

Chapter 4 investigates the throughput performances of the proposed receiver structures in collision scenarios. It provides an overview of FSA and describes what modifications of the current protocol are required in order to benefit from the proposed collision recovery. Furthermore, it suggests two different acknowledgement schemes applicable for the collision scenarios [33]. Moreover, it studies the throughput constraints due to the receiver structure and channel estimation for different collision scenarios [30]. It analytically derives optimal frame sizes, given that a certain number of collisions can be resolved. It studies the influence of the different number of acknowledged tags in a slot [27, 28]. It analyses theoretical limits of the inventory time and shows how the new method can approach such theoretical maxima [31]. Additionally, it investigates the expected frame duration and the expected number of acknowledged tags. The last section of the chapter provides a performance evaluation and the obtained results are compared with the performance of a standard compliant reader.

Conclusions chapter presents concluding remarks and discusses open issues and outlook.

Appendix presents the list of terms and symbols as well as the list of acronyms. Furthermore, it provides a derivation of a simple function in the ratio of the frame size to the tag population size for various throughput per slot calculations.

2 RFID COLLISION RECOVERY READER

This chapter defines the reader architecture that was studied throughout the thesis. It explains the employed channel model and describes the received signal in the defined setup. It proposes a Zero-Forcing (ZF) and a Minimum Mean Square Error (MMSE) receiver which allows the separation of up to $M = 2N_{\text{RA}}$ tags, where N_{RA} is the number of receiving antennas on the reader. The proposed algorithms are verified through simulations.

Additionally, it proposes a method for channel estimation with a modified tag response, a so-called “postpreamble”. The influence of the channel estimation on the performance is investigated by simulations. Furthermore, a collision recovery method through successive interference cancellation and projection of the constellation into the orthogonal subspace of the interference is proposed and the performance of the proposed method is analysed by means of simulations.

2.1 Reader

A reader with one transmit and N_{RA} receive antennas is considered as shown in Figure 2.1. The considered configuration is bistatic, dislocated [34]. In the reader range are N tags and it is assumed that R of them are simultaneously active.

2.2 Channel

In passive RFID systems a tag is powered by the reader with energy in the form of a continuous carrier transmission. For communicating with the reader, tags apply backscatter modulation. In [35,36], the authors proposed a two-way Rician channel model for RFID scenarios based on carried out channel measurements. They also showed that since the Rician factor strongly depends on the environment, a better fit to the measurement data was achieved by applying a double Rayleigh distribution. Thus, I assume that the channel is a double Rayleigh fading channel and is modelled as a multiplication of a forward channel h_j^f and a backward channel $h_{i,j}^b$ as shown in Equation (2.1), explained in [37].

$$h_{i,j} = h_j^f h_{i,j}^b, \quad (2.1)$$

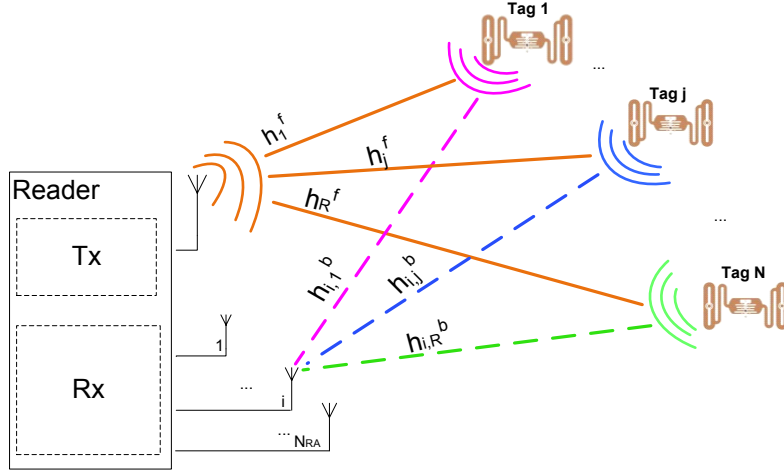


Figure 2.1: Communication between a single reader equipped with one transmit and N_{RA} receive antennas, and N tags.

where the index i represents antenna i and j denotes tag j .

As an example, the channel matrix between the reader's transmit antenna, two tags and four receive antennas is shown in Equation (2.2).

$$\mathbf{H}^c = \begin{bmatrix} h_{1,1} & h_{1,2} \\ h_{2,1} & h_{2,2} \\ h_{3,1} & h_{3,2} \\ h_{4,1} & h_{4,2} \end{bmatrix}. \quad (2.2)$$

The coefficients described above are illustrated in Figure 2.1.

2.3 Received Signal

The received signal can be written as:

$$\mathbf{r}^c(t) = \mathbf{H}^c \mathbf{a}(t) + \mathbf{I} + \mathbf{n}(t), \quad (2.3)$$

where \mathbf{H}^c denotes the $N_{RA} \times R$ channel matrix, R denotes number of active tags and $\mathbf{a}(t)$ is the $R \times 1$ modulation vector with the elements $a_j(t)$. Furthermore, $\mathbf{r}^c(t)$, \mathbf{I} , $\mathbf{n}(t)$ are the $N_{RA} \times 1$ column vectors of the received signal, the carrier leakage and noise, respectively.

Using the fact that $a_j(t)$, the modulation signal of tag j , is real valued, the received signal, presented by Equation (2.3), can be equivalently reformulated to:

$$\begin{bmatrix} \Re\{\mathbf{r}^c(t)\} \\ \Im\{\mathbf{r}^c(t)\} \end{bmatrix} = \begin{bmatrix} \Re\{\mathbf{H}^c\} \\ \Im\{\mathbf{H}^c\} \end{bmatrix} \mathbf{a}(t) + \begin{bmatrix} \Re\{\mathbf{I}\} \\ \Im\{\mathbf{I}\} \end{bmatrix} + \begin{bmatrix} \Re\{\mathbf{n}(t)\} \\ \Im\{\mathbf{n}(t)\} \end{bmatrix}, \quad (2.4)$$

where $\Re\{\cdot\}$ selects the real part and $\Im\{\cdot\}$ selects the imaginary part of the argument. In this way the number of equations is doubled. It allows the separation of up to $M=2N_{RA}$ tags.

In the following equations for the ZF and the MMSE receivers the channel matrix and the received signal have the form of:

$$\mathbf{H} = \begin{bmatrix} \Re\{\mathbf{H}^c\} \\ \Im\{\mathbf{H}^c\} \end{bmatrix}, \quad (2.5)$$

$$\mathbf{r}(t) = \begin{bmatrix} \Re\{\mathbf{r}^c(t)\} \\ \Im\{\mathbf{r}^c(t)\} \end{bmatrix}. \quad (2.6)$$

Perfect isolation of the reader transmit and received part is assumed and the carrier leakage is set to zero in order to simplify equations.

2.4 Receivers

In the following part optimal ZF and MMSE receivers are proposed.

2.4.1 Zero Forcing Receiver - ZF

The Zero Forcing receiver inverts the channel and eliminates inter-symbol interference (ISI) but at the expense of noise enhancement [38]. The ZF receiver is described by:

$$\mathbf{a}_{ZF}(t) = \left(\hat{\mathbf{H}}^H \hat{\mathbf{H}} \right)^{-1} \hat{\mathbf{H}}^H \left(\mathbf{r}(t) - \hat{\mathbf{H}} \bar{\mathbf{a}}(t) \right), \quad (2.7)$$

where $\hat{\mathbf{H}}$ is the matrix of the estimated channel, $\hat{\mathbf{H}}^H$ denotes its Hermitian transpose, $\bar{\mathbf{a}}(t) = E\{\mathbf{a}(t)\}$ and $\mathbf{a}_{ZF}(t)$ is the signal at the output of the ZF receiver. Since, the tag signal $\mathbf{a}(t)$ is modulated as on-off keying with $\bar{\mathbf{a}}(t) \neq 0$, in order to apply ZF, the mean value of the tag signal is multiplied by the estimated channel and is subtracted from the received signal. Furthermore, the tag signal is FM0 encoded and the baseband phase at every symbol boundary is inverted. In addition, a data-0 has a mid-symbol phase inversion. Thus, if the transmitted sequence contains even number of ones, the sequence is balanced (contains the same number of ones and zeros) and $\bar{\mathbf{a}}(t) = \frac{1}{2}$ [39]. If the transmitted sequence contains odd number of ones, then, $\bar{\mathbf{a}}(t) = \frac{1}{2} \pm \Delta$, where

$\Delta = \frac{1}{l_a}$ and l_a is the length of the transmitted sequence. In my work, I have chosen the sequences that contain even number of ones. If the sequence contains odd number of ones, that sequence is excluded and the new one is generated. Thus, the mean value of the tag signal is fixed to $\bar{\mathbf{a}}(t) = \frac{1}{2}$.

2.4.2 Minimum Mean Square Error Receiver - MMSE

A more sophisticated approach is an MMSE receiver that offers a balance between noise enhancement and ISI mitigation [38]. The MMSE filter is described by:

$$\mathbf{G}_{\text{MMSE}} = \left(\hat{\mathbf{H}}^H \hat{\mathbf{H}} + \sigma^2 \mathbf{I}_R \right)^{-1} \hat{\mathbf{H}}^H, \quad (2.8)$$

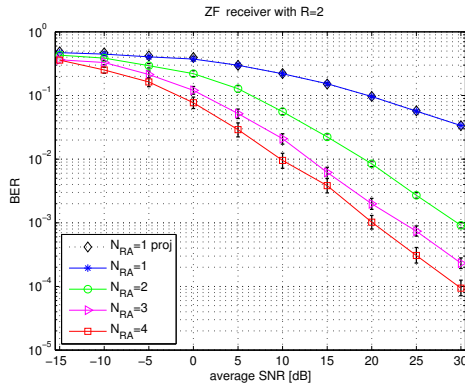
where σ^2 denotes the noise power, and \mathbf{I}_R is the $R \times R$ identity matrix. The signal at the output of the MMSE receiver is obtained by:

$$\mathbf{a}_{\text{MMSE}}(t) = \mathbf{G}_{\text{MMSE}} \cdot \left(\mathbf{r}(t) - \hat{\mathbf{H}}\bar{\mathbf{a}}(t) \right). \quad (2.9)$$

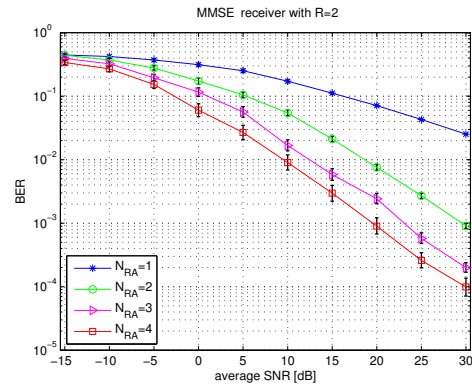
2.4.3 Performance Analysis

The performance of the proposed algorithm is analysed through MATLAB simulations. The Bit Error Ratio (BER) is computed by Monte Carlo simulations of a varying number of tag responses inside one slot in order to compare the performances. In the simulated system the RFID reader has four receive antennas. The number R of tags that are in the reader range and are transmitting in this slot, varies from one to eight. A Rayleigh fading channel is assumed. The individual Rayleigh channel coefficients are independent zero mean circularly symmetric complex-valued Gaussian random variables [23]. The simulation is run with different channel realizations and it is averaged over the total number of iterations. In order to have more precise insight with smaller confidence intervals, the number of iterations N_{iter} is chosen based on the SNR value and $N_{\text{iter}}(\overline{\text{SNR}}) = 50 \cdot 10^{\frac{\overline{\text{SNR}}[\text{dB}]}{10}} + 50$, where $\overline{\text{SNR}} \triangleq \frac{1}{N_{\text{RA}}} \sum_i \frac{E\{|h_{i,j}|^2 a_j^2\}}{N_0}$ is the average signal to noise ratio, and N_0 is the noise power spectral density. Thus, for higher SNR values the simulation is performed more times. This particular choice results in a good compromise, offering fast simulation and sufficiently small confidence intervals as depicted in the following figures. For each slot the channel parameters are calculated again. At this point perfect channel knowledge is assumed.

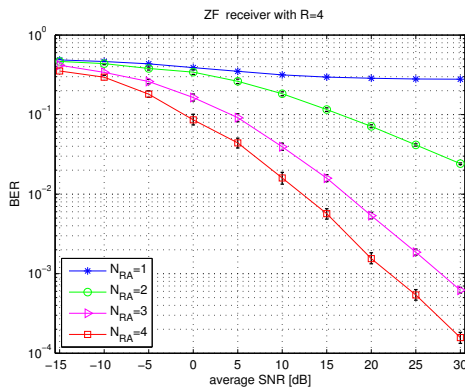
As shown in the figures (Figure 2.2a - Figure 2.2e) the ZF receiver is capable of recovering from collisions of the number of tags that is two times higher than the number of antennas. If at least two tags are active in the same slot, a collision occurs. A ZF receiver with one receiving antenna can resolve this collision. The obtained results are also verified through comparison with [23] (in Figure 2.2a, black dotted line with



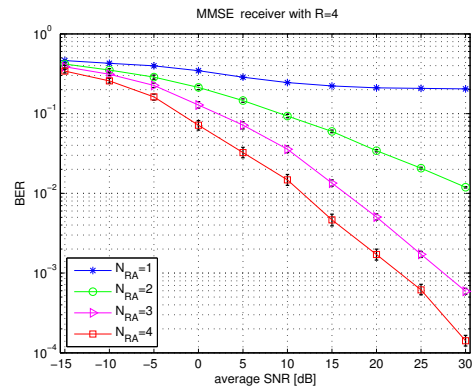
(a) ZF receiver with R=2



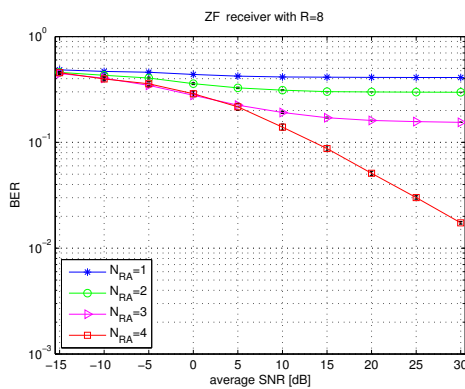
(b) MMSE receiver with R=2



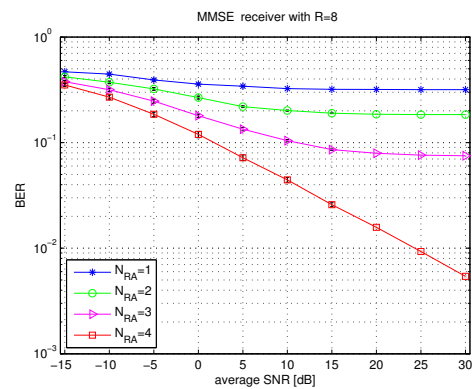
(c) ZF receiver with R=4



(d) MMSE receiver with R=4



(e) ZF receiver with R=8



(f) MMSE receiver with R=8

Figure 2.2: BER vs. SNR for ZF/MMSE receiver with R tags.

diamonds). Straightforward results are observed in case of four active tags and eight active tags. It is shown that a ZF receiver with two receiving antennas can resolve collisions of four tags. In the case of eight colliding tags four receiving antennas on the reader are necessary to recover from this collision. Similar results are obtained with MMSE receivers and the simulation results are illustrated in the figures (Figure 2.2b - Figure 2.2f). Around each point in the graphs confidence intervals of 95 % have been plotted.

In the figures (Figure 2.3a - Figure 2.3e) the number of successfully received packets NSRP is shown with respect to signal to noise ratio and different numbers of receive antennas at the reader.

The number of successfully received packets is calculated in the following way: Received packets are compared with transmitted packets. If an error in transmission has occurred, the number of packets with errors is incremented. That has been done for every received packet in one slot. The total number of packets with errors is subtracted from the total number of packets sent in the respected slot and in that way the number of successfully received packets is obtained. The same steps are conducted in every slot. At the end, the total number of successfully received packets is divided by the number of slots which correspond to that value of SNR.

If two tags are active in the same slot, a reader with one receive antenna is able to successfully receive more than 1.6 packets on average for the simulated SNR ratio. Furthermore, it can be observed that for a higher number of receive antennas, looking at the same SNR, the number of successfully received packets increases much faster. It can easily be shown that with a higher SNR, the reader can successfully receive two packets. Similar results are obtained for four and eight tags, transmitting in the same slot.

2.5 Channel Estimation

In order to resolve a tag signal from the received signal, a reader needs to estimate the channel. In the EPCglobal standard for UHF RFID [5] a tag response to the *Query* command consists of a preamble followed by a 16 bit-random number or pseudo-random number.

For channel estimation, the reader uses such preamble.

2.5.1 Tag Signal Modification

However, since the preamble is identical for all tags involved in a collision, it cannot be used for the channel estimation in collision scenarios. The bits that follow can neither be used, because they are not known in advance and they are different in each conversation round. Hence, an extension of the tag signal by including a "postpreamble"

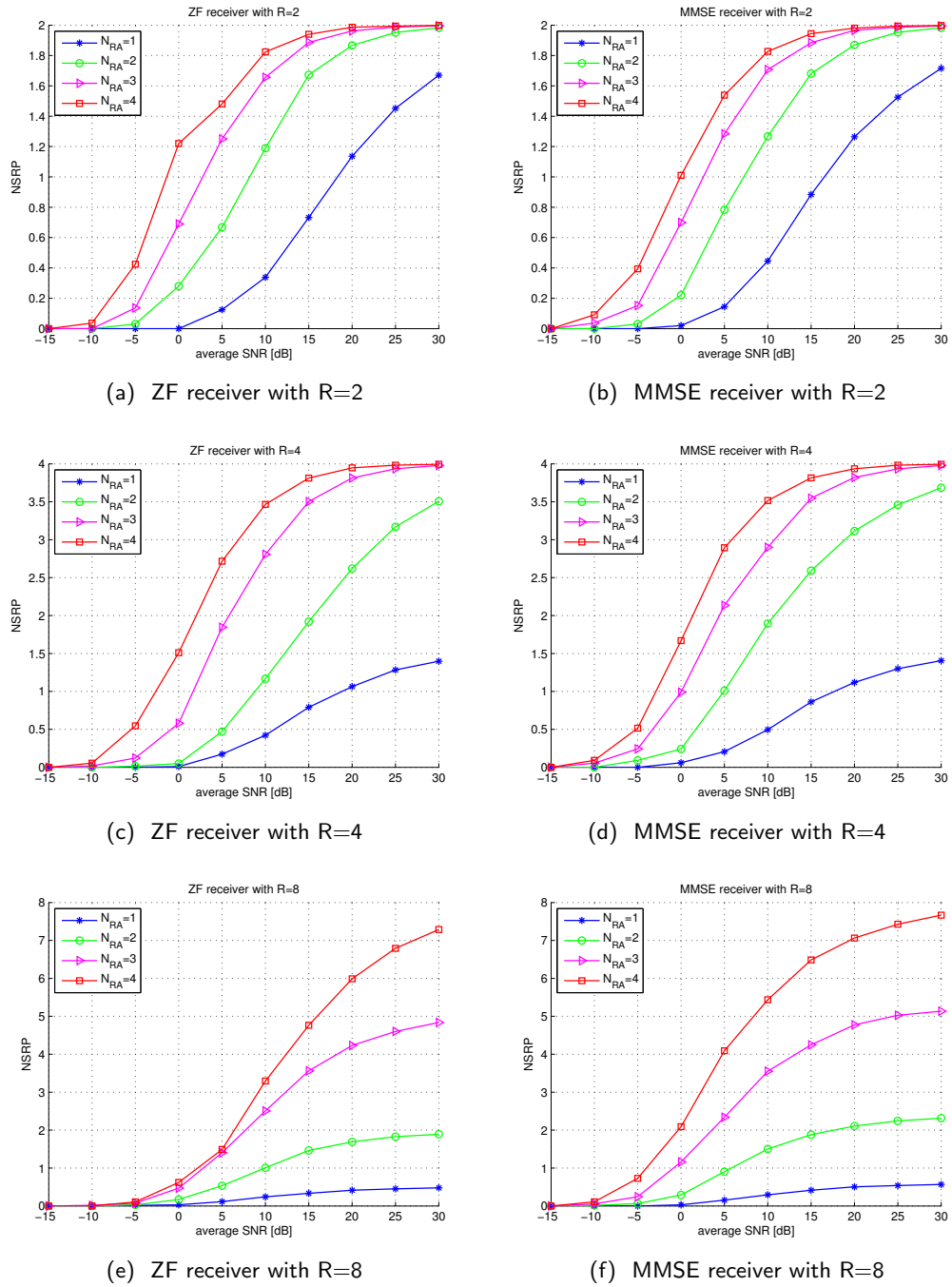


Figure 2.3: NSRP for ZF/MMSE receiver with R tags.

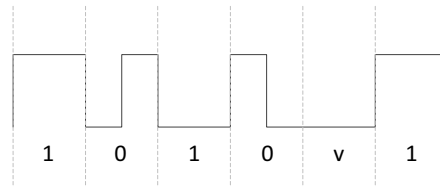


Figure 2.4: Preamble [5].

as shown in Figure 2.5 is proposed. In order to fulfil the channel estimation requirements, the “postpreamble” is designed to be different for each tag, and mutually orthogonal. Tags encode the backscattered data as either FM0 baseband or Miller modulated of a subcarrier at the data rate [5]. The challenge was to offer optimal channel estimation at minimum “postpreamble” length.

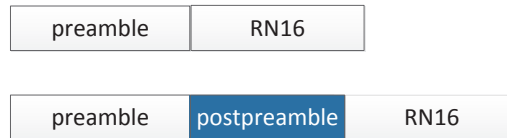


Figure 2.5: Tag response according to the EPC standard and the modified tag response (below).

2.5.2 Design of the “Postpreamble”

The length of the “postpreamble” is strongly influenced by the number of the tags I want to separate in the system. The FM0 coding doubles the amount of bits after the encoding process and does not allow the use of well known orthogonal sequences (i.e., Hadamard). Therefore, one can expect to find only a limited amount of mutually orthogonal sequences, that are equal to the half of the length of the encoded sequence at best. For example for the code length of 12 bits, there are only four mutually orthogonal sequences. Using a full search algorithm [40], also a set of eight mutually orthogonal sequences of length 16 is obtained. Since the collision recovery factor of the proposed reader is $M = 8$, the maximum number of colliding tags that can be separated is eight ($R_{\max} = 8$) and thus, a set of eight mutually orthogonal sequences is applied as a set of “postpreambles”.

Search-algorithm: Due to the extremely high number of possible vector sets, it is necessary to optimize the search algorithm for mutually orthogonal sequences. The algorithm iterates over increasing set sizes and in each iterations it searches for all unique sets of mutually orthogonal sequences of the size of the particular iteration. A set S_i of sequences \mathbf{p}_k with exactly i different sequences is called a set of mutually orthogonal sequences if it fulfills the following property:

$$\mathbf{p}_k^T \mathbf{p}_l = \begin{cases} 1, & k = l \\ 0, & \text{else,} \end{cases} \quad (2.10)$$

$$\forall \mathbf{p}_k, \mathbf{p}_l \in \mathbf{S}_i.$$

An iterative algorithm to find the largest set of mutually orthogonal sequences is developed. In each iteration it searches for all unique sets \mathbf{S}_i of mutually orthogonal sequences, which are denoted by \mathcal{W}_i . In the i^{th} iteration the algorithm searches for the set of all sets of unique mutually orthogonal sequences \mathcal{W}_i of size i based on the set \mathcal{W}_{i-1} obtained in the previous iteration. In the first step the algorithm searches for all unique possible sets of mutually orthogonal sequences of size one: \mathcal{W}_1 . The trivial solutions in the first iteration are all possible sequences. In the second iteration, all possible pairs of mutually orthogonal sequences are found: \mathcal{W}_2 . In the following iterations, based on the set of mutually orthogonal pairs of sequences \mathcal{W}_2 , algorithm searches for all unique sets of three mutually orthogonal sequences, resulting in \mathcal{W}_3 . The algorithm continues until it can still find at least one unique set of mutually orthogonal sequences of a bigger size.

The set of sequences \mathcal{S}_8 that is employed in the simulations, is shown in Table 2.1.

Table 2.1: A set of eight orthogonal sequences.

Sequence	
\mathbf{p}_1	1 -1 1 -1 1 -1 1 -1 1 -1 1 -1 1 -1
\mathbf{p}_{18}	1 -1 1 -1 1 -1 1 1 -1 1 -1 1 -1 -1
\mathbf{p}_{69}	1 -1 1 1 -1 1 -1 1 -1 1 -1 1 -1 1
\mathbf{p}_{86}	1 -1 1 1 -1 1 -1 -1 1 -1 1 1 -1 -1
\mathbf{p}_{171}	1 1 -1 1 -1 -1 1 -1 1 1 -1 1 -1 1
\mathbf{p}_{188}	1 1 -1 1 -1 -1 1 1 -1 -1 1 1 -1 -1
\mathbf{p}_{239}	1 1 -1 -1 1 1 -1 1 -1 -1 1 1 -1 -1
\mathbf{p}_{256}	1 1 -1 -1 1 1 -1 -1 1 1 -1 -1 1 -1

2.5.3 Least Squares Estimator - LS

The LS estimator estimates the channel coefficients by minimizing the squared discrepancies between the received signal, on the one hand, and the “postpreamble” on the other hand, using [41]:

$$\hat{\mathbf{H}}_{\text{LS}} = \arg \min_{\mathbf{H}} \|\mathbf{r}^{\text{pp}}(t) - \mathbf{S}_M \mathbf{H}\|^2. \quad (2.11)$$

The LS channel estimator for the “postpreamble” is given by

$$\hat{\mathbf{H}}_{\text{LS}} = \mathbf{r}^{\text{pp}}(t) \cdot \mathbf{S}_M^H (\mathbf{S}_M \mathbf{S}_M^H)^{-1}, \quad (2.12)$$

where \mathbf{S}_M denotes the set of the M “postpreambles” and $\mathbf{r}^{\text{pp}}(t)$ is the part of the received signal containing the “postpreamble”. A perfect knowledge of the “postpreamble” set, as well as that all tags involved in collision have a unique “postpreamble”, were assumed in the simulations conducted in Section 2.5.4.

2.5.4 Performance Evaluation

In Figure 2.6a, Figure 2.6c and Figure 2.6e the performance of the MMSE receiver from Section 2.4.2 with perfect channel knowledge is shown while in Figure 2.6b, Figure 2.6d and Figure 2.6f the corresponding performance of the MMSE receiver with estimated channels is presented. Around each point in the figures the confidence interval that contains 95% of the obtained results is plotted to evaluate the quality of the simulation.

Table 2.2: BER for MMSE receiver and R=2.

BER at 30 dB	Perfect Channel	Estimated Channel
$N_{\text{RA}} = 1$	$2.53 \cdot 10^{-2}$	$2.66 \cdot 10^{-2}$
$N_{\text{RA}} = 2$	$0.92 \cdot 10^{-3}$	$1.03 \cdot 10^{-3}$
$N_{\text{RA}} = 3$	$2.17 \cdot 10^{-4}$	$2.86 \cdot 10^{-4}$
$N_{\text{RA}} = 4$	$0.89 \cdot 10^{-4}$	$1.16 \cdot 10^{-4}$

A comparison of BER values from Figure 2.6a and Figure 2.6b, for the MMSE receiver and two colliding tags, is given in Table 2.2. From this it is observed that the MMSE receiver performs almost perfect with the proposed channel estimation method. The BER values are close to those values obtained with perfect channel knowledge.

Table 2.3: BER for MMSE receiver and R=4.

BER at 30 dB	Perfect Channel	Estimated Channel
$N_{\text{RA}} = 1$	0.2049	0.2052
$N_{\text{RA}} = 2$	$1.21 \cdot 10^{-2}$	$1.36 \cdot 10^{-2}$
$N_{\text{RA}} = 3$	$5.77 \cdot 10^{-4}$	$7.43 \cdot 10^{-4}$
$N_{\text{RA}} = 4$	$1.61 \cdot 10^{-4}$	$2.15 \cdot 10^{-4}$

In Table 2.3 a comparison of Figure 2.6c and Figure 2.6d is given, for the MMSE receiver and four tags transmitting in one slot. Inspecting the BER values it can be concluded that for the MMSE receiver with one receive antenna the BER ratio is too high and the collision cannot be resolved. At least two receive antennas are needed to recover from this collision. In this case the proposed channel estimation method provides very good results.

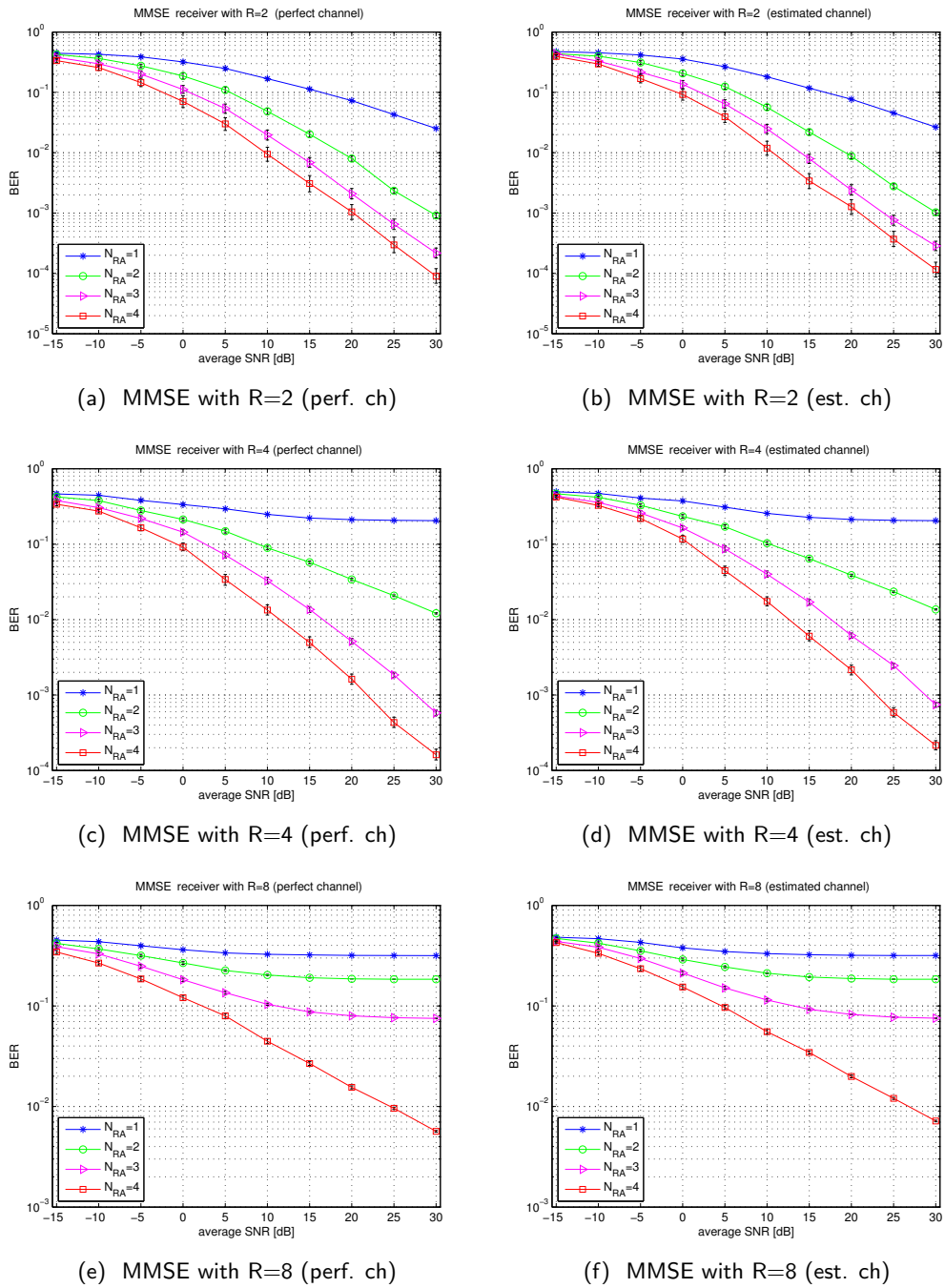


Figure 2.6: BER vs. SNR for MMSE receiver with R tags (perfect/estimated channel).

A comparison for the MMSE receiver and eight colliding tags, from 2.6e and 2.6f, is listed in Table 2.4. As expected for solving the collision of eight tags at least four receiving antennas are needed. In case of a smaller number of receiving antennas on the reader side, the resulting BER is too high. The obtained values are similar for

Table 2.4: BER for MMSE receiver and R=8.

BER at 30 dB	Perfect Channel	Estimated Channel
$N_{RA} = 1$	0.3170	0.3171
$N_{RA} = 2$	0.1842	0.1843
$N_{RA} = 3$	$7.53 \cdot 10^{-2}$	$7.56 \cdot 10^{-2}$
$N_{RA} = 4$	$5.66 \cdot 10^{-3}$	$7.17 \cdot 10^{-3}$

both scenarios, the scenario with perfect channel knowledge and the scenario with the estimated channels. The channel knowledge does not have much impact. Moreover, with four receiving antennas in both scenarios the MMSE receiver can recover from collisions, but as expected with perfect channel knowledge a bit better results are obtained.

The desired case is that all tags, that are participating in a collision, have orthogonal “postpreambles”. Thus, an additional constraint to this maximum is the channel estimation with the “postpreambles” set. Based on that, several possible scenarios can be distinguished.

2.6 Collision Scenarios

A set of eight mutually orthogonal “postpreambles” is considered as explained in Section 2.5.2. For easier understanding, for each “postpreamble” sequence, there is a corresponding colour as shown in Figure 2.7.

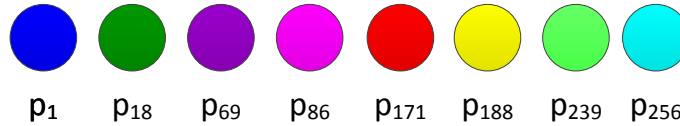


Figure 2.7: Set of “postpreambles” / colours.

If there are five tags transmitting in one slot, the following scenarios are possible:

Scenario 1: All tags involved in a collision have different/unique colours (different mutually orthogonal “postpreambles”). The probability of this scenario is:

$$P_{1+1+1+1+1} = \frac{8 \cdot 7 \cdot 6 \cdot 5 \cdot 4}{8^5} = 0.2051. \quad (2.13)$$

Scenario 2: Two out of five active tags have the same colour while the other three are different, with probability:

$$P_{2+1+1+1} = \frac{\binom{5}{2} \cdot 8 \cdot 7 \cdot 6 \cdot 5}{8^5} = 0.5127. \quad (2.14)$$

Scenario 3: Just one tag is having a distinct colour, the other four tags can be categorized

in two groups of two tags each with the same colour. The probability of this scenario is:

$$P_{2+2+1} = \frac{\binom{5}{2} \cdot \binom{3}{2} \cdot 8 \cdot 7 \cdot 6}{8^5} \cdot \frac{1}{2} = 0.1538. \quad (2.15)$$

Scenario 4: Two tags are having unique colours, while the other three are using the same colour:

$$P_{3+1+1} = \frac{\binom{5}{3} \cdot 8 \cdot 7 \cdot 6}{8^5} = 0.1025. \quad (2.16)$$

Scenario 5: Three tags are using the same colour while two tags are using an identical but different colour.

$$P_{3+2} = \frac{\binom{5}{3} \cdot \binom{2}{2} \cdot 8 \cdot 7}{8^5} = 0.0171. \quad (2.17)$$

Scenario 6: Only one tag has a distinct colour, the other four are identical.

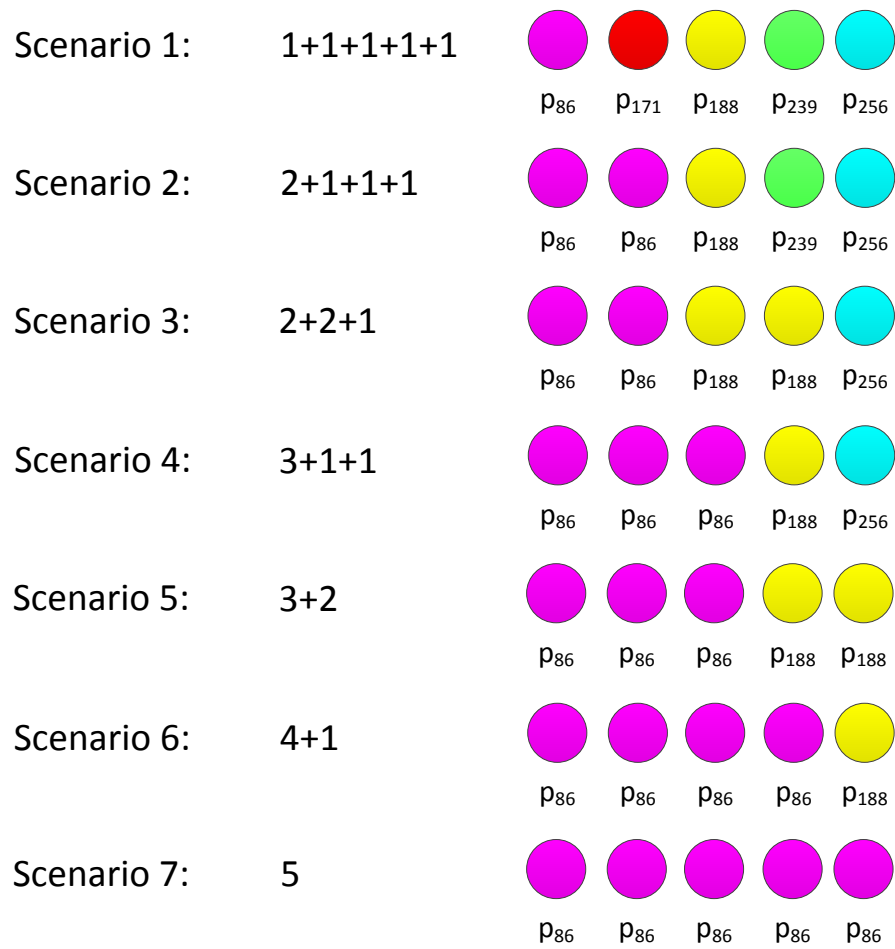
$$P_{4+1} = \frac{\binom{5}{4} \cdot 8 \cdot 7}{8^5} = 0.0085. \quad (2.18)$$

Scenario 7: All tags involved in the collision are using the same colour.

$$P_5 = \frac{\binom{5}{5} \cdot 8}{8^5} = 0.000242. \quad (2.19)$$

All scenarios for five tags transmitting in one slot are shown in Figure 2.8.

In Table 2.5, all scenarios are listed for up to eight tags colliding in one slot together with their probabilities assuming that eight tags per slot are the maximum that occurs. Based on the collision scenario, I propose the formula for calculating the probability when a set of C “postpreambles” is employed. The probabilities are calculated from a binomial distribution, taking into account the distribution of the “postpreambles” between collided tags. The collided set of tags is examined colour by colour. First, out of the total number of R colliding tags, tags with a common colour are chosen and so on. The numbers of the possible patterns are multiplied with all permutations of the “postpreamble” set and divided with the total number of possible patterns with the given set of “postpreambles” and R colliding tags. Furthermore, the obtained result is divided by the permutations of sets of tags with common colour, as shown in Equation (2.20):

Figure 2.8: Possible scenarios with $R = 5$ tags.

$$P_{s_l}(R) = \frac{\prod_{d=1}^D \binom{R - \sum_k R_k^{cc}}{R_d^{cc}} C!}{C^R \cdot (C - (D + U))!} \prod_{e=2}^R \frac{1}{S(e)!}, \quad (2.20)$$

where C is the number of “postpreambles” in a set (in this application $C = 8$ is selected), D denotes the number of “colliding” colours and R_d^{cc} represents the number of tags with the same colour for $d = 1, \dots, D$. Additionally, U is the number of “unique” colours. The values of D , U and R_d^{cc} for $d = 1, \dots, D$ are determined based on the corresponding scenario s_l ($l = 1, 2, \dots, S_l(R)$) as detailed in Table 2.5.

The remaining term, $S(e)$ is calculated as:

$$S(e) = \sum_{d=1}^D \mathbf{1}(R_d^{cc} = e), \quad e = 1, 2, \dots, R. \quad (2.21)$$

Here, $e = 1, \dots, R$ denotes the number of tags with the same colour and $\mathbf{1}(\cdot)$ is an indicator function:

$$\mathbf{1}(x) = \begin{cases} 1 & ; \text{if } x \text{ is true} \\ 0 & ; \text{else} \end{cases}. \quad (2.22)$$

Take for example, six tags transmitting in one slot; then $R = 6$ and just one tag is having a distinct colour $U = 1$, two tags are using the same colour $R_1^{cc} = 2$, and three tags have an identical but different colour $R_2^{cc} = 3$. Thus, the number of colliding colours is $D = 2$. In Table 2.5 this is Scenario 6 (3+2+1).

Each column of Table 2.5 lists various collision scenarios given a collision of R tags and each row of Table 2.5 represents a different collision scenario. In the first row of the table, Scenario 1 is listed. Here, all tags involved in a collision have a different “postpreamble”. In the second row Scenario 2 is found, where two out of all colliding tags have the same “postpreamble” while others have a different one, and so on. Thus, for $R = 2$ tags active in one slot, there are $S(R = 2) = 2$ scenarios, for $R = 3$ the number of scenarios is $S(R = 3) = 3$, for $R = 4$, the number is $S(R = 4) = 5$, and so on. The numbers in Table 2.5 represent the combination of tags with the same “postpreamble”. Indicated by the green colour are tags that can be successfully decoded due to their occurrence of a unique colour. Furthermore, the digit “2” in blue colour denotes those tags with a single occurrence of the same “postpreamble” that can be decoded by the projection method (Scenario 2) as will be explained in Section 2.7.2.

Table 2.5: Collision scenarios for up to eight colliding tags per slot.

S	R = 1	R = 2	R = 3	R = 4	R = 5	R = 6	R = 7	R = 8
u	$P_{s1} = 1$ 1	$P_{s1} = 0.875$ 1 + 1	$P_{s1} = 0.656$ 1 + 1 + 1	$P_{s1} = 0.410$ 1 + 1 + 1 + 1	$P_{s1} = 0.205$ 1 + 1 + 1 + 1 1	$P_{s1} = 0.077$ 1 + 1 + 1 + 1 1 + 1	$P_{s1} = 0.019$ 1 + 1 + 1 + 1 1 + 1 + 1	$P_{s1} = 0.002$ 1 + 1 + 1 + 1 1 + 1 + 1 + 1
M i x e d S c e n a r i o s		$P_{s2} = 0.125$ 2	$P_{s2} = 0.328$ 2 + 1	$P_{s2} = 0.492$ 2 + 1 + 1	$P_{s2} = 0.513$ 2 + 1 + 1 + 1	$P_{s2} = 0.385$ 2 + 1 + 1 1 + 1	$P_{s2} = 0.202$ 2 + 1 + 1 1 + 1 + 1	$P_{s2} = 0.067$ 2 + 1 + 1 1 + 1 + 1 + 1
			$P_{s3} = 0.016$ 3	$P_{s3} = 0.041$ 2 + 2	$P_{s3} = 0.154$ 2 + 2 + 1	$P_{s3} = 0.288$ 2 + 2 + 1 1	$P_{s3} = 0.337$ 2 + 2 + 1 1 + 1	$P_{s3} = 0.252$ 2 + 2 + 1 1 + 1 + 1
				$P_{s4} = 0.055$ 3 + 1	$P_{s4} = 0.103$ 3 + 1 + 1	$P_{s4} = 0.019$ 2 + 2 + 2	$P_{s4} = 0.084$ 2 + 2 + 2 1	$P_{s4} = 0.168$ 2 + 2 + 2 1 + 1
				$P_{s5} = 0.002$ 4	$P_{s5} = 0.017$ 3 + 2	$P_{s5} = 0.128$ 3 + 1 + 1 1	$P_{s5} = 0.112$ 3 + 1 + 1 1 + 1	$P_{s5} = 0.011$ 2 + 2 + 2 2
					$P_{s6} = 0.009$ 4 + 1	$P_{s6} = 0.077$ 3 + 2 + 1	$P_{s6} = 0.168$ 3 + 2 + 1 1	$P_{s6} = 0.067$ 3 + 1 + 1 + 1 1 + 1
					$P_{s7} = 2 \cdot 10^{-4}$ 5	$P_{s7} = 0.002$ 3 + 3	$P_{s7} = 0.017$ 3 + 2 + 2	$P_{s7} = 0.224$ 3 + 2 + 1 1 + 1
						$P_{s8} = 0.019$ 4 + 1 + 1	$P_{s8} = 0.112$ 3 + 3 + 1	$P_{s8} = 0.084$ 3 + 2 + 2 1
						$P_{s9} = 0.003$ 4 + 2	$P_{s9} = 0.028$ 4 + 1 + 1 1	$P_{s9} = 0.028$ 3 + 3 + 1 1
						$P_{s10} = 0.001$ 5 + 1	$P_{s10} = 0.017$ 4 + 2 + 1	$P_{s10} = 0.006$ 3 + 3 + 2
						$P_{s11} = 3 \cdot 10^{-5}$ 6	$P_{s11} = 0.001$ 4 + 3	$P_{s11} = 0.028$ 4 + 1 + 1 1 + 1
							$P_{s12} = 0.003$ 5 + 1 + 1	$P_{s12} = 0.042$ 4 + 2 + 1 1
							$P_{s13} = 6 \cdot 10^{-4}$ 5 + 2	$P_{s13} = 0.004$ 4 + 2 + 2
							$P_{s14} = 2 \cdot 10^{-4}$ 6 + 1	$P_{s14} = 0.006$ 4 + 3 + 1
							$P_{s15} = 4 \cdot 10^{-6}$ 7	$P_{s15} = 1 \cdot 10^{-4}$ 4 + 4
								$P_{s16} = 0.006$ 5 + 1 + 1 + 1
								$P_{s17} = 0.003$ 5 + 2 + 1
								$P_{s18} = 2 \cdot 10^{-4}$ 5 + 3
								$P_{s19} = 6 \cdot 10^{-4}$ 6 + 1 + 1
								$P_{s20} = 9 \cdot 10^{-5}$ 6 + 2
								$P_{s21} = 3 \cdot 10^{-5}$ 7 + 1
								$P_{s22} = 5 \cdot 10^{-7}$ 8

2.7 Tag Signal Recovery

Let me first consider an example by which I will explain how the proposed successive interference canceller with the projection concept typically works. In case when $R = 4$ tags are colliding and two colliding tags have the same colour while the others have different unique colours (Scenario 2) the vector of the signals received by $N_{\text{RA}} = 2$ antennas is:

$$\begin{bmatrix} \mathbf{r}_1^{pp}(t) \\ \mathbf{r}_2^{pp}(t) \end{bmatrix} = \begin{bmatrix} h_{1,1} & h_{1,2} & h_{1,3} & h_{1,4} \\ h_{2,1} & h_{2,2} & h_{2,3} & h_{2,4} \end{bmatrix} \begin{bmatrix} \mathbf{p}_a \\ \mathbf{p}_b \\ \mathbf{p}_c \\ \mathbf{p}_c \end{bmatrix} + \begin{bmatrix} \mathbf{n}_1(t) \\ \mathbf{n}_2(t) \end{bmatrix}, \quad (2.23)$$

where $\mathbf{r}_1^{pp}(t)$ and $\mathbf{r}_2^{pp}(t)$ are parts of the received signals containing the “postpreamble” from Antenna 1 and Antenna 2, respectively.

In this scenario, Tag 3 and Tag 4 share the same “postpreamble”, \mathbf{p}_c , and an LS channel estimation technique from Section 2.5.3 cannot be used. To overcome this situation, I propose a collision recovery procedure that consists of two phases. The first phase is performed by a successive interference cancellation (SIC) and the second is a projection of the constellation into the orthogonal subspace of the interference.

2.7.1 Successive Interference Cancellation

The successive interference cancellation [42] is used to take out the signals from the tags with unique colours. It is assumed that colliding tags are perfectly synchronized. The block diagram of the SIC architecture is shown in Figure 2.9. First, the channel is estimated based on the part of the received signal with “postpreambles” and the set of “postpreambles” \mathbf{S}_M . An LS estimator is employed as explained in Section 2.5.3.

After obtaining the channel estimation, the strongest tag signal is selected. The strongest tag signal corresponds to the strongest channel coefficient found as the maximum of $\|\hat{\mathbf{H}}\|_F^2$, where $\|\cdot\|_F^2$ denotes the Frobenius norm. In this search, the signals from tags with the same “postpreambles” are ignored. Furthermore, with an MMSE receiver from Section 2.4.2, $\mathbf{a}_{\text{MMSE}}(t)$ is extracted.

Later on, the signal from the strongest tag is remodulated and subtracted from the received signal:

$$\bar{r}_i(t) \leftarrow \bar{r}_i(t) - \hat{h}_{ij} \hat{a}_j(t). \quad (2.24)$$

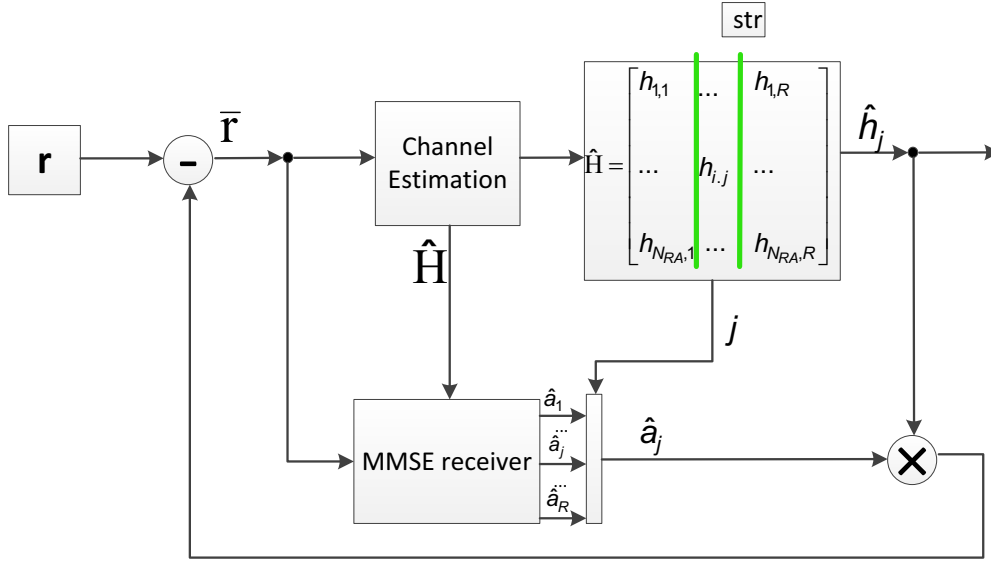


Figure 2.9: Block diagram of successive interference cancellation architecture.

Here, j denotes the signal from the strongest tag and i represents the index of the receive antenna. In vector form:

$$\bar{\mathbf{r}}(t) \leftarrow \bar{\mathbf{r}}(t) - \hat{\mathbf{h}}_j \hat{a}_j(t), \quad (2.25)$$

and $\hat{\mathbf{h}}_j = [\hat{h}_{1j}, \dots, \hat{h}_{ij}, \dots, \hat{h}_{N_{RA}j}]^T$ is the column vector of channel coefficients between reader, strongest tag j and receive antennas $i = 1, \dots, N_{RA}$. In this way, the received signal is cleaned from the influence of the strongest tag and that signal is used as the input signal for the next iteration, together with the set of “postpreambles” without the “postpreamble” of the strongest tag. In each iteration the channel coefficients are re-estimated. As an output, the signal from the strongest tag is obtained and the channel coefficients that correspond to that tag are stored.

In-phase/quadrature (IQ) diagrams of a received signal at antennas 1 and 2, when four tags are colliding, are presented in Figure 2.10. Here, it is difficult to detect states due to the superposition of many tag signals. During the successive interference cancellation, the signals from tags with a unique “postpreamble” are taken out. The remaining signal, after SIC, consists of the signals from the tags with the same “postpreamble”, Tag 3 and Tag 4, whose IQ diagrams are shown in Figure 2.11. The channel coefficients that correspond to this signals are estimated by a projection of the constellation into the orthogonal subspace of the interference from [23].

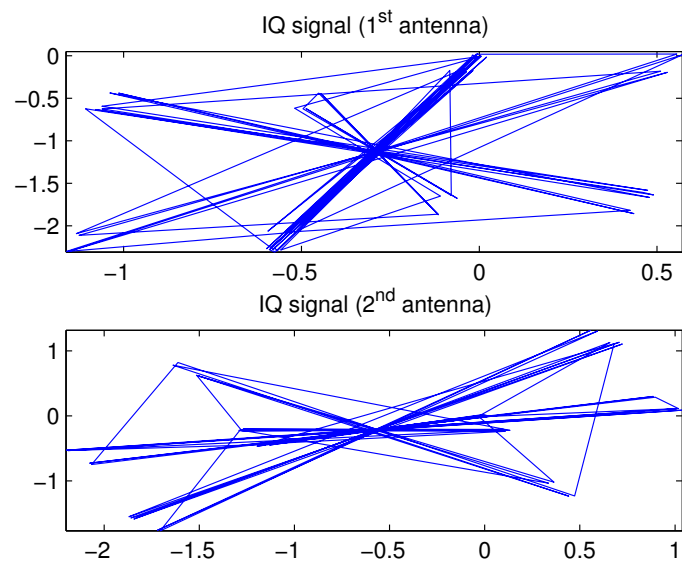


Figure 2.10: IQ diagram of the received signal from Tag 1 to Tag 4 at Antenna 1 and Antenna 2.

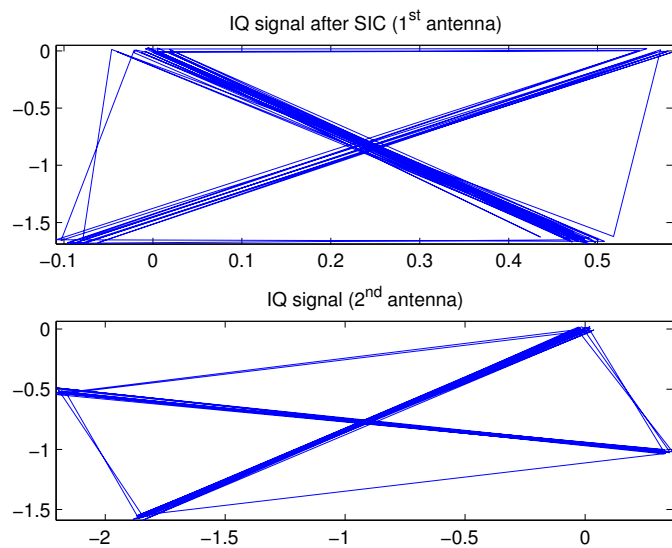


Figure 2.11: IQ diagram of the remaining signals (Tag 3 and Tag 4) at Antenna 1 and Antenna 2, after SIC.

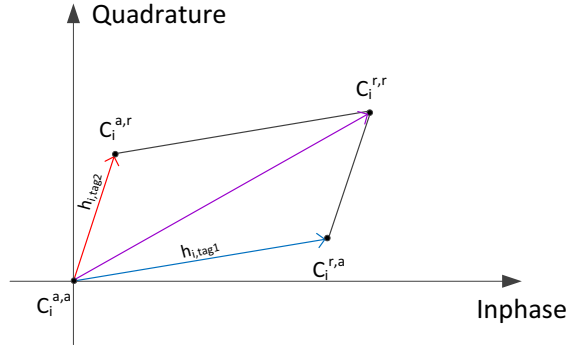


Figure 2.12: IQ diagram of the received signal.

2.7.2 Channel Estimation with Projections

An IQ diagram of a received signal with two colliding tags, in absence of noise and with a perfectly cancelled carrier leakage is shown in Figure 2.12. Hence, theoretically, $2^{R=2} = 4$ states in the IQ diagram should be distinguishable, since the signal after SIC consists of the signals originating from two tags. According to the EPCglobal standard for UHF RFID [5], a tag response to the *Query* command begins with a defined preamble shown in Figure 2.4. Thus, during such preamble, all tags modulate the same bits and the state when tags are reflecting can be estimated:

$$\hat{C}_i^{r,r} = \max_k \{r_i[k]\}_{t_{1bit}}, \quad (2.26)$$

where $r_i[k]$ is the sample of the received signal from antenna i taken within duration of the first preamble bit t_{1bit} . Thus, the reflecting state of both tags is found as a state with the highest level of the received signal, obtained within durations of the first preamble bit when both tags reply with bit "1", as shown in Figure 2.4.

The preamble consists just of bits 1 and 0 and during its duration, tags are moving between states $\hat{C}_i^{r,r}$ and $\hat{C}_i^{a,a}$ (subspace C_S). State $\hat{C}_i^{a,a} = E\{r_i[k]\}_T$ is determined as the average value of the received signal over time period T before the tag response. Since a perfect isolation of the transmit and receive part of the reader is assumed, the absorbing state $C_i^{a,a}$ of both tags is depicted in the coordinate origin of Figure 2.12. After the preamble, a "postpreamble" and an RN16 are transmitted, and the realization of the remaining states happens when tags modulate different data. This states are estimated as the points with the maximal signal strength in the subspace $C_{i\perp}^{r,r}$ orthogonal to $C_i^{r,r}$ [23]:

$$\hat{C}_i^{a,r} = \max_k \{r_{i\perp}[k]\}, \quad \hat{C}_i^{r,a} = \min_k \{r_{i\perp}[k]\}, \quad (2.27)$$

and $r_{i\perp}[k]$ is the signal component located in the subspace $C_{r\perp}$.

Since the modulation signals are on-off keying, the channel coefficients are:

$$\hat{h}_{i,1} = \hat{C}_i^{r,r} - \hat{C}_i^{a,r}, \quad \hat{h}_{i,2} = \hat{C}_i^{r,r} - \hat{C}_i^{r,a}, \quad (2.28)$$

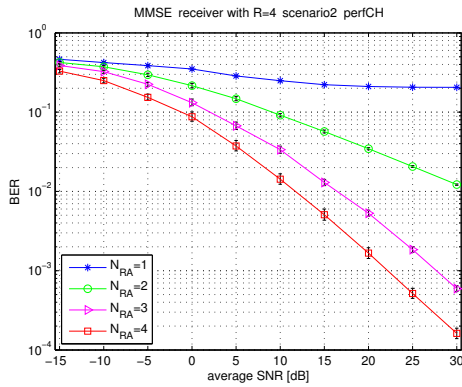
With this, the channel estimation procedure is completed and with the use of an MMSE receiver from Equation (2.9), the tag signals are extracted. In general, the signal that remains after SIC is formed of signals from tags with the same “postpreambles” which are disturbed with the channel, noise and errors accumulated through SIC. Due to this disturbances and errors, these states sometimes cannot be determined correctly.

2.7.3 Results

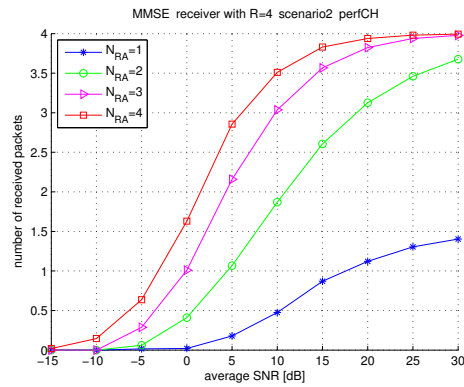
The performance of the proposed collision recovery is analysed through MATLAB simulations. In Figure 2.13a-Figure 2.13f, the obtained results for the MMSE receiver with different types of channel knowledge in the case of four tags ($R = 4$) transmitting in one slot are shown. Here, Scenario 2 from Table 2.5 is investigated with one pair of the tags with the same colour and two unique coloured tags (2+1+1). Figure 2.13a shows the BER of the receiver with perfect channel knowledge. With perfect knowledge of the channel coefficients, the “postpreamble” distribution does not have any influence on performance, as expected. In Figure 2.13b, the average NSRP per slot for different number of receiving antennas on the reader is presented. In the case of four tags transmitting in the same slot with two receive antennas, on average more than 3.6 packets can be successfully received at $\overline{\text{SNR}} = 30\text{dB}$. These two graphs will serve as an indicator of the highest achievable performance of the designed system.

Figure 2.13c and Figure 2.13d present results in the case of an LS channel estimation. Since here, two out of four tags are using the same sequence, the channel cannot be estimated properly and the MMSE receiver cannot resolve collisions. The BER curves are saturated at high error values and it seems that all packets are affected with errors. However, average NSRP values show that with the receiver that has more than one receive antenna, on average more than two packets can be received correctly. This is due to the fact that errors are mostly in packets from tags with the same “postpreambles” while the packets from other two tags are less affected with errors during the channel estimation process.

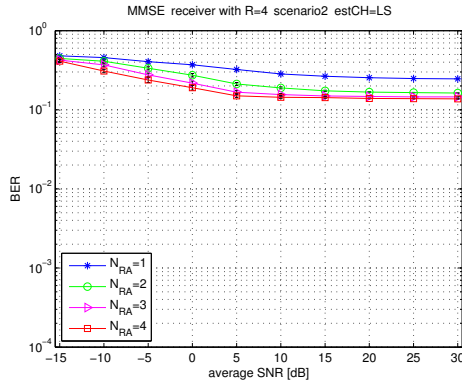
The performance of the RFID reader with proposed collision recovery through successive interference cancellation and projection of the constellation into the orthogonal subspace of the interference are shown in Figures 2.13e and 2.13f. It can be observed that by using the proposed method with two receive antennas, the collision of four tags is resolvable,



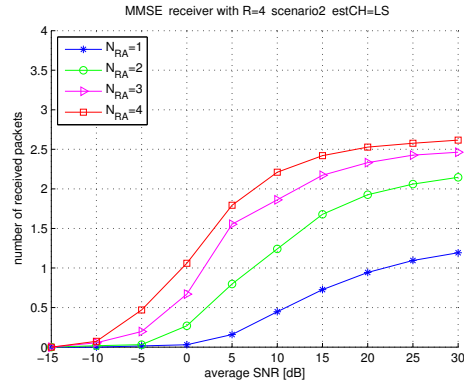
(a) BER over SNR (perf. ch)



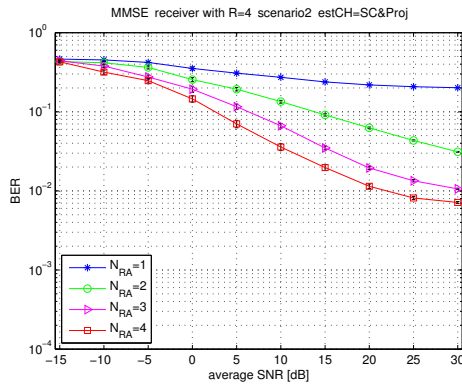
(b) NSRP over SNR (perf. ch)



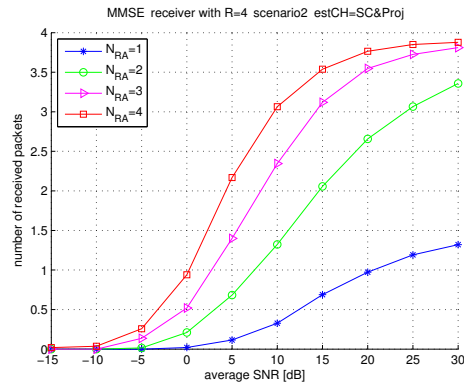
(c) BER over SNR (est. ch LS)



(d) NSRP over SNR (est. ch LS)



(e) BER over SNR (est. ch SIC Proj)



(f) NSRP over SNR (est. ch SIC Proj)

Figure 2.13: MMSE receivers $R = 4$, collision scenario: 2+1+1).

performances are comparable to the results obtained with perfect channel knowledge and on average more than 3.4 packets are received. However, by increasing the number of receiving antennas on the reader side, the BER curves are not following the trend of the reader with perfect channel knowledge. This is due to the fact that the performance

cannot be increased with this method after the necessary number of receiving antennas $N_{RA} = \frac{M}{2}$ is increased.

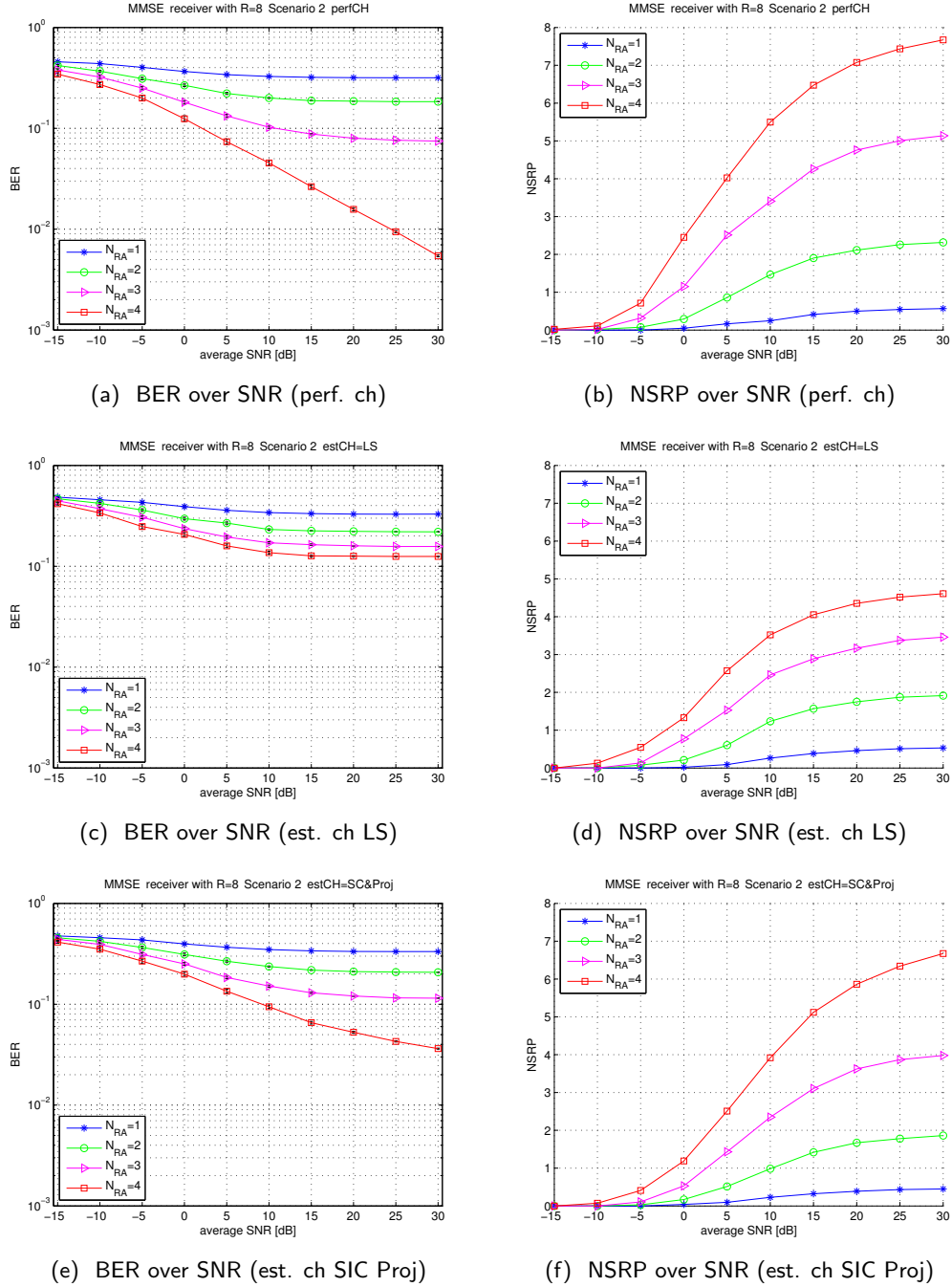


Figure 2.14: MMSE receivers $R = 8$, collision scenario: 2+1+1+1+1+1+1).

Additionally, simulation results for an extreme eight tag scenario are presented in the following. In this scenario two out of eight colliding tags have identical colour and the

remaining six tags have unique colours ($2 + 1 + 1 + 1 + 1 + 1 + 1$). Thus, these tags are expected to be resolved. In Figures 2.14a - 2.14f, the results for the MMSE receiver with up to four receive antennas ($N_{RA} = 1, 2, 3, 4$) are shown. Figures 2.14a and 2.14b represent BER and NSRP results, respectively, obtained by receivers with perfect channel knowledge. For these receivers channel estimation is not performed and the “postpreamble” distribution does not have any influence. Thus, there is no decrease in the system performance and they will be used as an reference to the highest achievable performance of the designed system.

Results obtained with the receivers that apply an LS channel estimation method instead are shown in Figures 2.14c and 2.14d, for BER and NSRP, respectively. It can be observed that since two out of eight colliding tags have the same “postpreamble”, the channel cannot be estimated correctly by an LS estimator and the MMSE receiver cannot recover from this collision. The BER curves are saturating at high values. Nevertheless, some packets are decoded correctly as the NSRP curves show that in average more than four packets can be correctly received with four antenna receivers ($N_{RA} = 4$). Hence, the errors are mostly concentrated in packets from tags with the same “postpreamble”, while the packets from the other six tags are less affected.

In Figures 2.14e and 2.14f, the results are presented, obtained from the proposed smart receiver with the two phase channel estimation and collision recovery. Even though the BER values are significantly higher when compared to the reader with perfect channel knowledge, the performances in NSRP are comparable. It can be observed that a reader with four receive antennas can successfully recover from this collision and in average can successfully receive almost seven packages.

2.8 Discussion and Conclusion

In this chapter, it is shown that with the proposed design of RFID reader it is possible to recover from collisions that have a number of tags two times higher than the number of receiving antennas. The channel model for two receiving antennas and two tags, already proposed in [23], is extended to a more general case. Simulation results for the optimal ZF and the MMSE receivers, which are able to resolve collisions of up to eight tags, are presented. The throughput increase of FSA RFID systems with physical layer collision recovery receivers is identified. In the performed analysis, it is assumed that the transmit and the receive part of a reader are perfectly isolated and that all carrier leakage is perfectly cancelled. Several carrier leakage cancellation techniques were proposed and evaluated in [43–49].

Furthermore, a method for channel estimation in collision scenarios is proposed. In the proposed method the tag signal is modified by adding a “postpreamble”, and the channel is estimated with a simple LS estimator. The influence of the estimated channel on the performance is investigated by simulations. The obtained results show that the

proposed method provides excellent results in comparison to perfect channel knowledge. There is not a significant decrease of the performance and still it is possible to recover from a collision as long as the number of tags is not larger than two times the number of receiving antennas at the reader. In [50], Ahmed et al. have proven the functionality of a set of sequences that contains “postpreambles” by means of a hardware demonstrator. Furthermore, I’ve investigated the performance of the proposed method with a linear minimum mean-square error (LMMSE) estimator [51, 52]. However, no further improvement is observed. Thus, there was no need to employ more complex estimators. Additionally, a collision recovery procedure for recovering from collision in which two of the colliding tags have the same “postpreamble”, i.e., the part of the signal used for channel estimation, is proposed. In the proposed method, first successive interference cancellation is performed during which the signals of tags with unique “postpreamble” are taken out. After that, the signal composed of tags with the same “postpreamble” remains. This collision is resolved with the projection of the constellation into the orthogonal subspace of the interference. The obtained results show that the proposed method provides satisfactory results. However, in order to employ the proposed SIC, perfect alignment of collided tag signals is required. Aside from that it is required that the tag signals have the same duration. However, these requirements are not fulfilled in practice. Recent papers have proposed special base functions to solve this problem [53, 54].

3 POSTPROCESSING BEAMFORMING

In order to approach the theoretical maxima, it is necessary to improve the collision recovery process, to make collisions less destructive and to resolve more tags from a collision. In this chapter, a relatively simple method that does not require any changes in the standard and can make collisions less destructive and resolve more colliding tags is proposed. In the proposed method a postprocessing of the received signal by employing a beamformer is performed. In this way, different groups of tags, active in the same slot, are processed with different gain factors. The behaviour of the proposed method in the system with collision recovery factor $M = 8$ that is optimized for a modified tag signal as proposed in Section 2.5.2 is studied. The obtained results are compared with the performance of an EPC protocol compliant reader.

Furthermore, in this chapter, deviations from some optimal prior controlled simulations are considered and a random tag behaviour is addressed. Tags randomly choose a slot for transmission, thus, the number of colliding tags can exceed M . Furthermore, in order to evaluate the proposed spatial filtering and to separately process signals coming from different angles of arrival, a geometrical channel model is employed for describing the influence of the multi antenna environment.

Moreover, in order to further increase the system throughput I propose a spatial filter that forms deep notches, or even a “stopband”, in certain range of angles and in that way decreases the number of colliding tags. With this, the reader becomes more robust, and can deal with even more than M colliding tags. Additionally, a semi-analytical formula for calculating the optimal frame size by taking into account spatial filter properties and the throughput is derived. Lastly, the influence of the proposed method is investigated and the results are compared with the performance of a conventional reader.

3.1 Geometrical Channel Model

The channel model, described in Section 2.2 is not convenient for the analysis of the performances of the reader with a beamformer. In order to employ spatial filtering of the received signal the use of a geometrical channel is more suitable.

Here, RFID multi-antenna system is composed of a reader with one transmit $N_{TA} = 1$ and four receive $N_{RA} = 4$ antennas. The receive antennas are organised as uniform linear array with separation of $d_s = \frac{\lambda}{2}$. My focus is on passive UHF RFID systems

operating at $f = 866$ MHz, thus, the corresponding antenna separation is $d_s = 0.17$ m. Furthermore, the Fraunhofer distance [55] that gives the limit between near and far field is $d_{n/f} \approx \frac{2D_r^2}{\lambda} = 1.56$ m, where $D_r = 3\frac{\lambda}{2}$ is the largest dimension of the radiator.

Figure 3.1 shows a communication between the reader and N tags. The solid lines denote the channels between the reader's transmit antenna and tags that are active in one slot, the forward channels. The channels between active tags and reader's receive antennas, the backward channels, are shown as dashed lines. Both channels are modelled as a geometrical line-of-sight (LOS) channel, with path loss and phase shift. A forward channel coefficient is:

$$h_j^f = \frac{\lambda}{4\pi d_j^f} e^{-j\frac{2\pi}{\lambda} \cdot \mathbf{u} \cdot \mathbf{p}_j'}, \quad (3.1)$$

where d_j^f is the distance between the reader's transmit antenna and tag j , \mathbf{u} denotes the unit vector $\mathbf{u} = [-\sin(\phi)\cos(\theta), -\sin(\phi)\sin(\theta), -\cos(\phi)]$ [56] and \mathbf{p}_j is the position vector $\mathbf{p}_j = [x - x_j, y - y_j, z - z_j]$. Here, the reader's transmit antenna has coordinates (x, y, z) , tag j is placed at (x_j, y_j, z_j) and ϕ and θ denote elevation and azimuth as shown in Figure 3.2. A backward channel coefficient is:

$$h_{i,j}^b = \frac{\lambda}{4\pi d_{i,j}^b} e^{-j\frac{2\pi}{\lambda} \cdot \mathbf{u} \cdot \mathbf{p}_{i,j}'}. \quad (3.2)$$

Here, $d_{i,j}^b$ denotes the distance between tag j and reader's receive antenna i with coordinates (x_i, y_i, z_i) , and correspondingly the position vector is $\mathbf{p}_{i,j}' = [x_j - x_i, y_j - y_i, z_j - z_i]$. The total channel is obtained as the multiplication of a forward channel and a backward channel $h_{i,j} = h_j^f \cdot h_{i,j}^b$ as explained in Section 2.2.

3.2 FFT Beamforming

A simple postprocessing of the received signal is proposed here in order to amplify the signal level of some colliding tags and to attenuate of the others. In this way, an artificial "near/far" effect is created which helps the receiver to hear some tags, from certain directions/sectors, better than tags from other directions. Thus, a spatial filter/beamformer is applied in the postprocessing.

The simplest way to generate a fixed beamforming is with the modified Fast Fourier Transform (FFT) algorithm as described in [57]. This algorithm forms the same number of equally spaced beams/sectors as the number of elements of a linear array.

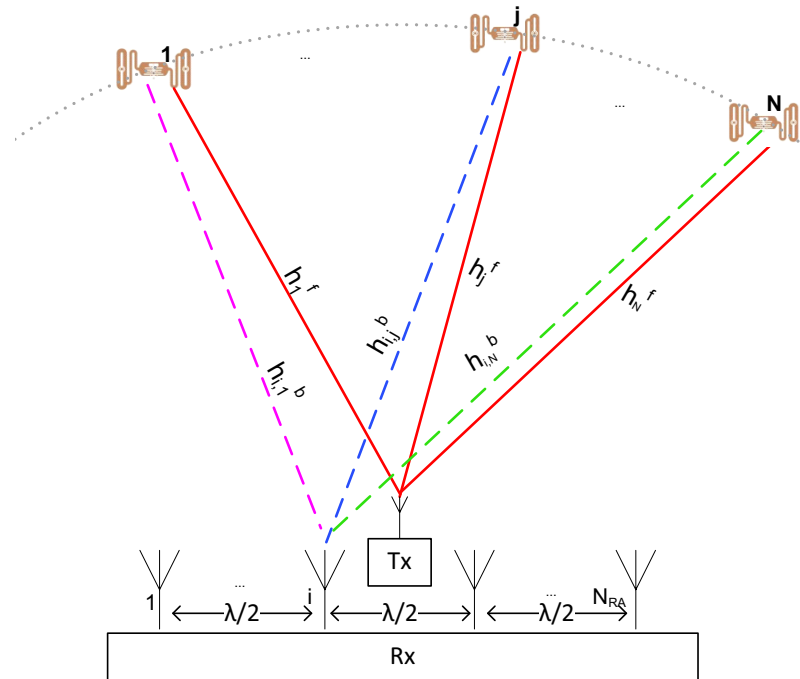


Figure 3.1: Communication between the RFID multi-antenna reader and N tags.

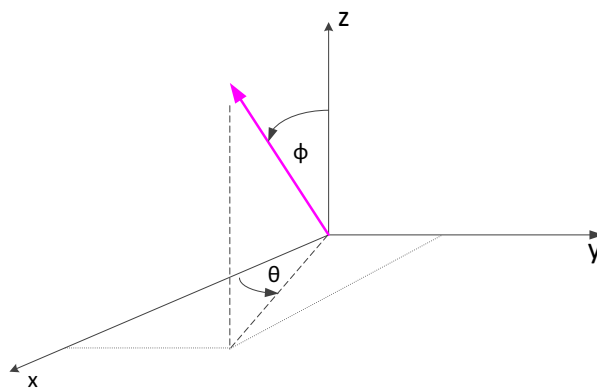


Figure 3.2: Azimuth and elevation.

3.2.1 FFT Weights

The factors of the spatial beams are generated as:

$$\text{AF}(\phi, \theta) = \mathbf{w}^H \mathbf{v}(\phi, \theta) \mathbf{g}(\phi, \theta), \quad (3.3)$$

where \mathbf{w} denotes the weights of the sector, $\mathbf{v}(\phi, \theta)$ is the steering vector and $\mathbf{g}(\phi, \theta)$ is the antenna pattern of a single array element. The array manifold vector is calculated as [56]:

$$\mathbf{v}(\phi, \theta) = e^{-j \frac{2\pi}{\lambda} \mathbf{a} \mathbf{p}'}. \quad (3.4)$$

Here, $\mathbf{p} \in \mathbb{R}^{N_{\text{RA}} \times 3}$ denotes the position vector of antenna array elements.

Using a four point FFT, the weights are calculated as follows:

$$\mathbf{w} = \frac{1}{4} \begin{bmatrix} 1 & 1 & 1 & 1 \\ 1 & e^{-j \frac{\pi}{2}} & e^{-j \pi} & e^{-j \frac{3\pi}{2}} \\ 1 & e^{-j \pi} & e^{-j 2\pi} & e^{-j 3\pi} \\ 1 & e^{-j \frac{3\pi}{2}} & e^{-j 3\pi} & e^{-j \frac{9\pi}{2}} \end{bmatrix} \quad (3.5)$$

$$= \frac{1}{4} \begin{bmatrix} 1 & 1 & 1 & 1 \\ 1 & -j & -1 & j \\ 1 & -1 & 1 & -1 \\ 1 & j & -1 & -j \end{bmatrix}. \quad (3.6)$$

3.2.2 FFT Sectors

Let us assume for now that each antenna element is omnidirectional with $\mathbf{g}(\phi, \theta) = 1$, $\forall \phi \in [0, \pi]$ and $\forall \theta \in [0, 2\pi]$. The obtained sectors are shown in Figure 3.3.

In order to have a more realistic calculation of the spatial beam factors an antenna pattern should be included. A simplest 2D model of a patch antenna pattern is based on the cavity model [55]:

$$\mathbf{g}(\theta) = \frac{\sin\left(\frac{k_0 h_s}{2} \sin(\theta)\right)}{\frac{k_0 h_s}{2} \sin(\theta)} \cos\left(\frac{k_0 L_{\text{eff}}}{2} \cos \theta\right), \quad (3.7)$$

where $k_0 = \frac{2\pi}{\lambda}$ is the wave number, $L_{\text{eff}} = \frac{\lambda}{2\sqrt{\epsilon_r}}$ is the effective length of the patch antenna, ϵ_r is the relative permittivity of the dielectric, and h_s is the height of the substrate as denoted in Figure 3.4.

Figure 3.5 shows the sectors obtained by taking into account the pattern generated according to Equation (3.7).

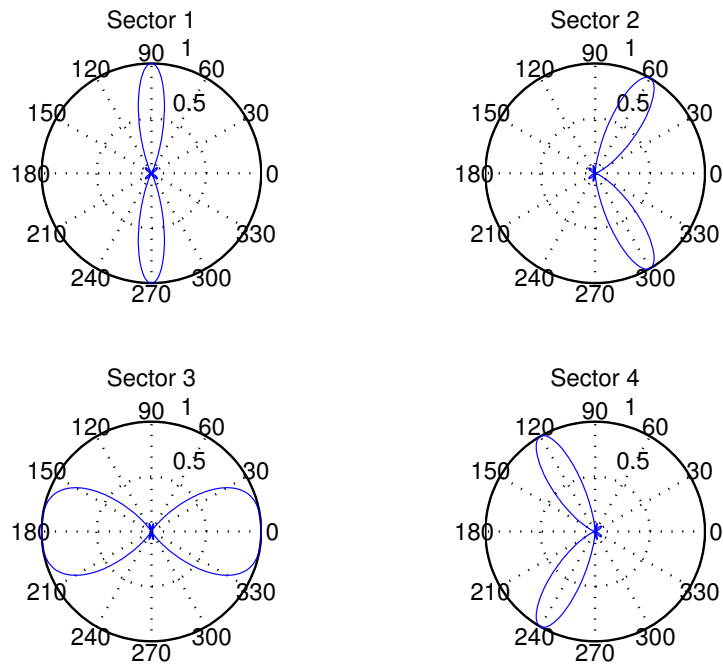


Figure 3.3: Sectors obtained by four point FFT weights.

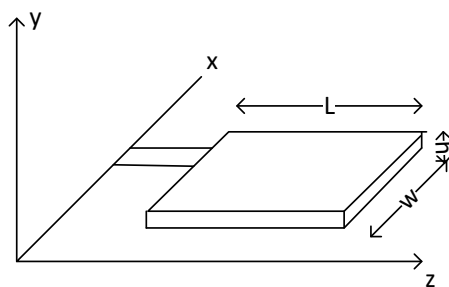


Figure 3.4: Rectangular patch antenna ($h = 0.1588$ cm, $\epsilon_r = 2.2$).

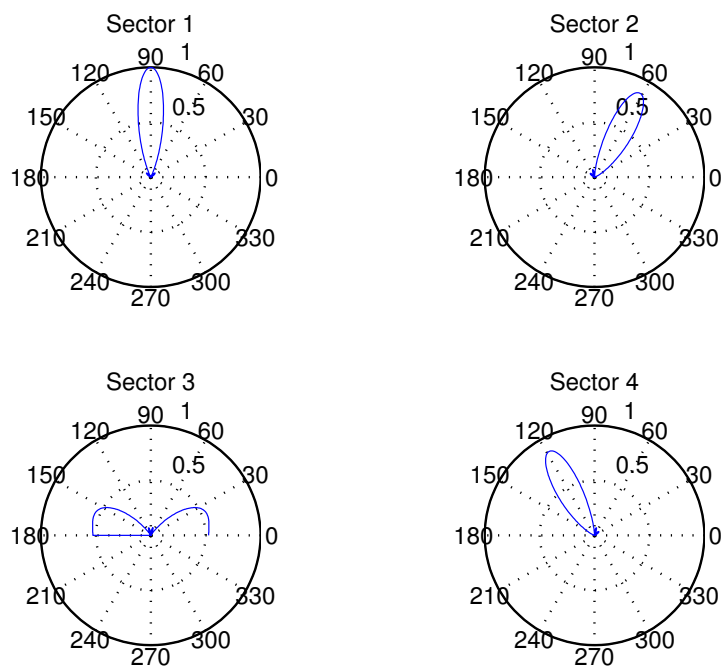


Figure 3.5: Sectors obtained by four point FFT weights and simple patch antenna pattern.

3.2.3 FFT Postprocessing

In order to evaluate the proposed collision recovery mechanism from Section 3.2.2 assume an RFID multi-antenna system that consists of one transmit and up to four receive antennas. Tags are distributed on a circular line in front of the reader as shown in Figure 3.1 on directions determined by $\theta \in [\frac{\pi}{6}, \frac{5\pi}{6}]$. Thus, all the tags are placed on the same distance from the reader's transmit antenna $d_j^f = 3\text{ m}$ for $\forall j = 1, \dots, N$. This means that all tag signals experience the same path loss and that the power of all colliding tags is the same at the receiver. The SNR has been averaged over the receive antennas and calculated as described in Section 2.4.3.

In this part, the performances of two different reader configurations are compared: a standard compliant reader with a single receive antenna and a reader with four receive antennas. With the first reader configuration, the performances of a reader without collision recovery capabilities $M = 1$ is evaluated. With the second reader configuration, the performance of the reader with a collision recovery factor $M = 8$ is investigated. In order to benefit from this collision recovery, the tag signal has been modified by adding a "postpreamble" as explained in Section 2.5.1. The 8-bit long "postpreamble" sequence is placed between the preamble and an RN16. In this way, the tag signal is extended and consequently, each slot is stretched $G = 1.364$ times. This modification also requires small changes in the standard. The reader performs collision recovery as described in Section 2.7.

Figure 3.6 shows the number of tags that are still left to be interrogated versus the number of slots in the case of readers with collision recovery factors $M = \{1, 8\}$. Receivers select optimal frame sizes: $\frac{F_{\text{opt}}}{N} = 1$ for a reader with $M = 1$ and $\frac{F_{\text{opt}}}{N} = 0.207$ for a reader with $M = 8$. When comparing the results for a conventional reader, obtained in the perfect LOS scenario with the results for the theoretical limits from Section 4.5.5, it can be observed that under LOS conditions the conventional reader is approaching its theoretical maximum. Moreover, the reader with collision recovery factor $M = 8$ is optimized to resolve collisions of up to eight tags and uses $N_{\text{RA}} = 4$ receive antennas. As described in Section 3.1, the receive antennas are separated by $\lambda/2$ thus, the signals received at different antennas are uncorrelated. However, since a total tag population of 1 000 is distributed along a circular line with the length $l = \frac{2d^f\pi}{2\pi} \cdot (\frac{5\pi}{6} - \frac{\pi}{6}) = 2\pi\text{ m}$, colliding tag signals have correlated channels with a high probability. This channel correlation leads to the lower performances of the reader with collision recovery factor $M = 8$ in the LOS setup, in comparison to the performances of the same reader in the double Rayleigh fading channel from Section 4.5.5 (listed in Table 4.14).

Figure 3.7 displays the result obtained with the offline spatial filtering of the received signal. This is achieved with the sectors defined in Section 3.2.2. Since this approach is expected to be beneficial in the case of colliding tags (due to an artificial "near/far" effect collisions can be made less destructive), the simulation is performed only for the receiver with collision recovery. The reader first employs the filters of Sector 1 and

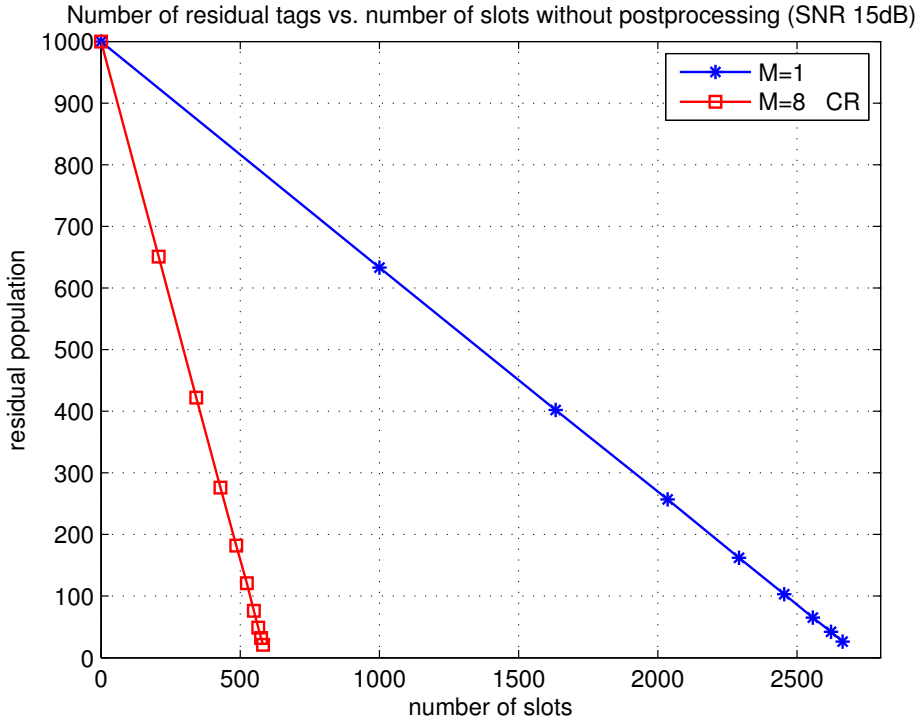


Figure 3.6: Number of residual tags vs. number of slots without postprocessing.

performs a collision recovery. In this way, colliding tags that are within the sector are amplified while other colliding tags are attenuated. The reader resolves some collisions while the rest is filtered with the filters of the next sectors and so on. As expected, with a postprocessing beamformer, the reader can resolve more collisions and read tags 9.77 times faster. By comparing Figure 3.6 and Figure 3.7, it is observed that with a postprocessing beamformer, the tags are read 2.08 times faster than when the reader, described in Chapter 2, with the same collision recovery factor but without postprocessing is employed.

3.2.4 Frame Optimization for FFT Postprocessing

Since with postprocessing beamforming, the reader became more robust and can resolve collisions more efficiently, the size of the frame can be shortened in order to evaluate the performances in the new circumstances. The new optimal frame size is calculated according to:

$$F_{\text{opt}}^{\text{new}} = \left(\frac{F_{\text{opt}}}{N} \right)^{\text{nop}} \cdot N^{\text{left}} \cdot \frac{1}{Q}, \quad (3.8)$$

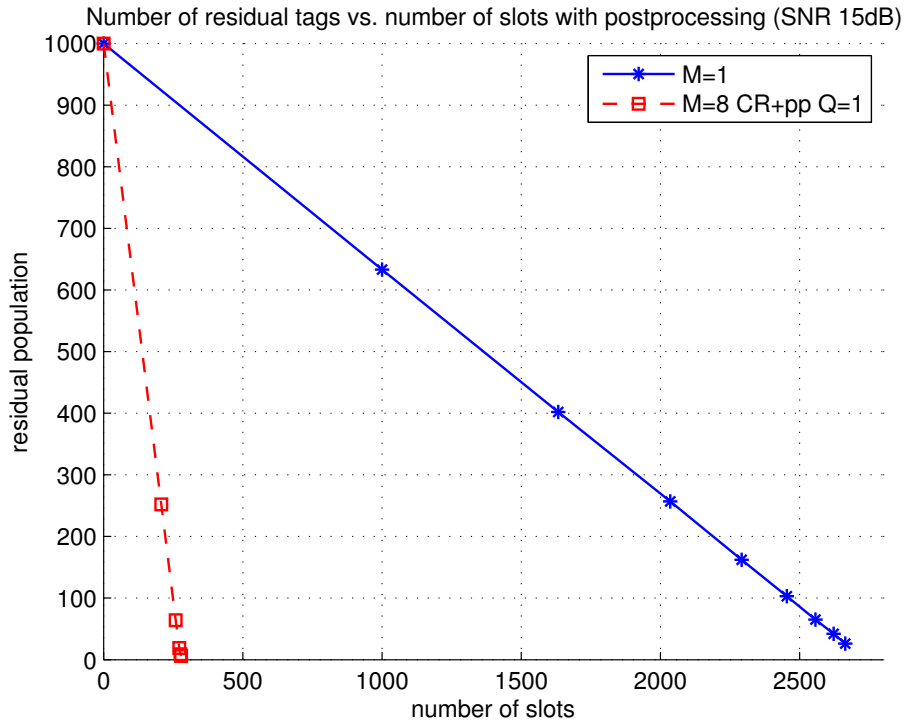


Figure 3.7: Number of residual tags vs. number of slots with postprocessing and $Q = 1$.

where N^{left} denotes the number of tags left for the next inventory round and Q is the so-called speed factor.

The results obtained for $Q = \sqrt{2}$ are displayed in Figure 3.8. Now, the new optimal frame size normalized to the residual tag population for a reader with a collision recovery factor $M = 8$ is 0.147. Thus, the new optimal frames contain less slots than optimal. This leads to a higher number of collisions $R \geq M$. However, by postprocessing beamforming the number of strongly colliding tags is decreased and collisions are resolved.

Furthermore, Figure 3.8 also depicts the result obtained for $Q = 2$. In this case normalized frame size is 0.104 for a reader with a collision recovery factor $M = 8$. For easier comparison results are listed in Table 3.1. It can be observed that if the speed factor Q is increased over a certain limit, the number of colliding tags will become too high and the proposed postprocessing beamforming cannot mitigate it as successfully as before. The number of strongly colliding tags within the sector increases over the collision recovery factor and the reader cannot resolve a collision. This leads to a longer interrogation time.

A comparative overview of the throughput versus averaged SNR for a reader with different collision recovery factors $M = 1$ and $M = 8$; with and without postprocessing is presented in Figure 3.9. The solid lines denote the reader without postprocessing.

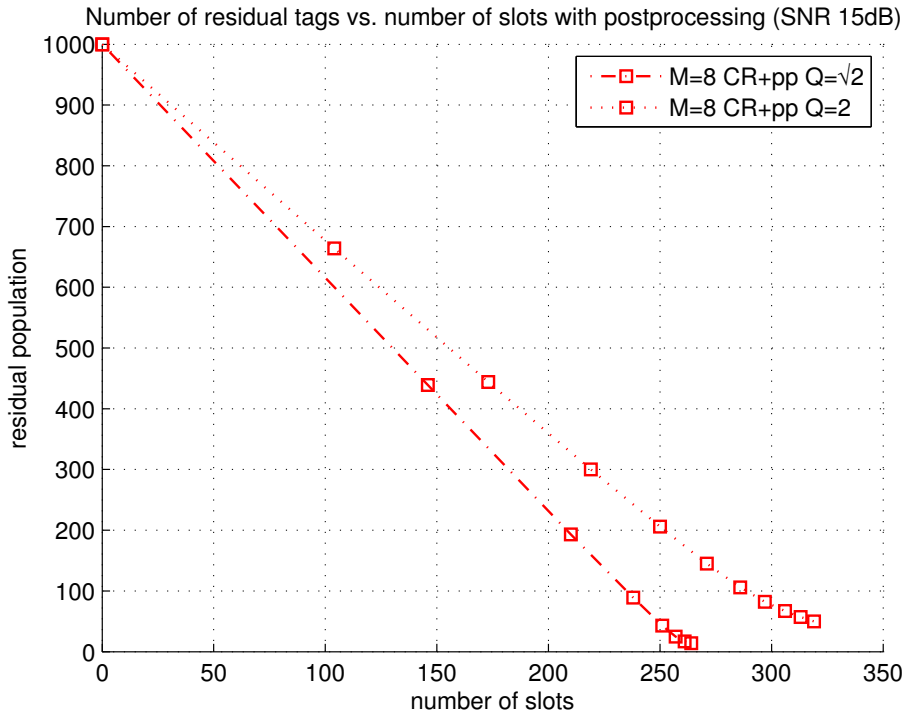


Figure 3.8: Number of residual tags vs. number of slots with postprocessing and $Q = \{\sqrt{2}, 2\}$.

Table 3.1: Number of slots elapsed with a collision recovery factor $M = \{1, 8\}$ at SNR=15 dB.

SNR=15 dB	$M = 1$	$M = 8$	$M = 8$ CR+PP		
			$Q = 1$	$Q = \sqrt{2}$	$Q = 2$
95%	2608	555	267	253	317
98%	2690	572	275	261	327
99.5%	2731	581	280	265	332

The dashed lines represent the reader that mitigates collisions by postprocessing beamforming and $Q = 1$. The dash-dot lines denote the reader with postprocessing and $Q = \sqrt{2}$. The reader with postprocessing and $Q = 2$ is represented by dotted lines. Around each point in Figures 3.9 and 3.10, a confidence interval that contains 95% of the obtained results is plotted to evaluate the quality of the simulations. It can be observed that for the lower SNR values the readers with $Q = 1$ have better performance. With increasing speed factor Q , frames become shorter and the number of colliding tags increases. However, at higher SNR values, readers become more robust and they can mitigate more successfully collisions with a higher number of tags. At SNR=15 dB the best performances are observed for $Q = \sqrt{2}$. In the case of a reader with collision recovery factor $M = 8$ and postprocessing achieves more than ten times higher throughput than a conventional reader.

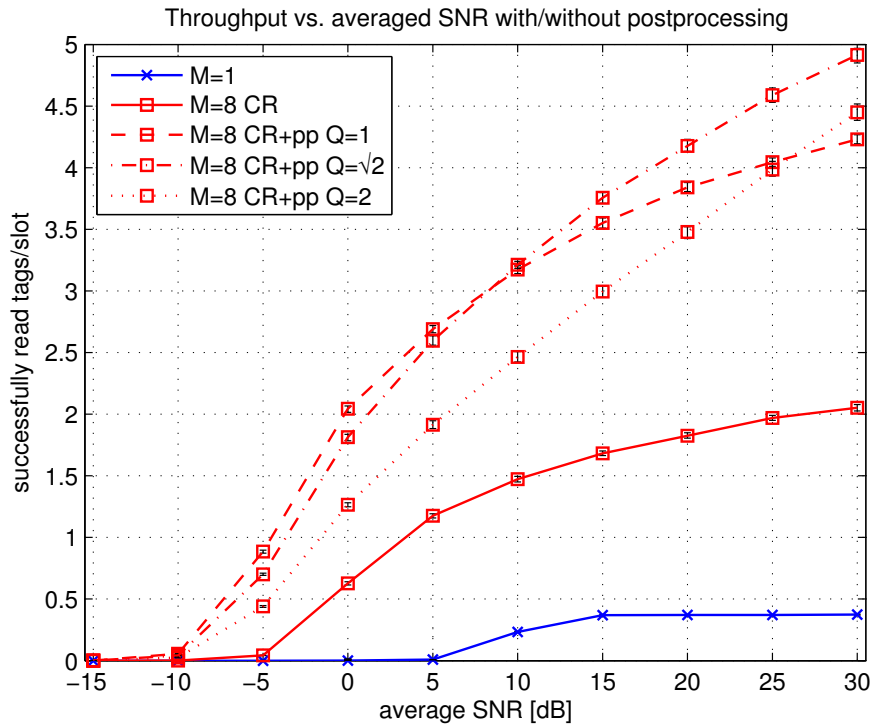


Figure 3.9: Throughput vs. averaged SNR for the reader with a collision recovery factor $M = \{1, 8\}$ with/without postprocessing.

A comparative overview of the number of slots for successfully reading 95% of the tag population versus speed factors Q is shown in Figure 3.10. The dashed lines denote the results obtained at SNR=15 dB, while the solid lines represent the results at SNR=30 dB. It can be observe for both curves that the optimal frame size is obtained for $Q \in [1, 2]$. For $Q \notin [1, 2]$ the number of slots in the frame is either too large or too small and with the receiver optimal performances are not achieved. Either the number of colliding

tags is below the reader's collision recovery factor and the potential of the reader is not fully used or the number of colliding tags is much higher and even with postprocessing, collisions cannot be mitigated collisions. The optimal speed for a reader with collision recovery factor $M = 8$ is $Q = 1.35$ at SNR=15 dB and $Q = 1.6$ at SNR=30 dB.

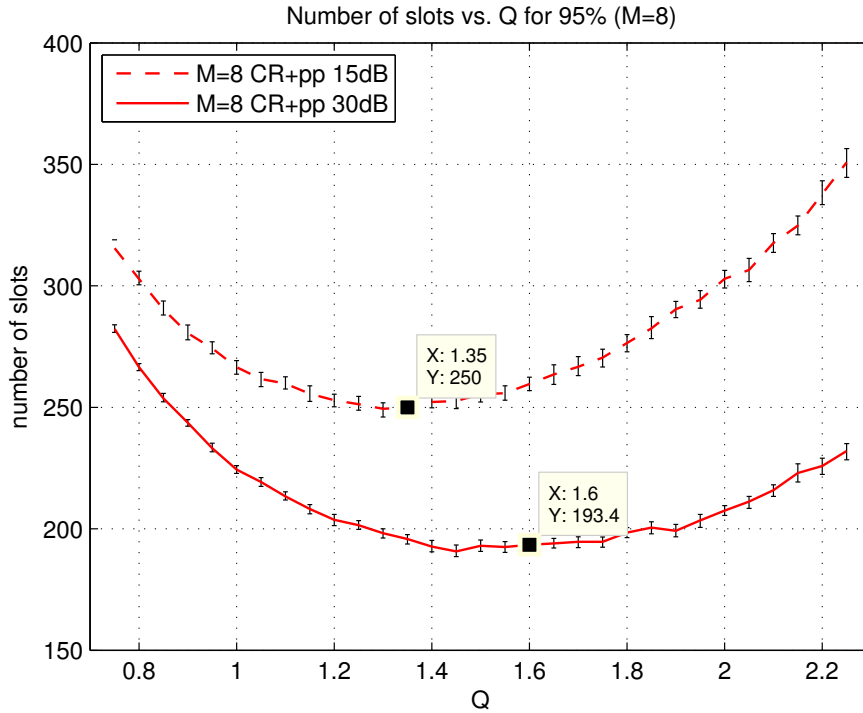


Figure 3.10: Number of slots used for successfully reading 95% of tag population vs. speed factor Q .

3.3 Eigenfilter Beamforming

In order to make the reader more robust to tag collisions and to have a more precise division of the readers area, I propose to use a better defined spatial filter in postprocessing. My intent is to design a filter that divides the reading area in “passbands” and “stopbands”. Thus, I could let $R \geq M$ tags collide in a frame, by making frames shorter, and then in an independent postprocessing of sectors, the number of colliding tags would be decreased by “cancelling” tags from certain ranges of angles.

3.3.1 Eigenfilter Weights

The proposed approach employs an eigenfilter design for spatial filtering in 2D [58]. An example of a desired filter characteristic is shown in Figure 3.11. In this example, the

“stopband” is placed in the range of $\theta_s \in \{90^\circ, 120^\circ\}$.

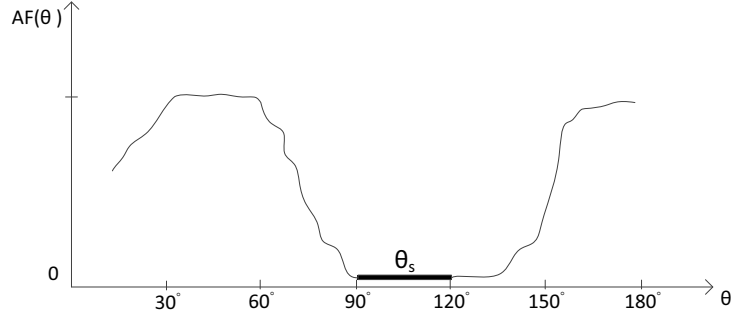


Figure 3.11: A desired filter characteristic with a “stopband” from $90^\circ - 120^\circ$.

As in [59] the filter is approximated with:

$$\text{AF}(\theta) \approx \sum_{i=1}^{N_{\text{RA}}} w_i^* v_i(\theta) = \mathbf{w}^H \mathbf{v}(\theta), \quad (3.9)$$

where $\mathbf{w} \in \mathbb{C}^{N_{\text{RA}} \times 1}$ is the weight vector with elements w_i ($\forall i = 1, \dots, N_{\text{RA}}$) and θ is an angle in the 2D plane. Additionally, $\mathbf{v}(\theta)$ denotes a steering vector $\mathbf{v}(\theta) = e^{-j \frac{2\pi}{\lambda} \mathbf{p}_x a(\theta)}$, where $\mathbf{p}_x \in \mathbb{R}^{N_{\text{RA}} \times 1}$ is a position vector composed of x -coordinates of antenna array elements and $a(\theta) = -\cos(\theta)$ [56].

In order to minimize the energy in the “stopband” [59]:

$$\begin{aligned} E_s &= \int_{\theta \in \theta_s} |\text{AF}(\theta)|^2 d\theta \\ &= \mathbf{w}^H \int_{\theta \in \theta_s} \mathbf{v}(\theta) \mathbf{v}^H(\theta) d\theta \quad \mathbf{w} = \mathbf{w}^H \mathbf{S} \mathbf{w}. \end{aligned} \quad (3.10)$$

A vector \mathbf{w} that achieves $\min_{\mathbf{w}} E_s$ is the eigenvector of \mathbf{S} , corresponding to the smallest eigenvalue [60, 61].

In the case of a linear array:

$$\mathbf{S} = \int_{\theta \in \theta_s} \mathbf{v}(\theta) \mathbf{v}^H(\theta) d\theta \quad (3.11)$$

$$= \int_{\theta \in \theta_s} e^{j \frac{2\pi}{\lambda} \mathbf{p}_x \cos(\theta)} e^{-j \frac{2\pi}{\lambda} \mathbf{p}_x^T \cos(\theta)} d\theta. \quad (3.12)$$

Formulating **S** element by element:

$$S_{a,b} = \int_{\theta \in \theta_s} e^{j \frac{2\pi}{\lambda} \cos(\theta)(x_a - x_b)} d\theta. \quad (3.13)$$

Here, $x_a - x_b$ denotes the distance between antenna a array element and antenna b array element. Since there is no closed form solution for Equation (3.13) an additional weight is introduced, as suggested in [62]:

$$c(\theta) = \begin{cases} 1, & \theta \in \theta_s = [\alpha_s, \beta_s]; \\ 0, & \theta \notin \theta_s \end{cases} \quad (3.14)$$

and $c(\theta)$ can be equivalently expressed in a Fourier series:

$$c(\theta) = \sum_{k=-\infty}^{\infty} c_k e^{-jk\theta} \quad (3.15)$$

with

$$c_k = \frac{1}{2\pi} \int_0^{2\pi} c(\theta) e^{jk\theta} d\theta. \quad (3.16)$$

Thus,

$$c_k = \begin{cases} k = 0, & c_k = \frac{\beta_s - \alpha_s}{2\pi}; \\ k \neq 0, & c_k = \frac{e^{j\beta_s k} - e^{j\alpha_s k}}{j2\pi k} \end{cases}. \quad (3.17)$$

By substituting Equations (3.15), (3.16) and (3.17) in Equation (3.13) and performing integration:

$$S_{a,b} = \sum_{k=-\infty}^{\infty} 2\pi (-j)^{-k} c_k J_k \left(\frac{2\pi}{\lambda} (x_a - x_b) \right), \quad (3.18)$$

where $J_k(\cdot)$ denotes the Bessel function of the first kind and order k . Based on the "stopband" width, I choose the number of sectors in the reader's area.

3.3.2 Eigenfilter Sectors

In case of a four-sector design the reader's area of 120° is divided in four sectors with a width of 30° each. For each sector weights are calculated as previously explained and the obtained weights for Sector 1, 2, 3 and 4, respectively, are:

$$\begin{aligned}\mathbf{w}_1 &= [0.13 - 0.20i, 0.67 + 0.00i, 0.37 + 0.55i, -0.09 + 0.22i]^T \\ \mathbf{w}_2 &= [0.13 + 0.20i, 0.67 + 0.00i, 0.37 - 0.55i, -0.09 - 0.22i]^T \\ \mathbf{w}_3 &= [-0.00 + 0.25i, -0.47 - 0.47i, 0.66 + 0.00i, -0.18 + 0.18i]^T \\ \mathbf{w}_4 &= [-0.18 + 0.18i, 0.66 + 0.00i, -0.47 - 0.47i, -0.00 + 0.25i]^T.\end{aligned}$$

Including these weights in Equation (3.9), antenna array factors for the four-sector design are obtained. Each antenna element is assumed to be omnidirectional with a unity gain. The normalized angular attenuation in dB introduced by postprocessing is:

$$\delta(\theta) = |\text{AF}_n(\theta)|^2 = \left| \frac{\text{AF}(\theta)}{\max_{\theta} \{\text{AF}(\theta)\}} \right|^2, \quad (3.19)$$

and the attenuation introduced by the four-sector postprocessor is shown in Figure 3.12.

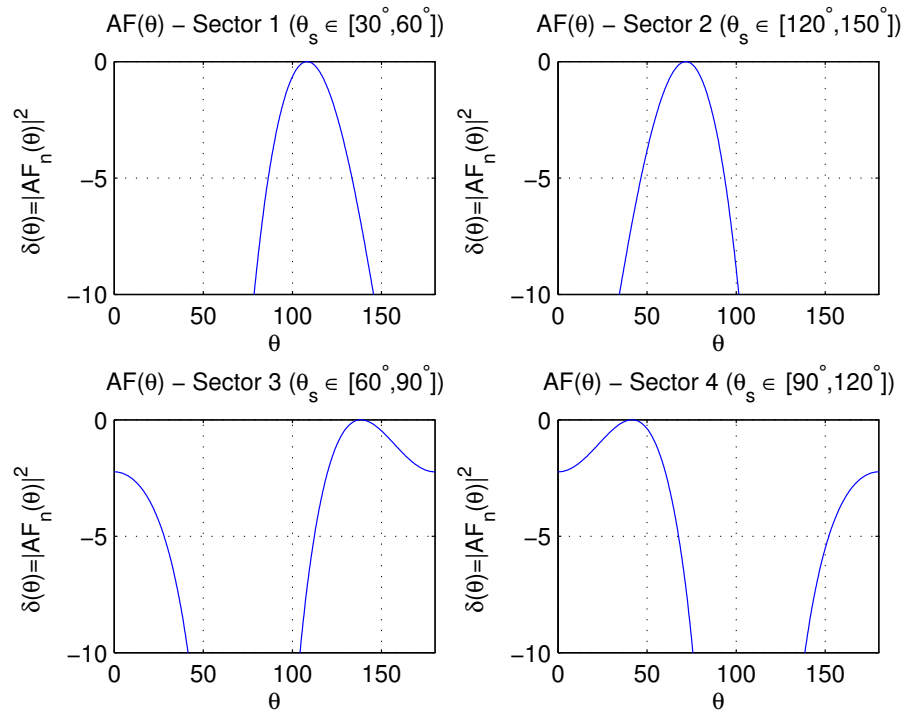


Figure 3.12: The normalized angular attenuation with four sectors.

When the reader's area is divided in six sectors with a width of 20° , the obtained weights of the eigenfilters for Sectors 1, 2, 3, 4, 5 and 6 read:

$$\begin{aligned}
\mathbf{w}_1 &= [0.16 + 0.16i, 0.67 + 0.00i, 0.48 - 0.46i, 0.01 - 0.23i]^T \\
\mathbf{w}_2 &= [0.16 - 0.16i, 0.67 + 0.00i, 0.48 + 0.46i, 0.01 + 0.23i]^T \\
\mathbf{w}_3 &= [0.00 + 0.23i, 0.67 + 0.00i, -0.01 - 0.67i, -0.23 + 0.01i]^T \\
\mathbf{w}_4 &= [0.00 - 0.23i, 0.67 + 0.00i, -0.01 + 0.67i, -0.23 - 0.01i]^T \\
\mathbf{w}_5 &= [-0.20 + 0.12i, 0.67 + 0.00i, -0.57 - 0.34i, 0.11 + 0.21i]^T \\
\mathbf{w}_6 &= [-0.20 - 0.12i, 0.67 + 0.00i, -0.57 + 0.34i, 0.11 - 0.21i]^T.
\end{aligned}$$

Antenna array factors for the six-sector design are calculated by substituting these weights in Equation (3.9). The attenuation introduced by the six-sector processor is shown in Figure 3.13.

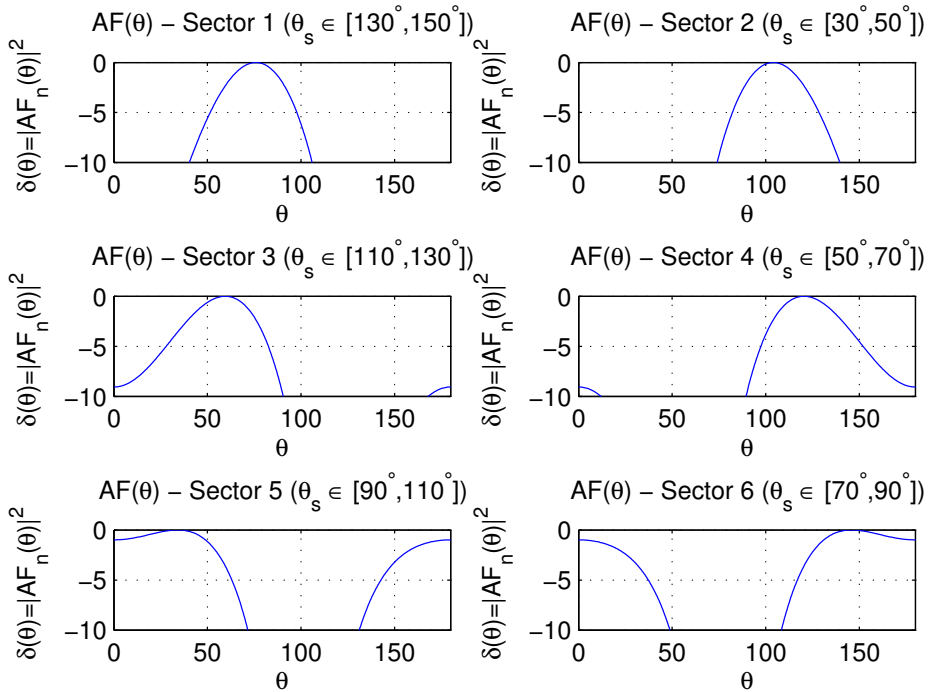


Figure 3.13: The normalized angular attenuation with six sectors.

As observed in Figure 3.12 and Figure 3.13, each “stopband” produces a high side lobe at a different range of angles and it can be interpreted as a sector’s “passband”. Due to a low number of antenna elements in the antenna array, these “passbands” are quite wide and are even overlapping. If the sectors would be without overlapping regions and a perfect channel knowledge would be available, a collision of up to $C_S \times M$ tags colliding

could be resolved, where C_S denotes the number of sectors. This means that under these perfect conditions, I could have C_S times shorter frames, which would lead to a readout speed factor increase of C_S times. However, due to the design imperfections, the readout speed factor is much smaller and the “passband” width and the overlapping region have to be taken into account. Based on that, I derive a semi-analytical formula in Section 3.3.3 for the optimal frame size and I calculate the readout speed factor depending on that.

3.3.3 Frame Optimization for Eigenfilter Postprocessing

Postprocessing with spatial filtering influences the strength of the colliding tags and depending on the angle of arrival some tags are attenuated or amplified. Depending on the attenuation level, tags can be regarded as a stronger or a weaker interference. Strongly attenuated tags through postprocessing can be assumed as a background noise. In order to take into account the influence of tags from all directions of arrival, a semi-analytical formula that considers the attenuation level of the interference as a system throughput with the corresponding SNR is derived. Hence, the impact of the colliding tags in the total system throughput is calculated by taking into account the level differences, introduced with the normalized angular attenuation $\delta(\theta)$ from Equation (3.19).

The throughput is averaged over the cover range as:

$$\overline{\text{TH}} = \frac{1}{2\pi} \int \text{TH}(\text{SNR} + \delta(\theta)) d\theta. \quad (3.20)$$

The readout speed factor is calculated as:

$$Q = \frac{\text{TH}^{\max}}{\overline{\text{TH}}}, \quad (3.21)$$

and the optimal frame size is determined based on the ratio of the frame size to the tag population size without postprocessing $\left(\frac{F_{\text{opt}}}{N}\right)^{\text{nopp}}$ as in Equation (3.8).

In order to perform the evaluation from Equation (3.20), it is necessary to be able to evaluate the throughput at any point. Thus, I have to find a fitting curve for the throughput. Using the MATLAB fitting tool, I found that the best fit to the throughput curve of the $M = 8$ reader from Section 4.5.3 is obtained by Gauss3 model with excellent agreement (RMSE = $2.3 \cdot 10^{-4}$):

$$\text{TH}(x) = a_1 e^{-\left(\frac{x-b_1}{c_1}\right)^2} + a_2 e^{-\left(\frac{x-b_2}{c_2}\right)^2} + a_3 e^{-\left(\frac{x-b_3}{c_3}\right)^2}, \quad (3.22)$$

with coefficients summarized in Table 3.2.

Table 3.2: Fitting coefficients

$$\begin{aligned} a_1 &= 2.047 & b_1 &= 30.76 & c_1 &= 15.41 \\ a_2 &= 1.01 & b_2 &= 12.9 & c_2 &= 9.715 \\ a_3 &= -0.6045 & b_3 &= 3.794 & c_3 &= 6.587 \end{aligned}$$

The obtained (perfect) fit is shown in Figure 3.14.

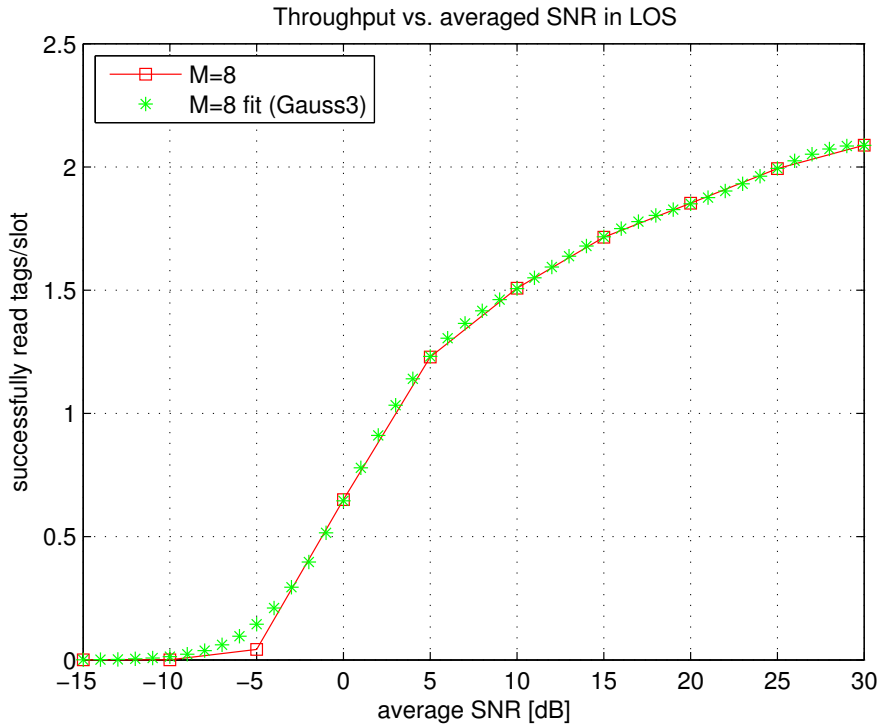


Figure 3.14: Throughput in LOS case vs. SNR and fitting by Gauss3.

Including $\delta(\theta)$ from Equation (3.19) in Equation (3.20) and in Equation (3.21), I find the optimal speed factor of $Q = 1.5$ which decreases the normalized frame size from $(F_{\text{opt}}/N)^{\text{nopp}} = 0.207$ to $(F_{\text{opt}}/N)^{\text{new}} = 0.138$ in the four-sector design. Furthermore, the optimal speed factor of $Q = 1.45$ in the six-sector design is obtained by including $\delta(\theta)$ from Equation (3.19) in Equation (3.20) and in Equation (3.21). This leads to $(F_{\text{opt}}/N)^{\text{new}} = 0.143$.

3.3.4 Eigenfilter Postprocessing

The performance analysis of the proposed spatial filtering is performed through MATLAB simulations. In the simulated setup the RFID reader consists of a single transmit antenna

and a four-element receive antenna array. This reader is designed to resolve collisions of up to eight colliding tags. For channel estimation purposes in collision scenarios, the tag signal is modified by including an additional “postpreamble” as in Section 2.5.1. All tags $j = 1, \dots, N$ are placed at $d_j^f = 3\text{ m}$ distance from the reader’s transmit antenna. With this arrangement all tags experience the same path loss, which facilitates the SNR evaluation. Furthermore, a population of $N = 1000$ tags is uniformly distributed on a part of a circular line determined by a 120° sector (azimuth angles $\theta = [30^\circ, 120^\circ]$). It is assumed that the tag responses are perfectly aligned and that the reader knows the size N_i of the tag population before each iteration. In order to evaluate the proposed spatial filter a channel between reader’s transmit antenna, tag, and the reader’s receive antenna array is modelled as a geometrical LOS channel, as explained in Section 3.1 and the multipath effect is ignored. Additive noise is assumed in the system, as well as errors accumulated through a collision recovery. The assumed errors come from an imperfect channel estimation, due to the limited set of eight “postpreambles”, propagated and accumulated errors over SIC, and a non-ideal projection of the constellation. As a performance measure I took the average number of successfully read tags per slot evaluated for different averaged SNRs (the displayed SNR is averaged over receive antennas as stated in Section 2.4.3).

In this experiment, tags randomly choose a slot within the announced frame for transmission. Since frames are optimized for the reader with the maximum collision recovery factor $M = 8$, slots with up to eight tags colliding occur with a probability of 93.5%. Slots with more than 12 tags colliding appear with a probability of less than 1%. The received signals are spatially filtered using different sector weights listed in Section 3.3.3, and the postprocessed signal is then taken in the collision recovery. During the collision recovery the reader first estimates the channel and based on its obtained estimates, determines the strongest tag signal and takes it out during the SIC. The process is repeated until all colliding tags with unique “postpreambles” are taken out. If at the end there is a single remaining pair of “postpreambles”, I try to resolve such remaining colliding signals by projecting the constellation into the orthogonal subspace of the interference. Successfully read out tags are switched off and they remain silent until the end of the readout process. The process is repeated over ten frames and averaged over $N_{\text{iterations}} = 25$. Furthermore, the experiment was repeated with a higher reading speed factor. Due to shorter frames, collisions of up to eight tags appear in less than 70% when the speed factor is $Q = 1.5$ and in less than 73% when $Q = 1.45$. Additionally, the obtained results are compared with the performance of a conventional reader, an EPC standard compliant reader without collision recovery capabilities, and with a reader with a collision recovery factor $M = 8$ but without postprocessor. Around each point a confidence interval that contains 95% of the obtained results is plotted to evaluate the quality of the obtained results.

Figure 3.15 gives an overview of the performances of three different setups. Solid lines represent the reader without postprocessing, while the dotted/dashed lines denote the

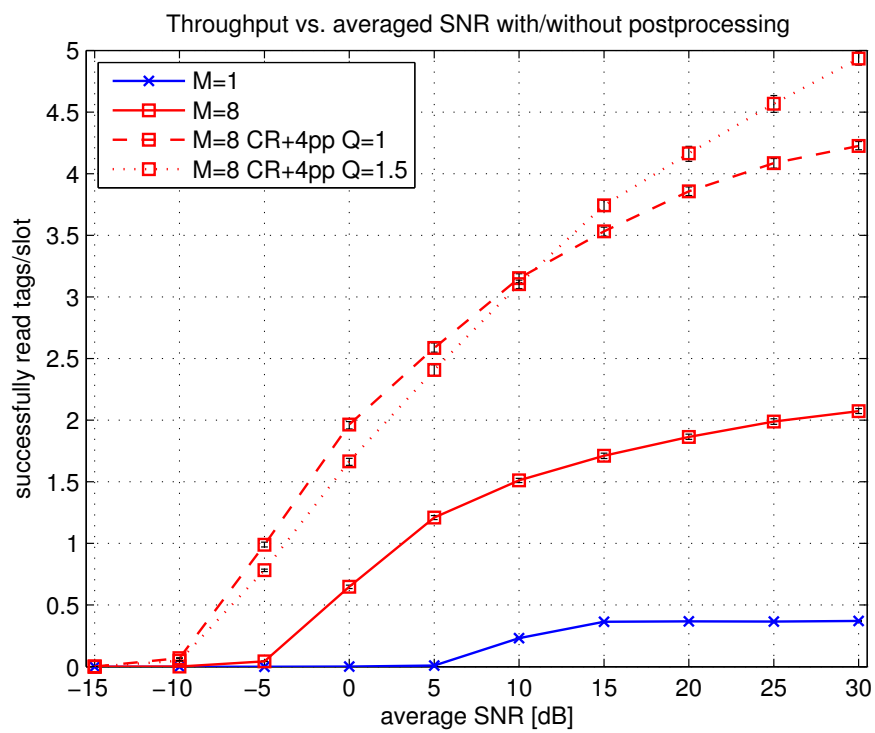


Figure 3.15: Throughput vs. averaged SNR for the reader with a collision recovery factor $M = \{1, 8\}$ with/without four-sectors postprocessing.

reader with a four-sector postprocessing. With spatial filtering the number of successfully read tags per slot is significantly increased, and the achieved system throughput at $\text{SNR} = 15 \text{ dB}$ is more than nine times higher than in the case of a conventional reader. Furthermore, it is observed that when the readout speed factor is increased and consequentially the frame becomes shorter, the reader can still successfully resolve colliding tags. Thus, with the help of the postprocessing, the reader becomes more robust, and the system throughput is now even more than ten times the throughput of a conventional reader.

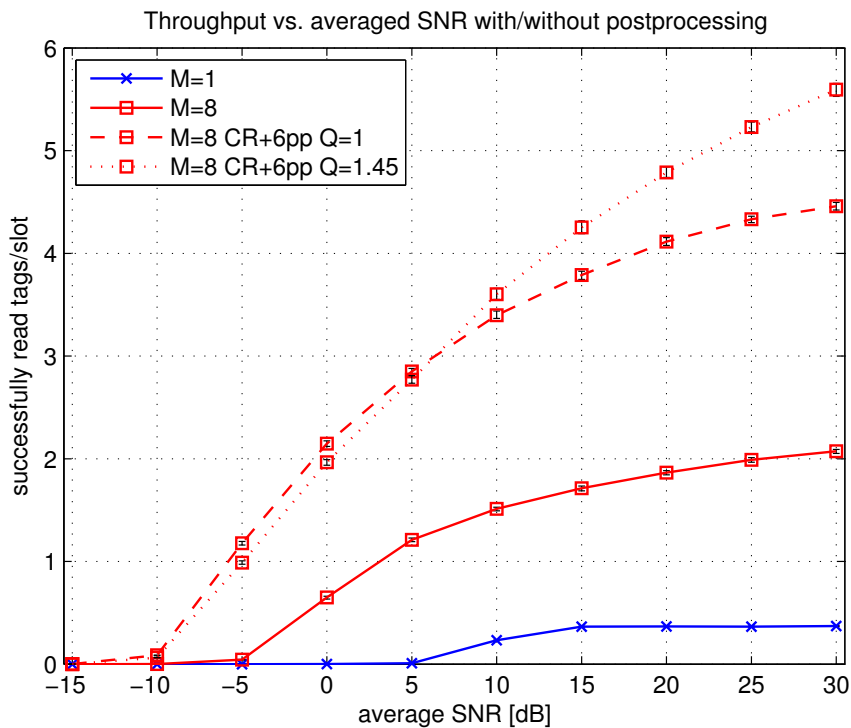


Figure 3.16: Throughput vs. averaged SNR for the reader with a collision recovery factor $M = \{1, 8\}$ with/without six-sectors postprocessing.

In Figure 3.16, a comparative overview of the performances of a reader with a collision recovery factor $M = 8$ with a six-sector postprocessing (red dashed/dotted lines) and without postprocessing (red solid line) is presented. Additionally, the performances of the conventional reader (blue solid line) are plotted. As expected, the system throughput is increased by the spatial filtering and with the speed factor of $Q = 1.45$, the performance of a reader is further improved especially in a high SNR region. With the proposed method almost 12 fold throughput increase is achieved at $\text{SNR} = 15 \text{ dB}$, while at the high $\text{SNR} = 30 \text{ dB}$ this increase is more than 15 times. For easier comparison results are summarized in Table 3.3.

Table 3.3: Successfully read tags per slot vs. averaged SNR.

System	SNR = 15 dB		SNR = 30 dB	
	Tps	R_{Tps}	Tps	R_{Tps}
$M = 1$	0.364	1	0.370	1
$M = 8$	1.712	4.70	2.074	5.60
$M = 8$ CR + 4pp $Q = 1$	3.532	9.70	4.224	11.41
$M = 8$ CR + 4pp $Q = 1.5$	3.744	10.28	4.881	13.18
$M = 8$ CR + 6pp $Q = 1$	3.789	10.40	4.459	12.04
$M = 8$ CR + 6pp $Q = 1.45$	4.252	11.67	5.594	15.11

Elapsed slots for successfully decoding 95%, 98% or 99.5% of the tag population with different readers at SNR = 15 dB are listed in Table 3.4 and at SNR = 30 dB are listed in Table 3.5.

Table 3.4: Number of slots elapsed for successfully decoding at SNR = 15 dB.

SNR=15 dB	$M = 1$	$M = 8$	$M = 8$			
			4 sectors		6 sectors	
			$Q = 1$	$Q = 1.5$	$Q = 1$	$Q = 1.45$
95%	2 608	555	269	254	251	223
98%	2 690	572	277	262	259	230
99.5%	2 731	581	282	266	263	234

Table 3.5: Number of slots elapsed for successfully decoding at SNR = 30 dB.

SNR=30 dB	$M = 1$	$M = 8$	$M = 8$			
			4 sectors		6 sectors	
			$Q = 1$	$Q = 1.5$	$Q = 1$	$Q = 1.45$
95%	2 565	458	225	195	213	170
98%	2 647	473	232	201	220	175
99.5%	2 687	480	236	204	223	178

Comparing Table 3.1 and Table 3.4 shows that in the case of a four-sector postprocessor, the performance of the reader with an eigenfilter beamforming is comparable to the performance of the reader with an FFT beamforming. In the case of a six-sector postprocessor, the reader with eigenfilter beamforming is 1.13 times faster than the reader with FFT beamforming. Thus, for time-sensitive applications, it is justified to employ a more complex reader with a six-sector postprocessing.

3.4 Discussion and Conclusion

In this chapter I have proposed the use of a simple postprocessing beamforming for improving the collision recovery. I have investigated the influence of the proposed FFT method on two reader configurations: a single antenna reader receiver, and a receiver with four receive antennas. In the first case, a tag signal is modelled according to the standard [5] and a conventional reader is employed. In the second case a tag signal is modified by adding a “postpreamble”. The number of strongly colliding tags is mitigated using postprocessing beamforming, collisions are resolved with a two phase approach and a significant improvement is observed. The proposed method considerably shortens the time necessary to interrogate tags.

Additionally, I have deviated from the optimal frame sizes and I have studied the behaviour in the new circumstances. I have observed that with the proposed postprocessing method, readers can recover even from $R \geq M$ tags colliding. The readers became more robust. However, if a number of offered slots becomes too small, the proposed postprocessing with fixed beams cannot mitigate any more and throughput decreases.

Furthermore, in this chapter I have suggested a new, more complex method for increasing the system throughput. The new spatial filter is modelled as an eigenfilter. My aim was to decrease the number of colliding tags by forming a “stopband”. Following such approach, I was able to focus on tag signals, arriving from different sectors independently in postprocessing. I have investigated the benefits of the proposed method, and I observed a throughput increase of more than 11.4 times with a four-sector postprocessor, while with a six-sector postprocessor, the increase was a bit more than 12 times at $\text{SNR} = 30$ dB.

Moreover, I derived a semi-analytical relation between spatial filter pattern and a throughput, and based on that I have calculated the optimal frame size. With the frame size optimized for the postprocessor, even larger gain in system throughput is achieved. A throughput increase of more than 13 times was detected in a four-sector case, while with six-sectors, the increase was more than 15 times. I have shown that the proposed method considerably shortens the time necessary to interrogate tags.

Throughout this chapter a perfect knowledge of the tag population size for calculating optimal frame sizes is assumed. However, the reader does not know the tag population size and has to estimate it. Estimations methods are proposed in [10–12, 63–69]. Additionally, for easier evaluation of the proposed sector postprocessing, multipath propagation is ignored. In order to obtain results in a more realistic environment, it is necessary to adapt the channel model and to include multipath effect. The first step could be to model the multipath effect by a model with a few scatterers. In that way, the received signal includes scattered signals as well and those signals have an additional delay, phase shift and attenuation due to scattering. However, that would lead to a much more complex tracking of the signal components that correspond to the same tag. In order

to benefit from the multipath, the reader would have to be able to align the received scattered signals that correspond to the same tag.

4 FSA WITH COLLISION RECOVERY

In this chapter, the throughput performances of advanced receiver structures in collision scenarios are investigated. Section 1 gives an overview of FSA. In Section 2, necessary modifications of the existing protocol are presented. In addition to that, two different methods of acknowledging colliding tags are proposed.

In Section 3, the constraints to the throughput due to the receiver structure and channel estimation for different collision scenarios are studied. More specifically, the throughput of FSA systems with up to four receive antennas that can recover from a collision of up to eight tags on the physical layer and acknowledge J tags involved in that collision is analysed.

The expected frame duration and the expected number of acknowledged tags have been investigated in Section 4. The study is conducted with perfect dynamically adjusted frame sizes, and with quantized frames. Furthermore, the frame size is further optimized by taking into account different slot durations.

Section 5 provides a performance evaluation. The proposed schemes are evaluated by means of Monte Carlo simulations. The obtained results are compared with the performance of a standard compliant reader. Moreover, the inventory time, i.e., the number of slots necessary to successfully decode all tags in the reader range, is calculated and compared for different receiver types. Furthermore, in order to obtain a fairer comparison of different collision recovery schemes, time spent for tag identifications is calculated.

4.1 FSA Overview

FSA is an interrogation scheme, which is used for scheduling the transmission of tags. The reading cycle is divided into time slots, which are grouped in frames. At the beginning of the reading cycle, the reader announces the frame start and the number of the slots in the frame. The first slot in a frame starts with the preamble followed by the *Query* command, while the consecutive slots begin with the frame synchronization command followed by *Query Repeat*. Unidentified tags from the reader's area choose one of the slots for transmission. Thus, it can happen that some of the slots are empty, some of the slots contain the reply of one tag (singleton slots) and in some of the slots more tags are active causing collisions. Durations of the slots, according to the standard,

are shown in Figure 4.1 and the mentioned abbreviations are listed in Table 4.1. The timing parameters are taken from [5, 70].

Table 4.1: Abbreviations.

P	preamble
PP	postpreamble
QRep	Query Repeat
RN16	16-bit random number
FS	frame sync
ACK	acknowledgment
PC	protocol control
EPC	electronic product code
CRC	16-bit CRC code
T_1	timing parameter $70.7 \mu s$
T_2	timing parameter $18.7 \mu s$
T_3	timing parameter $62.5 \mu s$

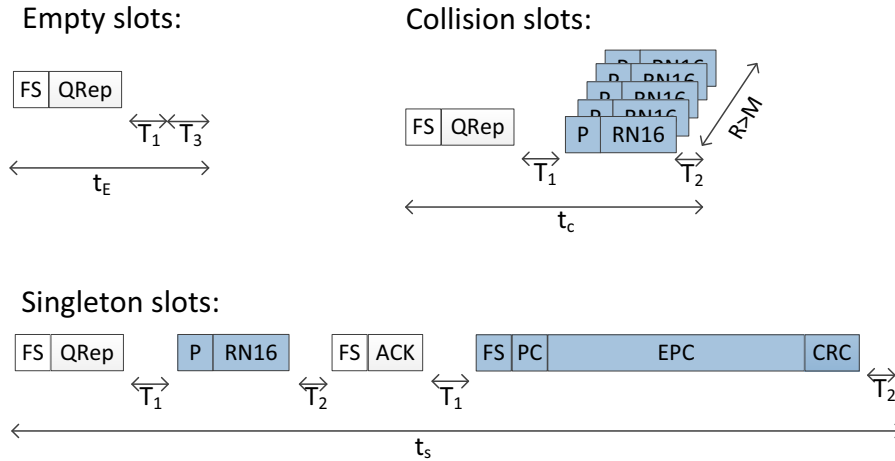


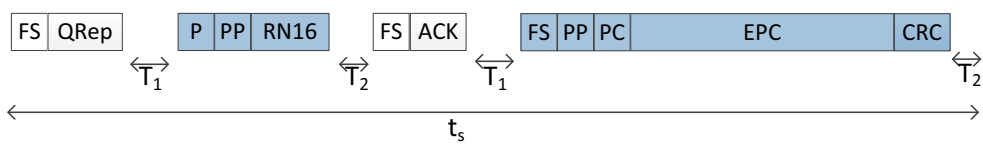
Figure 4.1: Slot durations in FSA.

For a conventional reader without CR, only slots without a collision can be decoded successfully, and it is well known that the maximal throughput is achieved when the frame size F is the same as the tag population size N . If more than one tag is active in one slot, a collision at the air interface occurs and the entire slot is discarded. With CR capable readers, and some changes in the protocol, it is possible to use the information from slots with a collision to increase the throughput together with shorter frame sizes.

4.2 Modifications in FSA

As explained in Section 2.5, in order to employ a collision recovery, a tag reply to a *Query* command is modified by adding a “postpreamble”. New slot durations are prolonged for $t_{pp} = 0.12$ ms and are shown in Figure 4.2. The duration of empty slots stay unchanged.

Singleton slots:



Non resolvable collision slots:

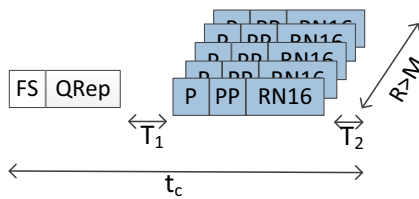


Figure 4.2: Modified slot durations in FSA due to “postpreamble” PP.

If the number of colliding tags is higher than the collision recovery factor M , none of the colliding tags can be acknowledged. However, if the number is smaller, then, based on the collision scenario, some of the colliding tags can be resolved. I propose two ways to send acknowledgements to the resolved tags. The first one is described in Figure 4.3. Here, the acknowledgements are sent to the resolved tags in the consecutive order. This requires changes in the standard both on the reader and on the tag side, since, the tags have to wait for a longer time for their acknowledgements.

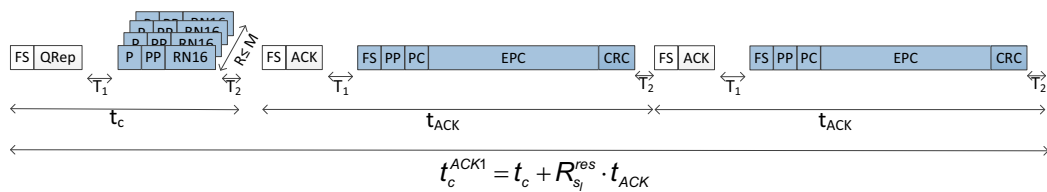


Figure 4.3: Acknowledgements of the resolved tags - type one.

The second proposed option employs the fact that the collision has already been resolved and that the reader knows how to separate signals from the colliding tags. Thus, as shown in Figure 4.4, the tags send their data at the same time and the collided signal can be resolved again. In this case, the changes are just on the reader side.

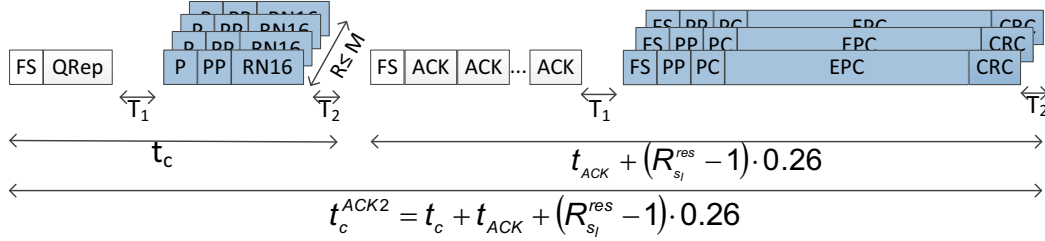


Figure 4.4: Acknowledgements of the resolved tags - type two.

Standard slot durations and the modified durations are listed in Table 4.2. As observed from Table 4.2, the durations of the collision slots with $R \leq M$ tags colliding, for both acknowledgement schemes (ACK type 1 and ACK type 2), depend only on the number of the $R_{s_l}^{res}$ resolved tags.

Table 4.2: Slot durations in collision scenarios.

	stand. [ms]	modified [ms]
empty slot duration t_E	0.21	0.21
singleton slot t_S	2.58	$2.58 + t_{pp}$
acknowledge time t_{ACK}	2.09	$2.09 + t_{pp}$
coll. slot - non res. t_C	0.49	$0.49 + t_{pp}$
- $R_{s_l}^{res}$ res. tags t_C^{ACK1}	×	$t_C + R_{s_l}^{res} \cdot t_{ACK}$
- $R_{s_l}^{res}$ res. tags t_C^{ACK2}	×	$t_C + t_{ACK} + (R_{s_l}^{res} - 1) \cdot 0.26$
postpream. duration t_{pp}	×	0.12
difference Δt between the first and cons. slots	0.25	0.25

4.3 Throughput Constraints

In order to evaluate the performance of FSA systems with CR, theoretical bounds are calculated in the following. These bounds are determined by the receiver structure, the tag signal modification and the channel estimation. Furthermore, the number of simultaneously acknowledged tags is denoted as J . The maximum number of J is given by M , but J can also be limited by the standard (the current standard only allows for $J = 1$) and/or the capabilities of the receiver technique. By introducing such a variable J , the expected throughput improvements can be studied beforehand and later compared with the true achievable values of J based on the receiver capabilities.

4.3.1 Receiver Structure Constraints

Acknowledged $J = 1$ tag

In this case one of these R tags is chosen and acknowledged ($J = 1$) while the responses from other tags are discarded.

The expected number of slots with exactly R tags transmitting is given by [18]:

$$E\{\mu_R\} = F \binom{N}{R} \left(\frac{1}{F}\right)^R \left(1 - \frac{1}{F}\right)^{N-R}, \quad (4.1)$$

where μ_R is a random variable indicating the number of slots with exactly R tags transmitting, $E\{\cdot\}$ denotes the expected value and N represents the number of tags within the reader range.

The reader is capable of recovering from collision with $R \leq M$ tags transmitting in the same slot. If more than M tags collide, the slot is unreadable. The reader chooses one of these R tags and acknowledges this single tag ($J = 1$) while the other tag's responses are discarded. For this scenario, can be computed directly from (4.1).

$$T_{ps} = \frac{1}{F} \sum_{R=1}^M E\{\mu_R\} = \sum_{R=1}^M \binom{N}{R} \left(\frac{1}{F}\right)^R \left(1 - \frac{1}{F}\right)^{N-R}. \quad (4.2)$$

The frame size F can be optimized in order to maximize the average throughput. In Figure 4.5 the expected throughput curves of receivers which are capable of recovering from collision of up to M tags are shown for a tag population of $N = 1000$. The expected throughput increases with M and converges toward one successful readout per slot for $M \rightarrow \infty$. In Table 4.3 the optimal values of frame size and average throughput are shown. The values are related to the tag population size for the reader which is capable of recovering from a collision of $M = \{1, 2, 4, 8\}$ tags and acknowledge one tag ($J = 1$).

Table 4.3: Optimal frame size F_{opt} and expected throughput for readers resolving $M = \{1, 2, 4, 8\}$ collisions and $J = 1$.

System	F_{opt}/N	T_{ps}	R_{Tps}
1	1	0.368	1.000
2	0.707	0.587	1.595
4	0.452	0.817	2.220
8	0.265	0.962	2.614

With this method a 2.6 fold throughput increase is achieved for receivers with $N_{RA} = 4$ antennas which are capable of recovering from up to eight tags colliding in one slot.

It is feasible to further increase the throughput by acknowledging more than one tag.

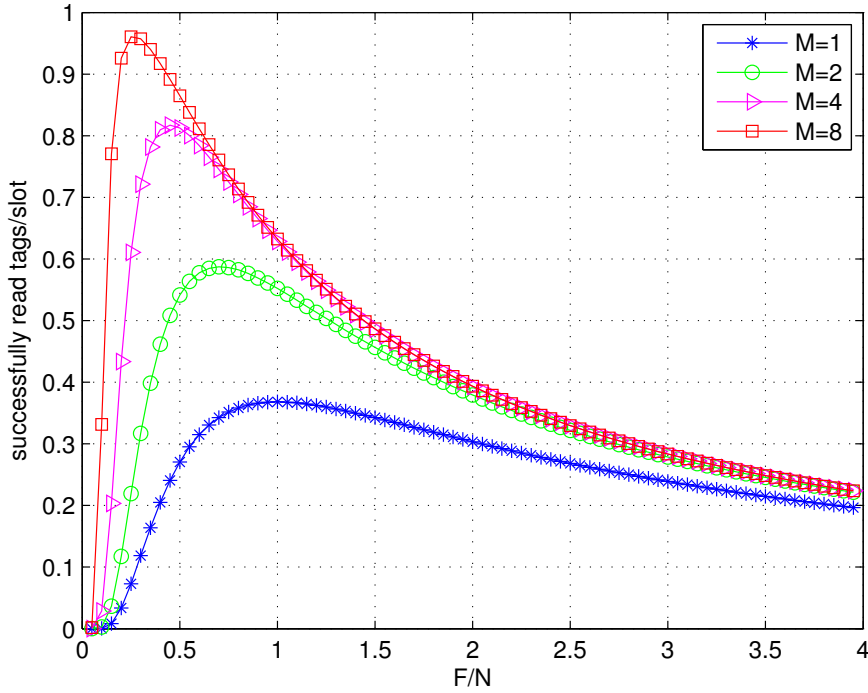


Figure 4.5: Expected throughput for $J = 1$ in respect to frame size to tag ratio F/N .

Given the number N of the tag population and the frame size F , the throughput for a collision recovery factor M under the assumption that up to J tags per slot can be acknowledged is computed [23]:

$$\begin{aligned}
 T_{\text{psJ}} = & \sum_{R=1}^J \binom{N}{R} \left(\frac{1}{F}\right)^R \left(1 - \frac{1}{F}\right)^{N-R} R \\
 & + \sum_{R=J+1}^M \binom{N}{R} \left(\frac{1}{F}\right)^R \left(1 - \frac{1}{F}\right)^{N-R} J. \quad (4.3)
 \end{aligned}$$

The first sum in Equation (4.3) represents the throughput increase due to the fact that the collision recovering from R tags while acknowledging up to J tags can be ensured. The second part considers the throughput increase due to collision recovery of $J < R \leq M$ tags. The second sum goes up to M , thus the slots with a higher number of tags colliding, $R > M$, are not resolvable and do not contribute to the throughput. Based on [23], the ratio F/N of frame size and tag population for such scenarios is optimized.

Acknowledged up to $J = 2$ tags

Figure 4.6 shows the theoretically expected throughput curves of receivers with a collision recovery factor $M = \{2, 4, 8\}$ and up to two tags ($J = 2$) acknowledged in one slot, together with the curve with a collision recovery factor of $M = 1$, representing conventional receivers that can deal with only one transmitting tag per slot. The calculations are performed for a tag population of $N = 1000$.

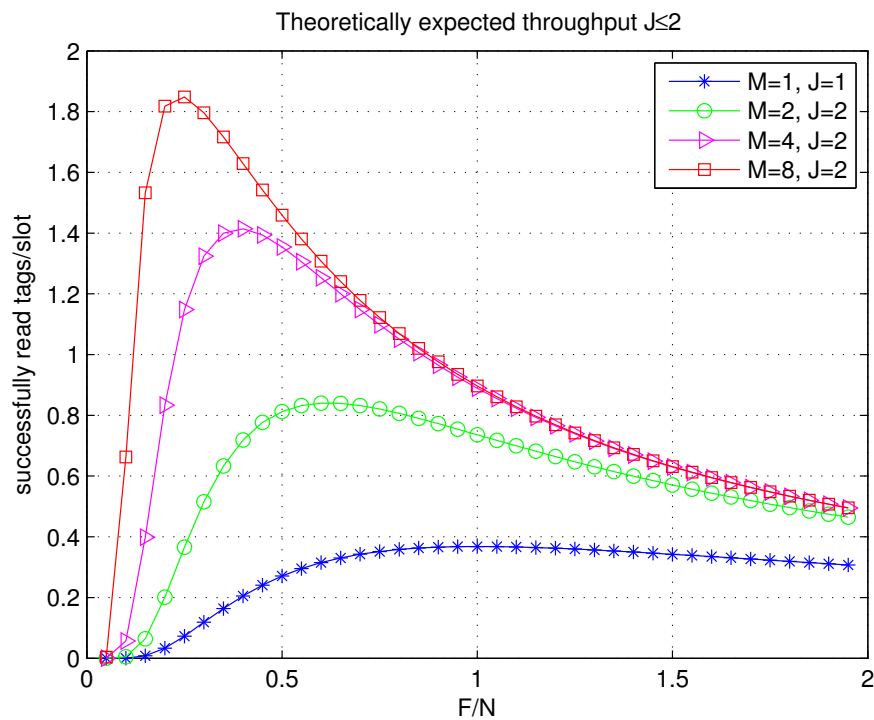


Figure 4.6: Expected throughput for $J \leq 2$ with respect to the ratio F/N .

Table 4.4 shows the optimal values of the frame size, and the corresponding maximum theoretical throughput as well as the relative improvement with respect to a conventional system with $M = 1$. The optimal frame size values are normalized to the tag population size and are presented for the reader with a collision recovery factor $M = \{2, 4, 8\}$ and up to two tags ($J = 2$) acknowledged in a slot.

Figure 4.7 shows the dependence of the expected throughput on the collision recovery factor M and the number of acknowledged tags J in one slot. For both, ($J = 1$) and ($J = 2$), the throughput significantly increases with the collision recovery factor M . For receivers capable of recovering from up to eight tags colliding in one slot (i.e., $N_{RA} = 4$), the receiver which can acknowledge one tag shows a throughput increase of 2.614 times while the receiver that can acknowledge two tags in one slot offers even a 5.033 times higher throughput, compared to the throughput of a conventional receiver.

Table 4.4: Optimal ratio F_{opt}/N and maximal theoretical throughput for readers resolving $M = \{1, 2, 4, 8\}$ collisions and $J \leq 2$.

System	F_{opt}/N	T_{PSJ}	$R_{T_{\text{PSJ}}}$
$M = 1 \quad J = 1$	1	0.368	1.000
$M = 2 \quad J = 2$	0.618	0.841	2.285
$M = 4 \quad J = 2$	0.391	1.415	3.845
$M = 8 \quad J = 2$	0.235	1.852	5.033

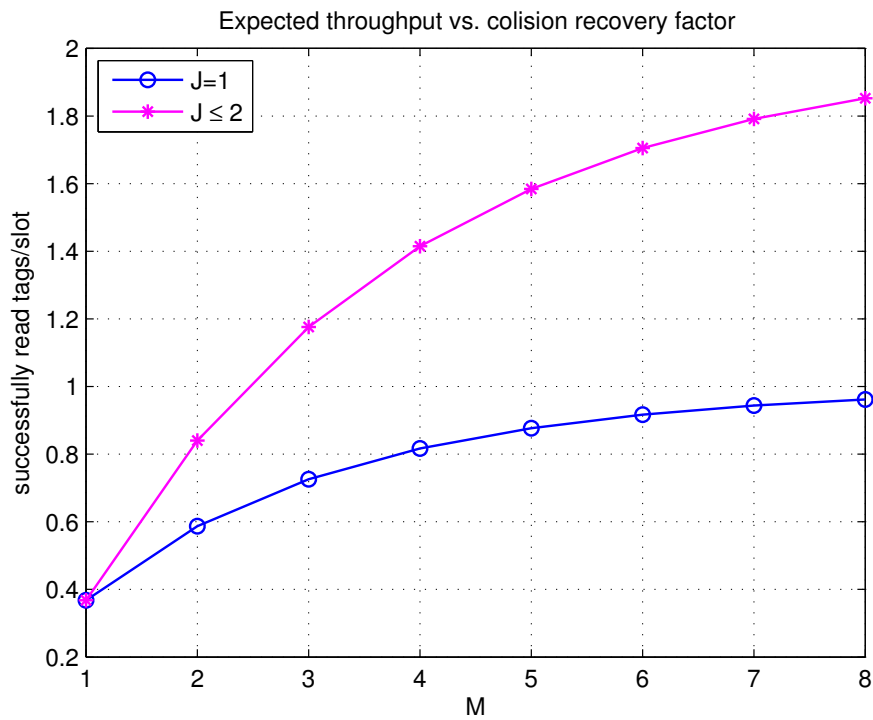


Figure 4.7: Expected throughput vs. collision recovery factor M with the optimal ratio F_{opt}/N .

Acknowledged up to $J = M$ tags

The maximal theoretical throughput per slot, obtained for an optimal reader that can recover from a collision of $R \leq M = 2N_{\text{RA}}$ tags and acknowledge ($J = M$) in the case of perfect channel knowledge reads:

$$T_{\text{ps}_M} = \sum_{R=1}^M \binom{N}{R} \left(\frac{1}{F}\right)^R \left(1 - \frac{1}{F}\right)^{N-R} R. \quad (4.4)$$

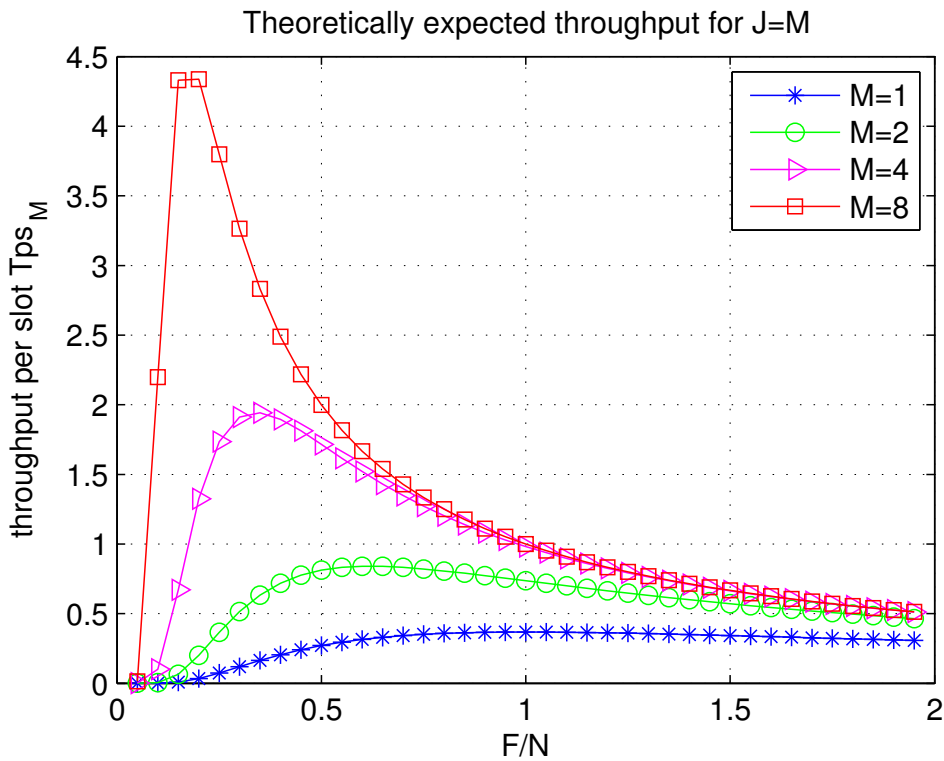


Figure 4.8: Expected throughput as a function of slots per tag population F/N for $J = M = 2N_{\text{RA}}$ acknowledgements following Equation (4.4).

Figure 4.8 shows successfully read tags per slot with respect to the normalized frame size. The throughput curves follow with very good agreement a simple function in the ratio F/N ; see Appendix C.1 for more details. The maximal theoretical throughput per slot T_{ps} for a reader with different collision recovery factor M is listed in Table 4.5. This maximum is obtained for the optimal frame size F_{opt} , which is normalized by the tag population size N . Furthermore, for each case the relative improvement $R_{T_{\text{ps}_M}}$ in T_{ps_M} with respect to a conventional system with $C = 1$, $J = 1$ is listed.

Table 4.5 shows the optimal ratio F_{opt}/N and the corresponding maximum theoretical throughput per slot T_{ps} . The last column labelled $R_{T_{\text{ps}}}$ lists the relative improvement

in Tps with respect to a conventional system with $C = 1$, $J = 1$.

Table 4.5: Optimal ratio F_{opt}/N , maximal theoretical throughput per slot and its relative improvement.

System	F_{opt}/N	Tps_M	R_{Tps_M}
$M = 1 \quad J = 1$	1	0.368	1.000
$M = 2 \quad J = 2$	0.618	0.841	2.285
$M = 4 \quad J = 4$	0.339	1.944	5.283
$M = 8 \quad J = 8$	0.173	4.479	12.171

By assuming an optimal receiver structure and a tag population of $N = 1\,000$, the maximal theoretical throughput per slot is 4.479, achieved for a frame that contains only 173 slots. However, the values obtained here are in the case of perfect channel knowledge, which is much higher than what can be expected to achieve with a feasible receiver. In order to recover from a collision when applying an MMSE receiver (Equation (2.9)), the channel need to be estimated. For channel estimation additional “postpreambles” are introduced. In the following paragraph, the influence of the tag signal modification to the system throughput is investigated.

4.3.2 “Postpreamble” Constraints

Assume the tag response to the *Query* command has been modified according to Section 2.5.1. As explained there, a “postpreamble” is added in order to support channel estimation and the desired case is that all tags involved in a collision, have orthogonal “postpreambles” to distinguish them. For easier explanation, I will use the term “tags with different colours” to denote the tag’s property of having different “postpreambles”. If a uniform distribution of “postpreambles” between tags in the population is assumed, the tag population of size N can be seen as C partitioned tag populations, each with the average size N/C , where C is the number of different colours (number of different “postpreambles” in a set) as shown in Figure 4.9. Theoretically, as long as there is a tag of unique colour among the active tags in a slot, the related signal can be differentiated and this tag can be acknowledged. Even if there are two tags with the same colour involved in a collision, it is expected to recover from that particular collision and to acknowledge both tags by applying the projection method proposed in [23].

Now, under the assumption that up to J_C tags with identical colour can be can acknowledged per slot, given the tag population size N , the frame size F and C different “postpreambles” in a set, the Tps is:

$$\text{Tps}_C = C \sum_{R_C=1}^{J_C} \binom{\frac{N}{C}}{R_C} \left(\frac{1}{F}\right)^{R_C} \left(1 - \frac{1}{F}\right)^{\frac{N}{C} - R_C} R_C, \quad (4.5)$$

where R_C denotes the number of tags per slot with identical colour.

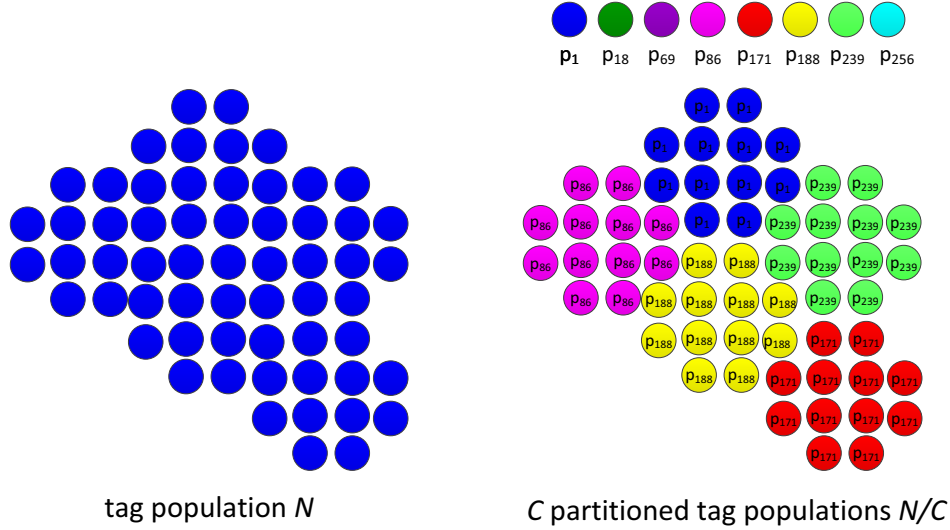


Figure 4.9: Left: Tag population N , right: C partitioned populations with N/C tags each.

Figure 4.10 shows the theoretically expected throughput per slot curves. The throughput curves follow with very good agreement a simple function in F/N ; see Appendix C.2 for more details. The first two curves, blue ($-*-$) and green ($-\circ-$), are simulated for a tag population size of $N = 1000$ according to Equation (4.4) for $J = M$, while the magenta ($-\triangleright-$) and red ($-\square-$) curves are calculated with the partitioned tag population of size $C \times \frac{N}{C} = 8 \times 125$, Equation (4.5). The conventional receiver that can deal with just one tag transmitting per slot and acknowledge that single tag ($J = 1$) is presented by the blue curve. Here, the theoretical maximum throughput per slot is 0.368 and is achieved for the frame size equal to the tag population size. The green curve represents a receiver that can recover from a collision of two tags and acknowledges both signals ($J = 2$). In this case the maximal throughput per slot is obtained for a shorter frame size and is 0.841. Due to the shortening of the frame by 38.2% (see Table 4.6), the overall throughput is further increased by $2.285/0.618 = 3.697$. For the next two curves, $C = 8$ different partitions of tags are assumed. For the magenta curve, eight different partitions of tags are in the reader range and the throughput benefits just from the existence of tags with single unique colours that are correctly acknowledged ($J_C = 1$), while the red curve represents also a throughput increase due to the recovery from a collision of pairs of colours ($J_C = 2$). Here, the throughput is further increased and for $C = 8$ and $J_C = 1$ the relative increase is $8.030/0.125 = 64.24$, while for $C = 8$ and $J_C = 2$ it is even $18.361/0.077 = 238.45$. However, due to the additional “postpreamble” also a slot duration increase of 26.67% needs to be taken into account.

Table 4.6 shows the optimal values of the frame size normalized by N , the corresponding

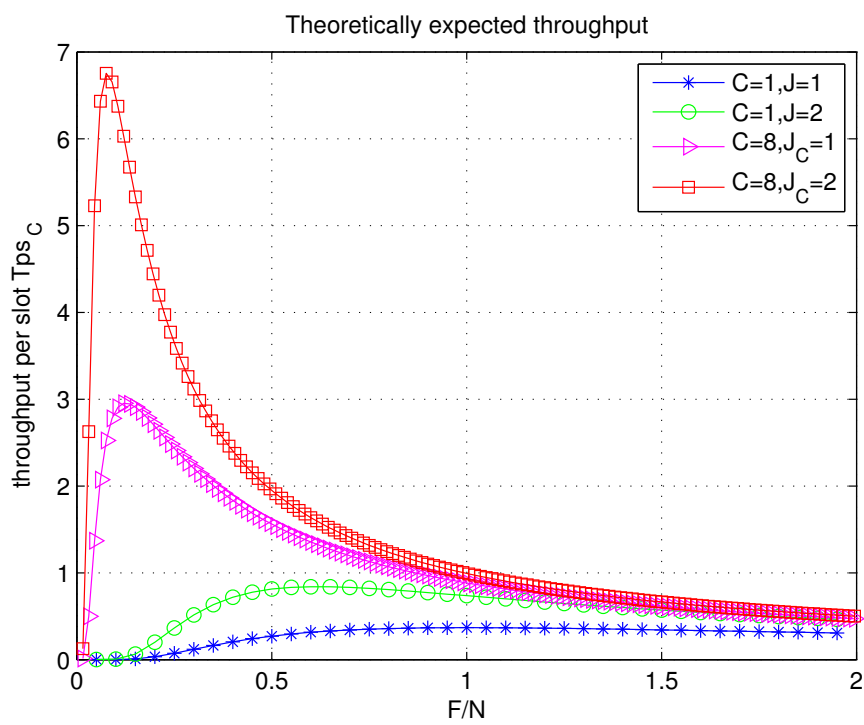


Figure 4.10: Expected throughput as a function of slots per tag population F/N for $C = \{1, 8\}$ colours and $J = \{1, 2\}$ acknowledgements following Equation (4.5).

maximum T_{ps_C} , as well as the relative improvement in T_{ps_C} with respect to a conventional system with $C = 1, J = 1$. The last column labelled $R_{T_{pf}}$ lists the relative improvement $R_{T_{pf}}$ in throughput per frame with respect to a conventional system with $C = 1, J = 1$ calculated as:

$$R_{T_{pf}} = \frac{T_{pf}}{T_{pf}^{C=1,J=1}} = \frac{\frac{T_{ps_C}}{F_{opt}} \cdot \frac{1}{G}}{\frac{T_{ps_C}^{C=1,J=1}}{F_{opt}^{C=1,J=1}}} = \frac{\frac{T_{ps_C}}{F_{opt}/N} \cdot \frac{1}{G}}{\frac{0.368}{1}}. \quad (4.6)$$

Here, shorter frames (F_{opt}) are taken into account and the stretching of the frames by an additional “postpreamble” (G) that is required for $C > 1$ colour. The signal of a tag consists of a preamble (6 bits), a “postpreamble” (8 bits) and an RN16 (16 bit) and each bit is encoded with FM0. Thus, the frame stretching factor is $G = \frac{6+8+16}{6+16} = 1.364$. In spite of the small loss due to G , the relative improvement $R_{T_{pf}}$ can climb up to 174.8.

Table 4.6: Optimal ratio F_{opt}/N , maximal theoretical throughput per slot T_{ps} , its relative improvement and the relative improvement in throughput per frame.

System	F_{opt}/N	T_{ps_C}	$R_{T_{ps_C}}$	$R_{T_{pf}}$
$C = 1 \quad J = 1$	1	0.368	1.000	1.000
$C = 1 \quad J = 2$	0.618	0.841	2.285	3.697
$C = 8 \quad J_C = 1$	0.125	2.955	8.030	47.096
$C = 8 \quad J_C = 2$	0.077	6.757	18.361	174.824

However, such considerations are too optimistic as the following example shows. For N_{RA} receive antennas only $R \leq M = 2N_{RA}$ tags can be resolved. Consider for example a scenario in which each of the $C = 8$ colours appears twice. Then, there are in total $R = C \cdot R_C = 16$ tags in this slot but with $N_{RA} = 4$ only eight tags can be resolved. Practically, Equation (4.5) needs at least to be constrained by $C \cdot J_C \leq M$. Furthermore, the channel cannot be estimated in all collision scenarios. Thus, tighter bounds in the following are derived.

4.3.3 Channel Estimation Constraints - Cyan Set Constraints

In Equation (4.4) it is assumed that the reader resolves all tags in each slot in any collision scenario up to $R = M$, and acknowledges $J = M$ tags. For a reader that can detect and acknowledge only the green and blue parts of the collisions on Table 2.5 (further on this joint set is called the **Cyan Set**), the analytically obtained maximal theoretical throughput per slot is:

$$T_{ps_f} = \sum_{R=1}^M P_R \cdot \left(\sum_{l=1}^{S_l(R)} P_{s_l}(R) \cdot R_{s_l}^{sol}(R) \right). \quad (4.7)$$

Here, P_R is calculated as:

$$P_R = \binom{N}{R} \left(\frac{1}{F}\right)^R \left(1 - \frac{1}{F}\right)^{N-R}, \quad (4.8)$$

and represents the probability that exactly R tags are active in one slot.

Now, the probability $P_{s_l}(R)$ (as listed in Table 2.5, and calculated according to Equation (2.20)) of each scenario s_l ($l = 1, 2, \dots, S_l(R)$) and the number $R_{s_l}^{\text{sol}}(R)$ of tags that can be resolved in each scenario (joint set of blue and green numbers from corresponding rows of Table 2.5) have been taken into account. Theoretically expected values of the throughput per slot are shown in Figure 4.11. The throughput curves follow with very good agreement an approximated function $\text{Tps}_f(F/N)$; see Appendix C.3 for more details. Values of the maximal theoretical throughput per slot together with the optimal frame size normalized to the tag population size are shown in Table 4.7 for $N_{\text{RA}} = \{1, 2, 4\}$ receive antennas allowing for collision recovery factors of $M = \{1, 2, 4, 8\}$.

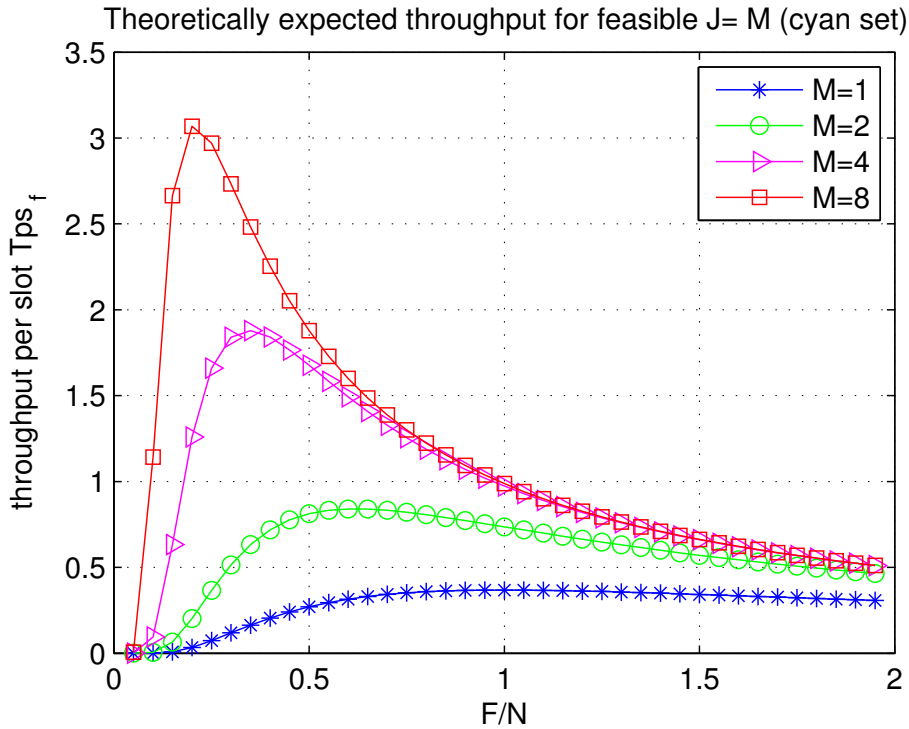


Figure 4.11: Expected throughput as a function of slots per tag population F/N for $J = M = 2N_{\text{RA}}$ acknowledgements in Cyan Set following Equation (4.7).

Comparing Table 4.5 and Table 4.7 it is observed that for higher values of the collision recovery factor M , the loss in Tps performance increases because the number of unresolved tags becomes much higher.

Table 4.7: Optimal ratio F_{opt}/N , maximal theoretical throughput and its relative improvement in [Cyan Set](#).

System	F_{opt}/N	Tps_f	R_{Tps_f}
$M = 1 \quad J = 1$	1	0.368	1.000
$M = 2 \quad J = 2$	0.618	0.841	2.285
$M = 4 \quad J = 4$	0.345	1.879	5.106
$M = 8 \quad J = 8$	0.207	3.073	8.351

4.4 Tag Identifications

As previously mentioned, a conventional reader can only acknowledge the tags from singleton slots and the expected number of acknowledged tags in a frame is calculated as follows:

$$\gamma_{\text{conv}} = F \cdot P_R(1), \quad (4.9)$$

where F denotes the number of slots in the frame and $P_R(R)$ is the probability that exactly R tags are active in one slot and is calculated according to Equation (4.8).

The expected frame duration is calculated as shown below:

$$t_{\text{conv}} = F \cdot \left(P_R(0) \cdot t_E + P_R(1) \cdot t_S + \sum_{R=2}^N P_R(R) \cdot t_C \right), \quad (4.10)$$

where the slot durations are provided in Table 4.2.

However, if a reader is capable of a collision recovery, aside from the singleton slots also some of the collision slots can be acknowledged. As explained in Section 4.2, two different types of collision slots can be distinguished. Collision slots with more than M tags colliding where none of the colliding tags can be resolved and collision slots with $R \leq M$. In the latter case, some of the colliding tags, depending on a collision scenario could be resolved.

Now, the expected number of acknowledged tags in a frame becomes:

$$\gamma = F \cdot \left(P_R(1) + \sum_{R=2}^M P_R(R) \cdot \sum_{l=1}^{S_l(R)} P_{s_l}(R) \cdot R_{s_l}^{\text{sol}}(R) \right), \quad (4.11)$$

where $S_l(R)$ is the number of scenarios in case of R colliding tags and $P_{s_l}(R)$ is the probability of scenario S_l calculated as in Section 2.6, Equation (2.20).

As proposed in Section 4.2, there are two acknowledgement schemes which differ in the slot durations t_C^{ACK1} and t_C^{ACK2} . Depending on the chosen scheme, the duration

of the collision slot with the acknowledgement part will be calculated as a function of the number of resolved tags $t_C^{\text{ACK1/2}}(R_{s_l}^{\text{sol}})$, as listed in Table 4.2. The expected frame duration depends on the acknowledgement scheme that is employed and is obtained as:

$$t_F = F \cdot (P_R(0) \cdot t_E + P_R(1) \cdot t_S) + \quad (4.12)$$

$$F \cdot \left(\sum_{R=2}^M P_R(R) \cdot \sum_{l=1}^{S_l(R)} P_{s_l}(R) \cdot t_C^{\text{ACK1/2}}(R_{s_l}^{\text{sol}}(R)) \right) +$$

$$F \cdot \left(\sum_{R=M+1}^N P_R(R) \cdot t_C \right).$$

In Table 4.8, Table 4.9 and Table 4.10 expected frame durations and the expected number of identified tags in a frame are listed, as well as the averaged identification time per tag (given in brackets) for the two proposed acknowledgement schemes. The values are calculated for a conventional reader (according to Equation (4.9) and Equation (4.10)) and three readers with collision recovery capabilities $M = \{2, 4, 8\}$ (according to Equation (4.11) and Equation (4.12)). In case of a reader with $M = 2$, the tag signal is according to the standard (without modifications) and a projection of the signal constellation into the interference subspace is employed for collision recover. Thus, t_E , t_S and t_C have the standard durations while t_C^{ACK1} and t_C^{ACK2} are calculated as detailed in Table 4.2 with $t_{pp} = 0$. Furthermore, I have calculated the expected frame durations and the expected numbers of identified tags for three different frame sizes.

4.4.1 Perfect DFSA

Here, I assume that the frame size is perfectly optimized to the tag population size and is calculated as:

$$F_{\text{DFSA}} = F^{\text{norm}} \cdot N. \quad (4.13)$$

Here, F^{norm} is the optimal frame size for a reader with the corresponding collision recovery factor normalized to the tag population size. In case of a conventional (standard compliant) reader with $M = 1$, the normalized frame size is $F^{\text{norm}} = 1$, for a reader with $M = 2$ is $F^{\text{norm}} = 0.618$, for $M = 4$ is $F^{\text{norm}} = 0.345$ while for a reader with $M = 8$, the normalized optimal frame size is $F^{\text{norm}} = 0.207$ as listed in Table 4.7.

As expected, by employing collision recovery, the identification time decreases. Furthermore, as observed in Table 4.8, the second acknowledgement scheme, ACK type 2, significantly shortens the necessary identification time.

Table 4.8: Expected Identification time for ACK type 1 and ACK type 2 in perfect DFSA.

	Tags	Id. Time - ACK 1 [ms]	Id. Time - ACK 2 [ms]
$M = 1$	368.06	1 157 (3.14)	
$M = 2$	519.46	1 355 (2.61)	1 061 (2.04)
$M = 4$	648.20	1 604 (2.47)	862 (1.33)
$M = 8$	636.04	1 508 (2.37)	645 (1.01)

4.4.2 DFSA= 2^Q

According to the standard the announced frame size has to be a quantized. Thus, I calculate the expected values for a frame size as $F_{2^Q} = 2^{\langle \log_2(F) \rangle}$ from Equation (4.13), where $\langle \cdot \rangle$ represents the rounding. Now, the frame size for a reader with $M = 1$ is $F_{2^Q} = 1024$. For a reader with $M = 2$ is $F_{2^Q} = 512$, while readers with $M = 4$ and $M = 8$ announce the same frame size of $F_{2^Q} = 256$.

Table 4.9: Expected Identification time for ACK type 1 and ACK type 2 in quantized 2^Q DFSA.

	Tags	Id. Time - ACK 1 [ms]	Id. Time - ACK 2 [ms]
$M = 1$	376.79	1 182 (3.14)	
$M = 2$	419.13	1 107 (2.64)	853 (2.04)
$M = 4$	433.21	1 092 (2.52)	561 (1.29)
$M = 8$	753.76	1 791 (2.38)	801 (1.06)

Now, the frame sizes differ from their expected optimum and the expected values are shown in Table 4.9. In case of a reader with $M = 1$, there are more slots than necessary and the number of empty slots is increased. However, this increase is almost negligible and the average identification time stays the same. In case of $M = 8$, there are 1.24 times more slots and consequently the number of slots with a lower number of collisions is increased. This leads to a longer identification time per tag on average. A reader with $M = 2$ announces less slots than optimal, which leads to more collision slots with $R \geq M$ tags and consequently longer identification time per tag on average. In case of a reader with $M = 4$ even with the shorter frame size, the averaged identification time per tag for ACK type 2 is shorter than in the optimal frame case. This is because the number of collisions with more tags is increased but still some of the tags can be resolved and their acknowledgements are sent at the same time.

4.4.3 DFSA= 4^Q

In this part, I examine the behaviour of the proposed acknowledgement schemes with a higher quantization level. Here the frame size is calculated as $F_{4^Q} = 4^{(\log_4(F))}$, and now readers with $M = 1$ and $M = 2$ have frames with $F_{4^Q} = 1024$ slots and readers with $M = 4$ and $M = 8$ announces frames with $F_{4^Q} = 256$ slots.

Table 4.10: Expected Identification time for ACK type 1 and ACK type 2 in quantized 4^Q DFSA.

	Tags	Id. Time - ACK 1 [ms]	Id. Time - ACK 2 [ms]
$M = 1$	376.79	1 182 (3.14)	
$M = 2$	744.74	1 951 (2.62)	1 614 (2.17)
$M = 4$	433.20	1 093 (2.52)	561 (1.29)
$M = 8$	753.76	1 791 (2.38)	801 (1.06)

Here, a reader with $M = 2$ announces longer frames than necessary and that leads to the longer identification time per slot on average as listed in Table 4.10. As observed here, there is a slight improvement in the identification time for ACK type 1 comparing to the identification time necessary for ACK type 1 in Subsection 4.4.2. That is due to the fact that there are less collision slots, and the collision recovery scheme is not efficiently employed. On the other hand, readers with $M = 1$, $M = 4$ and $M = 8$ stay with the same values.

By comparing Tables 4.8, 4.9 and 4.10, the same trends are observed. With an increased collision recovery factor, the identification time decreases. Thus, even with the suboptimal frame sizes the averaged identification time per tag does not change significantly.

4.4.4 Optimized Frame Size

A different response of the two proposed acknowledgement schemes to the variations in the frame lengths is observed. The frame sizes in Section 4.3.3 were calculated without taking into account slot durations, thus, are not optimal any more. Thus, I search for the new optimal frame size $F_{\text{opt}}^{\text{norm}}$ that minimises the identification time per tag, i.e.,

$$F_{\text{opt}} = \arg \min_F \frac{t_F}{\gamma}. \quad (4.14)$$

In Figures 4.12 and 4.13, the identification time per tag for readers with collision recovery factors $M = 2$, $M = 4$ and $M = 8$ for ACK type 1 and ACK type 2 is plotted together with the time that a conventional reader with $M = 1$ spends for identifying one tag.

As shown in Figure 4.12, the identification time per tag is minimized and the new frame size is longer than the optimal frame size from Section 4.3.3. This is due to the long

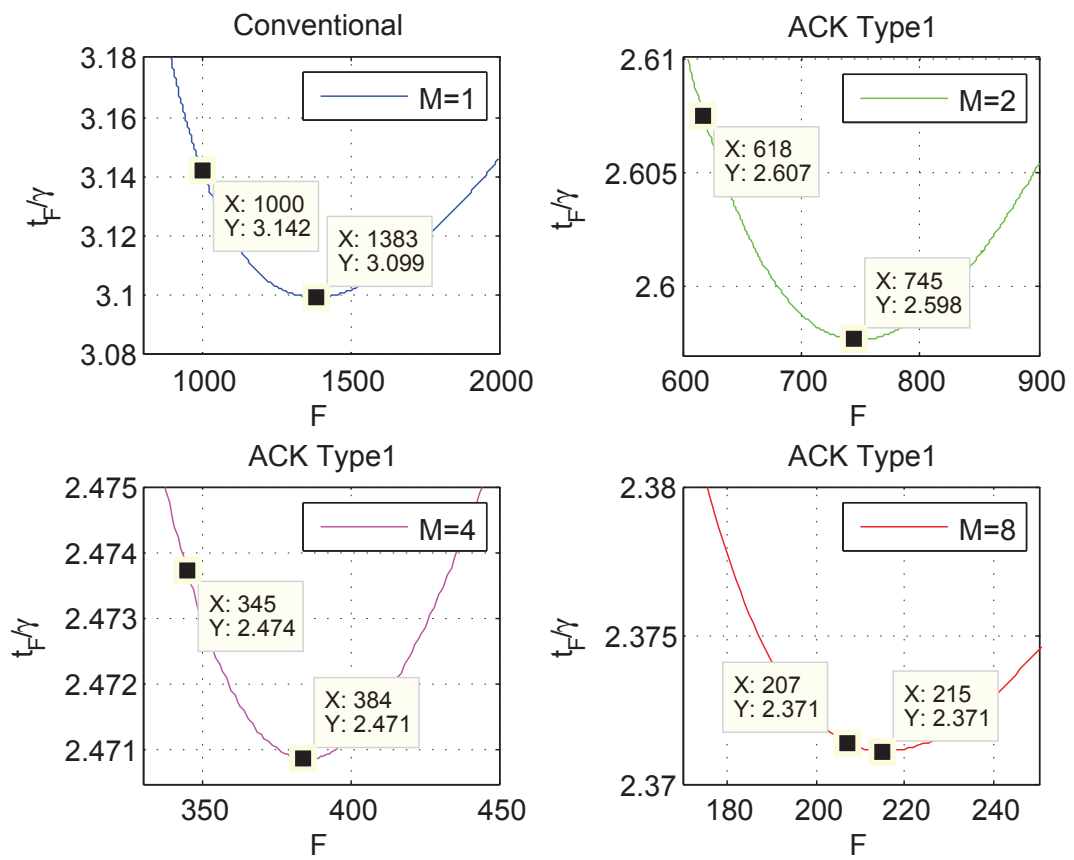


Figure 4.12: Identification time per tag vs. frame size F with ACK type 1. The theoretical optimal value F_{opt} and the true value F_{DFSA} are depicted.

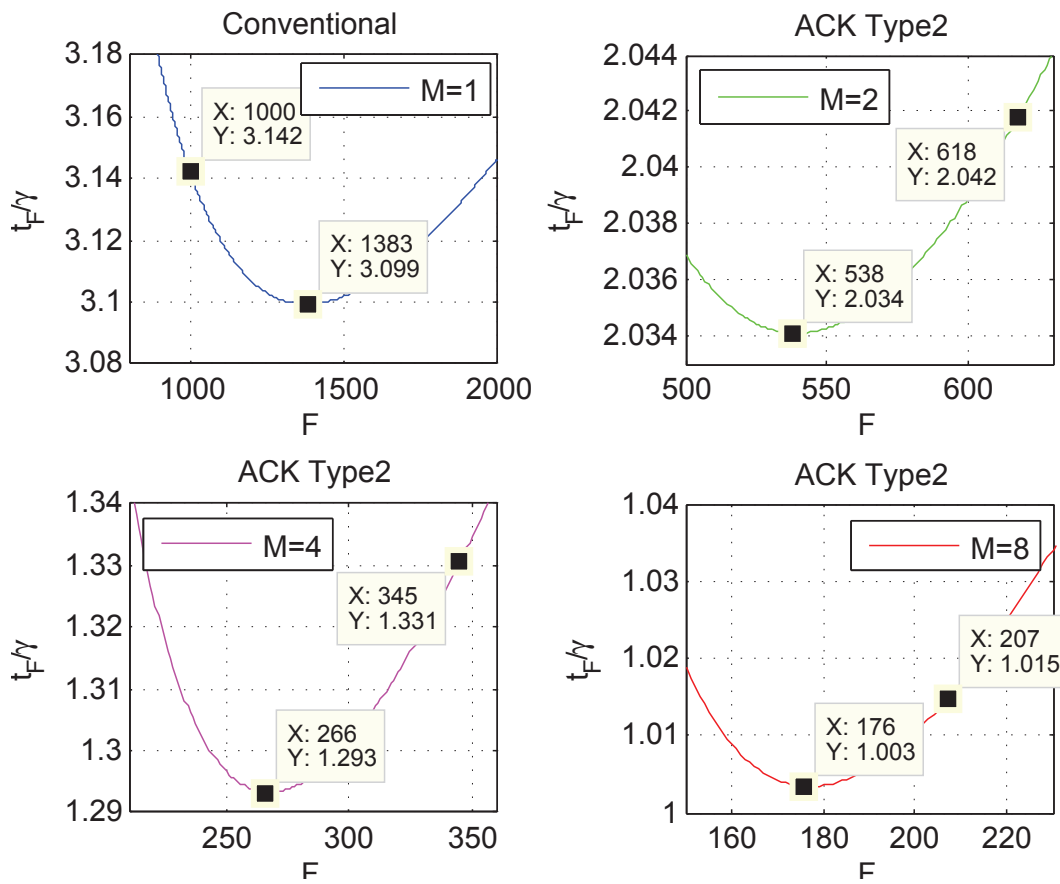


Figure 4.13: Identification time per tag vs. frame size F with ACK type 2. The theoretical optimal value F_{opt} and the true value F_{DFSA} are depicted.

duration of ACK type 1 scheme in addition to the different durations of t_E , t_S and t_C . When ACK type 2 scheme is employed and more colliding tags are acknowledged almost simultaneously, the shortest identification time per tag is obtained for the frame sizes that are shorter than the optimal frame sizes from Section 4.3.3, as shown in Figure 4.13. However, it can be seen by carefully examining Figure 4.12 and Figure 4.13 that the difference between the identification time per slot in the frame with F_{DFSA} slots and in the frame with F_{opt} does not differ much. Thus, with the additional frame optimization the total identification time will not change significantly. Since the differences are so small, I select the simple rule, according to Equation (4.13), for calculating the frame size in Section 4.5.6.

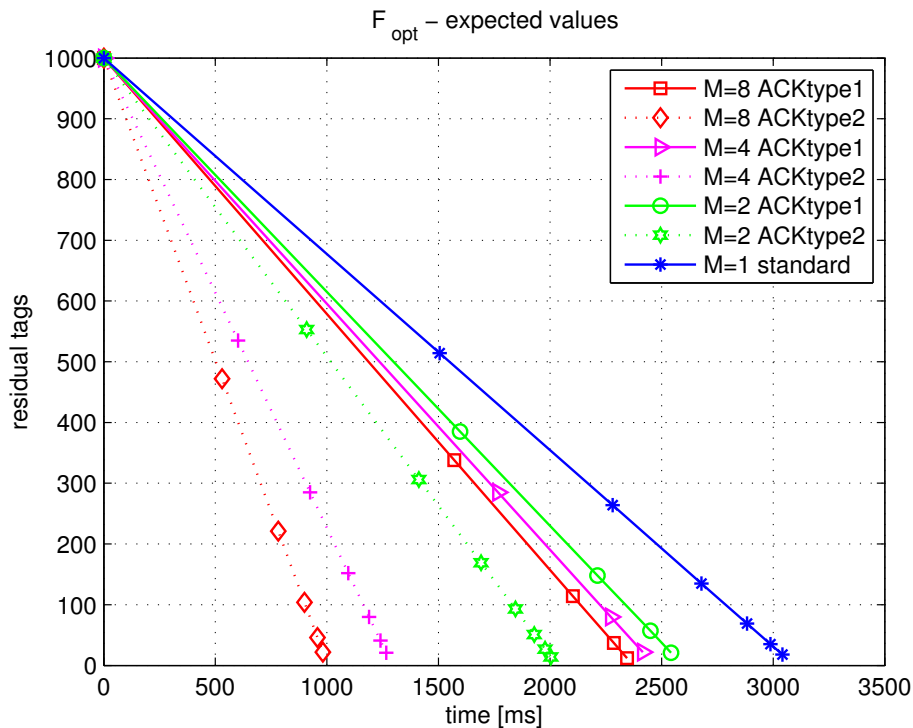


Figure 4.14: Residual tags vs. elapsed time with the frame sizes optimized according to Equation (4.14).

In Figure 4.14 a comparative overview of the two proposed schemes, ACK type 1 and ACK type 2, with the frame sizes optimized according to Equation (4.14) is depicted. At the beginning of each frame k , the number of residual tags is recalculated:

$$N_k = N_{k-1} - \langle \gamma_{k-1}(F_{opt,k-1}) \rangle, \quad (4.15)$$

where N_{k-1} denotes the number of the unidentified tags after $k-2$ frames, $\gamma_{k-1}(F_{opt,k-1})$ is the expected number of tags identified in the frame $k-1$ calculated according to Equation (4.11) (or Equation (4.9) in case of a conventional reader) and $\langle \cdot \rangle$ represents the

rounding.

4.5 Performance evaluation

As additional performance measure, the throughput per slot of readers that can recover from collision and acknowledge J tag for different levels of the average SNR is investigated.

4.5.1 For $J = 1$ Acknowledged Tag

In Figure 4.15 a comparative overview of the expected throughput for MMSE receivers is presented when up to eight tags transmit in the same slot under various receive antenna numbers. The maximum of the theoretically expected throughput from Section 4.3.1, Equation (4.2), is indicated by dashed horizontal lines. The lines correspond to the receivers with a collision recovery factor $(M = 1, J = 1)$, $(M = 2, J = 1)$, $(M = 4, J = 1)$ and $(M = 8, J = 1)$, according to Equation (4.2), respectively. The receivers with perfect channel knowledge are represented by solid lines and the receivers with estimated channel knowledge by dotted lines. For both scenarios, corresponding groups of curves are approaching their theoretical limits, and it can be observed that with the increase of SNR the curves saturate. Table 4.11 shows the expected throughput values at an SNR of 30 dB.

Table 4.11: Expected throughput of FSA ($J=1$).

Throughput at 30 dB	Perfect Channel	Estimated Channel
$N_{RA} = 1 \ R = 1$	0.3533	0.3522
$N_{RA} = 1 \ R = 2$	0.5658	0.5647
$N_{RA} = 2 \ R = 4$	0.8151	0.8151
$N_{RA} = 4 \ R = 8$	0.9621	0.9621

4.5.2 For $J = 2$ Acknowledged Tags

A comparative overview of the expected throughput for the MMSE receivers with the possibility to recover from collisions and to acknowledge two tags is shown in Figure 4.16. The receiver decodes two of the received packets. The packets are from the strongest of all received signals. The chosen received packets are compared with the corresponding transmitted packets. If there is an error in transmission, the number of packets with errors is increased. The same steps are performed in each slot. Finally, the average number of packets with errors (averaged over the slots) is subtracted from the number of acknowledged tags ($J = 2$). In the case with singleton slots, just one tag is transmitted per slot; then just that packet is examined and the average number of packets with

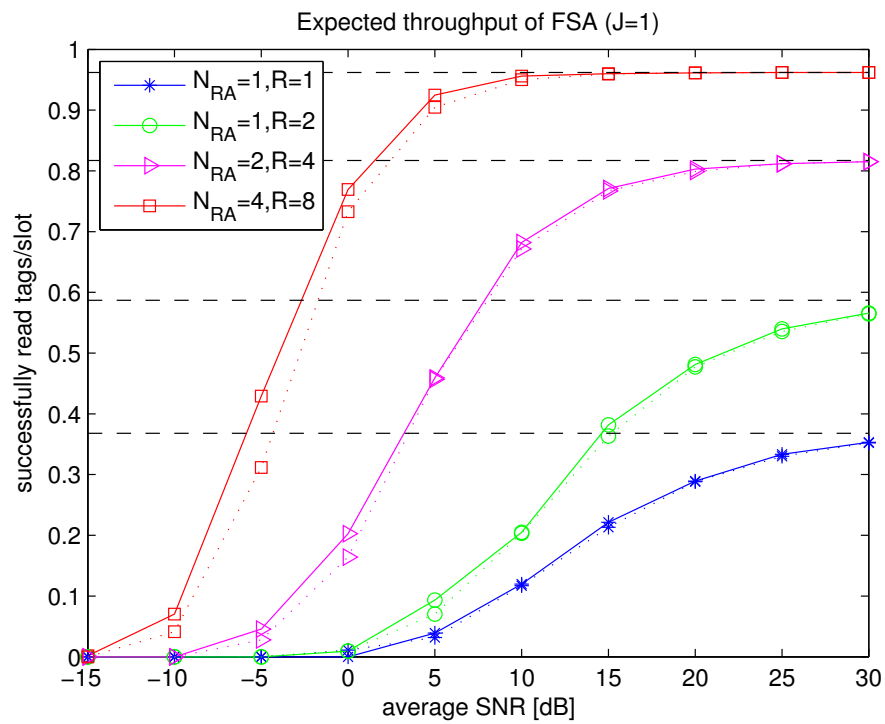


Figure 4.15: Expected throughput of FSA scheme for one tag acknowledged ($J=1$) in a perfect (solid lines), estimated (dotted lines) channel and theoretical maxima from Equation (4.2) (dashed lines).

errors is subtracted from $J = 1$. The obtained result represents the success ratio of the simulated system (the average number of packets in a slot that are correctly received) $Sd_{i,R}$ with i receive antennas when R tags are transmitting in the same slot. The expected throughput is calculated as:

$$T_{\text{FSA},i} = \sum_{R=1}^M P_R \cdot Sd_{i,R}. \quad (4.16)$$

Here P_R denotes the probability that exactly R tags (out of the total number of tags N), are transmitting in one slot. The MMSE receiver is shown with different numbers of receive antennas at the reader and with up to eight tags transmitting in the same slot. As in the previous graph the horizontal dashed lines indicate the maximum of the theoretically expected throughput for receivers with collision recovering factor ($M = 2, J = 2$), ($M = 4, J = 2$), ($M = 8, J = 2$), according to Equation (4.3), respectively. For comparison also the blue curve that represents a conventional receiver with $M = 1$ and $J = 1$ as well as its theoretical maximum are plotted. Corresponding groups of curves, for the receivers with the perfect channel knowledge (solid lines) as well as with estimated channels (dotted lines), are approaching their theoretical limits. The relative improvements shown in Table 4.6 are in accordance with the relation between curves that are representing the proposed receivers and the conventional receiver. From Table 4.12 it can be observed that with the proposed acknowledgement of two tags per slot, a throughput increase of more than five times is achieved compared with the conventional system in both cases.

Table 4.12: Expected throughput of FSA ($J \leq 2$).

Throughput at 30 dB	Perfect Channel	Estimated Channel
$N_{\text{RA}} = 1 \quad R = 1 \quad J = 1$	0.3533	0.3522
$N_{\text{RA}} = 1 \quad R = 2 \quad J = 2$	0.7481	0.7445
$N_{\text{RA}} = 2 \quad R = 4 \quad J = 2$	1.3830	1.3810
$N_{\text{RA}} = 4 \quad R = 8 \quad J = 2$	1.8370	1.8370

4.5.3 For $J = M$ Acknowledged Tags

The throughput per slot is calculated again for all tags that a reader with $i \in \{1, 2, 4\}$ receive antennas and collision recovery factor M can resolve and acknowledge from a collision ($R = 1, \dots, M$). The probability that exactly R tags are active in one slot is taken into account. Furthermore, for each number of colliding tags R , the corresponding probabilities of solvable scenarios, listed in Table 2.5 are also included. All solvable scenarios are simulated separately and averaged over N_{iter} iterations. The simulation results are multiplied with the corresponding scenario probability and with the corresponding probability that exactly R tags are active in one slot. By combining all individual colli-

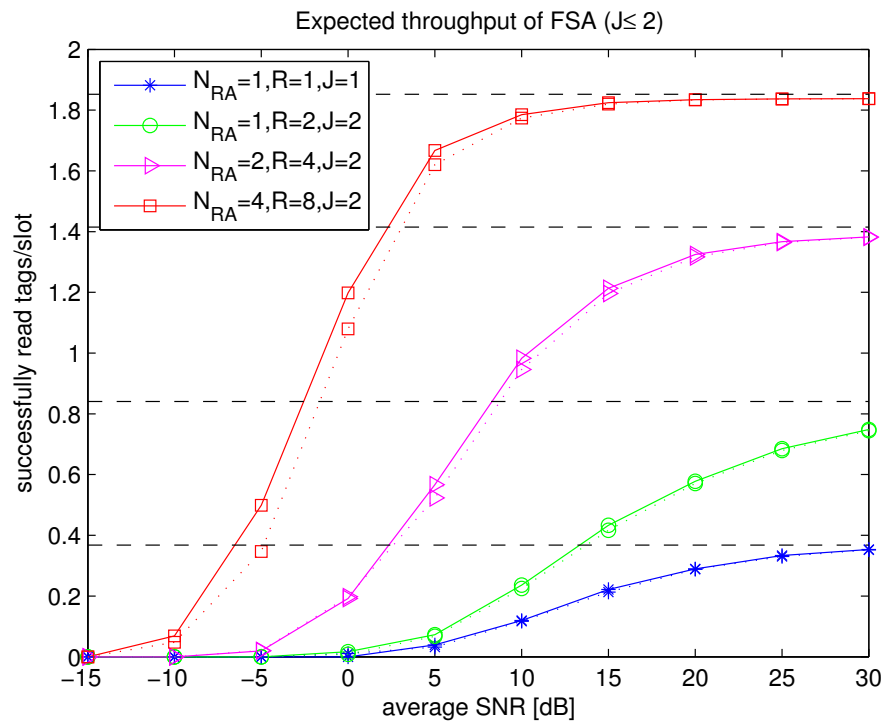


Figure 4.16: Expected throughput of FSA scheme for up to two tags acknowledged ($J \leq 2$) in a perfect (solid lines), estimated (dotted lines) channel and theoretical maxima from Equation (4.3) (dashed lines).

sion scenarios, the throughput per slot can be calculated semi-analytically as a function of SNR:

$$\text{Tps}_{\text{FSA},i}(\text{SNR}) = \sum_{R=1}^M P_R \cdot \left(\sum_{l=1}^{S_l(R)} P_{s_l}(R) \cdot \text{Sd}_{i,R}^{s_l}(\text{SNR}) \right),$$

$$i = 1, 2, \dots, N_{\text{RA}} \quad (4.17)$$

where $\text{Sd}_{i,R}^{s_l}(\text{SNR})$ denotes the average number of successfully decoded tags in a system with i receive antennas in Scenario s_l , $l = 1, 2, \dots, S(R)$. Variable $\text{Sd}_{i,R}^{s_l}(\text{SNR})$ represents the average number of packets in a slot that are correctly received and at best it is close to $R_{s_l}^{\text{sol}}(R)$. The values of $\text{Sd}_{i,R}^{s_l}(\text{SNR})$ are taken from simulations and are thus dependent on the SNR. In Equation (4.17) P_R represents the probability that exactly R tags are active in one slot and this probability is calculated based on Equation (4.8) for the optimal value F_{opt} taken from Table 4.7. The probabilities of collision scenarios are taken from Table 2.5.

In the case of perfect channel knowledge, the collision scenarios are irrelevant and thus the even simpler semi-analytical relation is obtained:

$$\text{Tps}_{\text{FSA},i}^{\text{opt}}(\text{SNR}) = \sum_{R=1}^M P_R \cdot \text{Sd}_{i,R}(\text{SNR}). \quad (4.18)$$

Here, the probability P_R is calculated according to Equation (4.8) for F_{opt} taken from Table 4.5 and the values of $\text{Sd}_{i,R}(\text{SNR})$ correspond to those of $\text{Sd}_{i,R}^{s_l}(\text{SNR})$ but are now obtained from simulations with perfect channel knowledge.

A comparative overview of the expected throughput per slot for the MMSE receiver with a different number of receive antennas in case of up to eight tags transmitting in one slot is presented in Figure 4.17. In the simulations all cases from $R = 1$ to $R = 8$ collisions are included, which is equivalent to 93.5% of all cases for the given value of the optimal frame size F_{opt} . The simulation results in Figure 4.17 reflect very well that only 74.3% of these cases can be resolved. The missing 6.5% of collisions due to $R > 8$ do not change the results considerably. The maxima of the theoretically expected throughputs based on perfect channel knowledge are indicated by the horizontal solid lines according to Equation (4.4), also listed in Table 4.5 (third column Tps), while the maxima of the theoretically expected throughputs from “postpreamble”-based channel estimation are represented by the dotted horizontal lines according to Equation (4.7) also listed in the third column Tps of Table 4.7. In Figure 4.17 the receivers with perfect channel knowledge are represented by solid curves (obtained based on Equation (4.18)), and the proposed receivers with “postpreamble”-based channel estimation in the [Cyan Set](#) are represented by dotted curves (obtained based on Equation (4.17)). In both cases, the

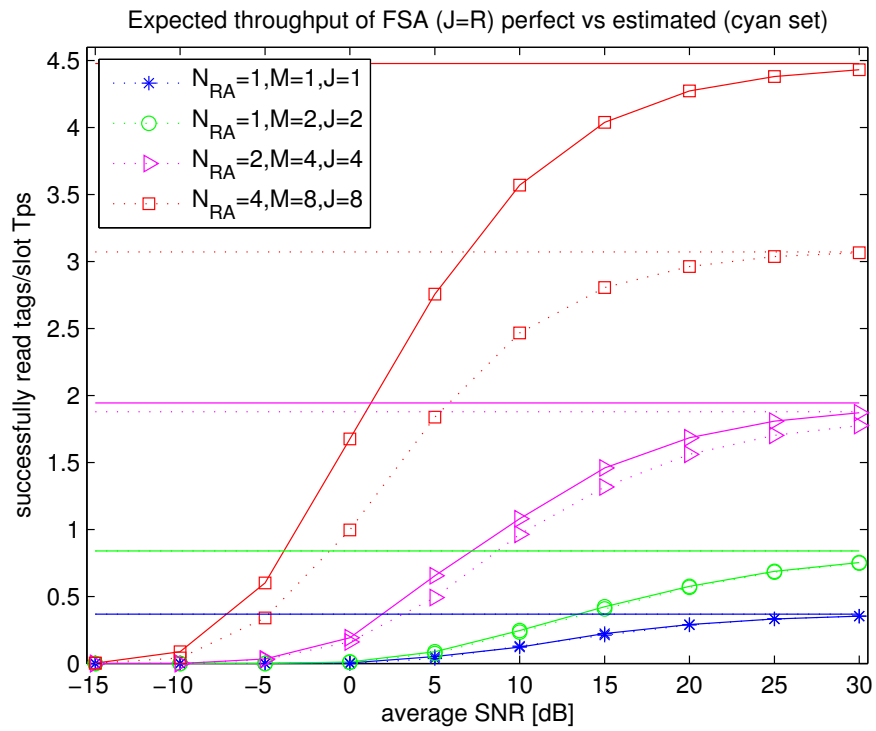


Figure 4.17: Throughput in the case of perfect channel knowledge (from Equation (4.18)) vs. throughput based on “postpreamble” channel estimation in [Cyan Set](#) (from Equation (4.17)). Continuous horizontal lines are bounds according to Equation (4.4), dashed horizontal lines are following Equation (4.7).

corresponding groups of curves are approaching their theoretical maxima very well. At high SNR the simulated curves attain their theoretical maxima from Equation (4.4) (case with perfect channel knowledge) and from Equation (4.7) (case with “postpreamble”-based channel estimation). While the curves for single antenna systems with $M = 1$ and $M = 2$ are exhibiting the same performance with “postpreamble”-based channel estimation as with perfect channel knowledge, for two antennas there is a slight loss visible and for $N_{RA} = 4$ antennas the loss due to channel estimation is quite pronounced. It can be observed that at a high SNR of 30 dB, the throughput per slot increases dramatically when compared to the conventional reader even though the performance is hampered by channel estimation losses. In case of a receiver with channel estimation and collision recovery factor $M = 8$, the throughput per slot is still more than eight times higher than that of a conventional system (plotted with the blue curve (—*—)). Even though not all of the collision scenarios have been covered with the proposed receiver but just the [Cyan Set](#), the obtained results are quite satisfactory.

4.5.4 Tag Identifications (in slots)

Based on Figure 4.17, the Tps for the different values of SNR is observed and according to that the number of tags that are left for the next frame in the same inventory round is recalculated. For a receiver with collision recovery factor $M = 8$, for example, the Tps value at the SNR=15 dB is $\text{Tps}^{15\text{ dB}} = 2.805$. The theoretically expected maximal throughput per slot is $\text{Tps}_F = 3.073$ for $F_{\text{opt}}/N = 0.207$ (Table 4.7). Taking into account the optimal frame duration, the average number of tags that are successfully decoded within the duration of the first frame is $N^{\text{dec}} = \text{round}(\text{Tps}^{15\text{ dB}} \cdot F_{\text{opt}}) = 581$. Thus, for the next inventory round $N^{\text{left}} = 419$ tags are left. On the other hand, a conventional receiver has a maximal throughput per slot $\text{Tps} = 0.368$ for a frame size equal to the tag population size $F_{\text{opt}}/N = 1$, and at the SNR = 15 dB, $\text{Tps}^{15\text{ dB}} = 0.212$. Accordingly, within the first frame duration a conventional receiver successfully reads out $N^{\text{dec}} = 212$ tags and $N^{\text{left}} = N - N^{\text{dec}} = 788$ tags are left for the next round.

Assuming that the reader recalculates optimal frame sizes for the residual tag population $N^* = N^{\text{left}}$ before announcing the next frame, the following Figure 4.18 and Figure 4.19 are obtained. For the new tag population, the optimal frame size is calculated according to the ratio from Table 4.7, and $N^{\text{dec}} = \text{round}(\text{Tps}^{15\text{ dB}} \cdot F_{\text{opt}})$. The new residual tag population is $N^{\text{left}} \leftarrow N^* - N^{\text{dec}}$, and so on.

The number of residual tags, tags that still have not been decoded, versus the number of elapsed slots is shown in Figure 4.18. For the reader with collision recovery factor $M = 1$, a number of 4 693 slots (22 frames) is necessary to decode 99.5% of the tags in the reader range. A reader with collision recovery factor $M = 2$ needs 2 447 slots (19 frames) to decode 99.6%, while the readers with higher collision recovery factors are

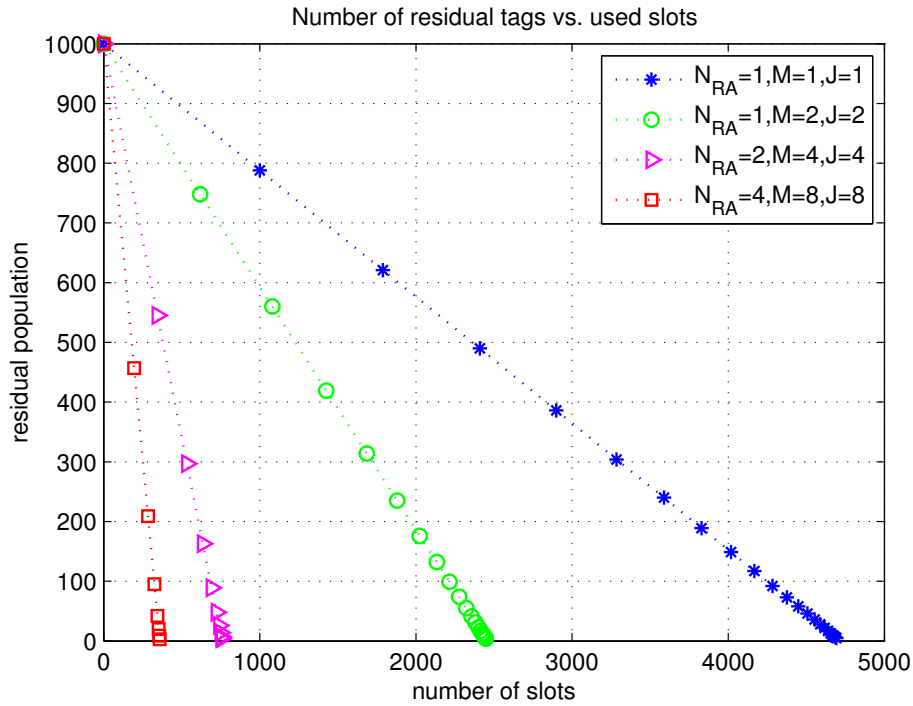


Figure 4.18: Number of residual tags vs. number of required slots.

much faster. The reader that is capable of recovering from a collision of up to four tags active in a slot $M = 4$ and acknowledge all of them, spends 775 slots (19 frames) for successfully decoding 99.6% and the reader with $M = 8$ decodes 99.7% of tags in just 355 slots (7 frames).

In Figure 4.19 the number of decoded tags versus the frame index is shown for different receivers. These values are also listed in Table 4.13 along with the optimal frame sizes F_{opt} .

Table 4.13: Number of decoded tags and frame duration at SNR = 15 dB.

$M = 1$		$M = 2$		$M = 4$		$M = 8$	
F_{opt}	N^{dec}	F_{opt}	N^{dec}	F_{opt}	N^{dec}	F_{opt}	N^{dec}
1 000	212	618	252	345	455	195	543
788	167	462	188	188	248	89	248
621	131	346	141	102	134	41	114
490	104	259	105	56	74	19	53
386	82	194	79	31	41	8	22
304	64	145	59	17	22	4	11
240	51	109	44	9	12	2	6

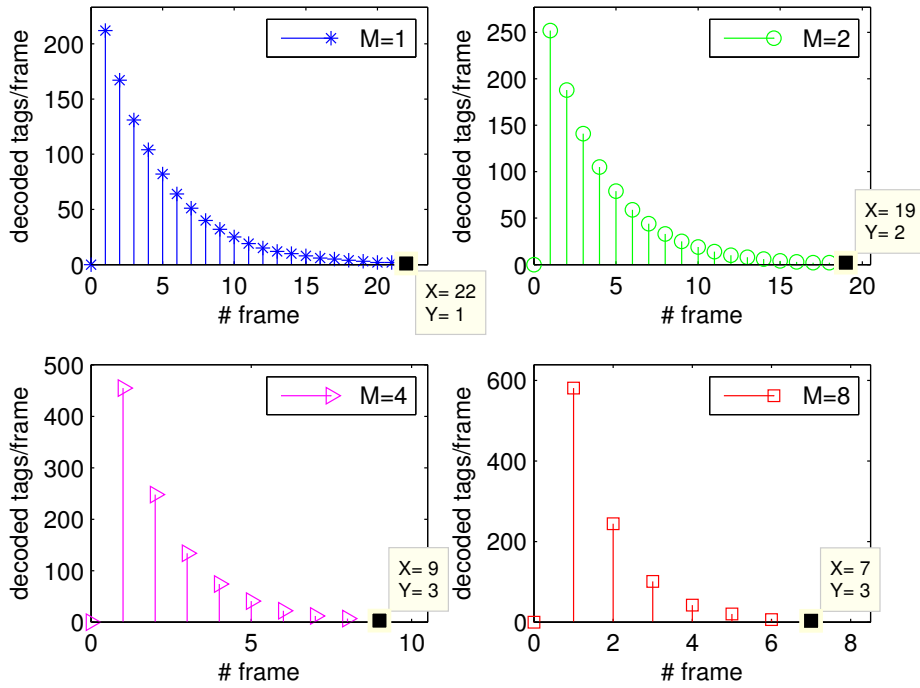


Figure 4.19: Number of decoded tags vs. number of frames.

Table 4.14: Number of slots spent for decoding 95%, 98% and 99.5% and relative improvement at $\text{SNR} = 15$ dB for $N_{\text{RA}} = \{1, 2, 4\}$ antennas and corresponding collision recovery factor $M = \{1, 2, 4, 8\}$.

Slots Rel. Imp.	$M = 1$	$M = 2$	$M = 4$	$M = 8$
95%	4 481	2 334	720	341
	1	1.920	6.224	13.141
98%	4 623	2 408	743	352
	1	1.920	6.222	13.134
99.5%	4 693	2 445	754	357
	1	1.920	6.224	13.146

In Table 4.14 the necessary number of slots is presented for reading a fixed percentage of the tag population together with the relative improvement compared to the conventional reader with collision recovery factor $M = 1$. In case of the proposed smart collision recovery reader receiver, the relative improvement is larger than 13 times at a realistic SNR of 15 dB. As compared to the throughput increase at SNR = 30 dB, the relative improvement at SNR = 15 dB is much higher and in accordance with Figure 4.17 as expected.

4.5.5 Theoretical Maxima of Tps in FSA

In Section 4.5.4, the results are obtained at a Signal to Noise Ratio of SNR=15 dB. Continuously increasing the SNR results in saturating the throughput and reaching its theoretical limit. Knowing the ratio of $\frac{F_{\text{opt}}}{N}$ and the throughput maxima Tps_f , which now corresponds to the theoretical limit, the number of slots spent for successfully decoding the tag population can be recalculated as explained in Section 4.5.4. The results obtained are listed in Table 4.15. Here, the receivers with perfect channel knowledge are represented by solid lines and the receivers with the “postpreamble”-based channel estimation are represented by dotted lines. Each marker denotes the number of residual tags at the end of the frame.

Table 4.15: Number of slots elapsed for decoding 95% and relative improvement for $M = \{1, 2, 8\}$ at theoretical maxima.

95%	$M = 1$	$M = 2$	$M = 8$
Slots	2579	1130	309
Rel.Imp.	1	2.28	8.34

Furthermore, with perfect channel knowledge at the receiver, all collisions of up to $R \leq M = 8$ can be resolved. Then the theoretical maxima of the throughput is even higher and the optimal ratio $\frac{F_{\text{opt}}}{N}$ is smaller. Based on the new value of the theoretical maxima and optimal frame size, which is again dynamically adopted to the residual tag population, the number of slots spent for successfully decoding 95% of the tag population is listed in Table 4.16. For receivers with collision recovery factors $M = 1$ and $M = 2$, theoretical limits are the same as in the previous case, as shown in Figure 4.20. For a receiver with a collision recovery factor $M = 8$ a significant improvement is observed.

Table 4.16: Number of slots elapsed for decoding 95% and relative improvement for $M = \{1, 2, 8\}$ at theoretical maxima in case of perfect channel knowledge.

95%	$M = 1$	$M = 2$	$M = 8$
Slots	2579	1130	212
Rel.Imp.	1	2.28	12.16

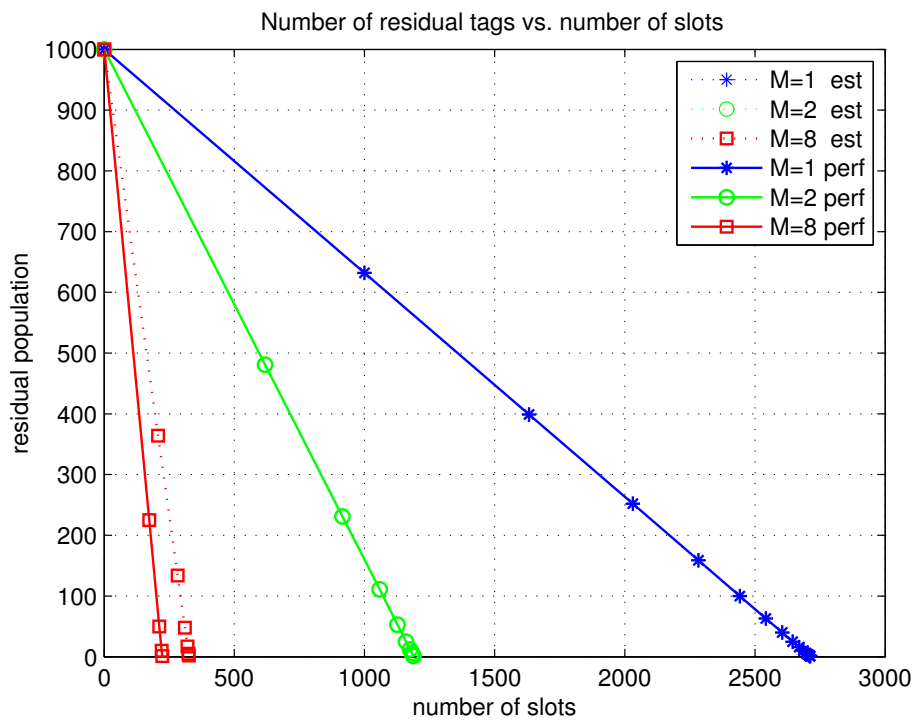


Figure 4.20: Number of residual tags vs. number of slots corresponding to the theoretical maxima in the case of perfect channel knowledge (solid lines) and in the case of the “postpreamble”-based channel estimation (dotted lines).

4.5.6 Time Spent for Tag Identifications

The performance of the proposed methods is evaluated by Monte Carlo simulations. In the simulated system, $N = 1000$ tags are present in the reader's area. Since there are eight "postpreambles" in the set, tags are divided in eight groups each with one "postpreamble" sequence. The tags randomly choose one of the available F slots for transmission. Inspecting slot by slot, the number of active tags in each slot is determined. All singleton slots are acknowledged and the number of identified tags is increased. Additionally, if there are less than M tags colliding in a slot then the "postpreambles" are examined (based on the tag's group) and all tags with a unique "postpreamble" are acknowledged. Furthermore, a single pair of tags with a matching "postpreamble" is acknowledged (in the case where all other colliding tags have unique "postpreambles"). Together with this procedure, slot durations are calculated as explained in Section 4.2. After the frame is finished, for the new frame just unidentified tags are competing and a new frame size is dynamically adjusted.

I have evaluated the proposed methods with three different dynamically adjusted frame sizes as explained in Section 4.4.

Perfect DFSA

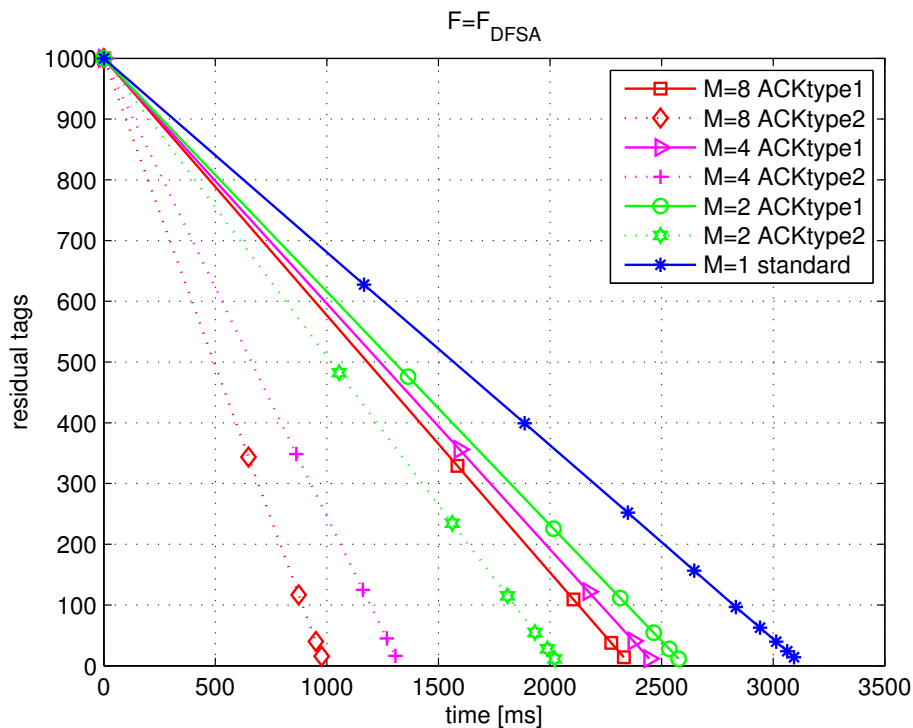


Figure 4.21: Residual tags vs. elapsed time in perfect DFSA.

In Figure 4.21 a comparative overview of the performances of readers with collision recovery factor $M = 2$, $M = 4$ and $M = 8$ is given. The solid lines represent the performances of readers that employs ACK type 1 while the dotted lines depict the performances of readers with ACK type 2. Each point in the figure shows how many unidentified tags are left as well as the current duration of the frame. The obtained results are compared with the performance of a conventional reader with $M = 1$. For easier comparison I have found the fitting of simulated curves and based on that I have calculated identification times necessary to successfully read out 95%, 98% and 99.5% of tags. The obtained values are listed in Table 4.17.

Table 4.17: Identification time (ACK type 1 vs. ack type 2) for reading out 95%, 98% and 99.5% of tags in perfect DFSA.

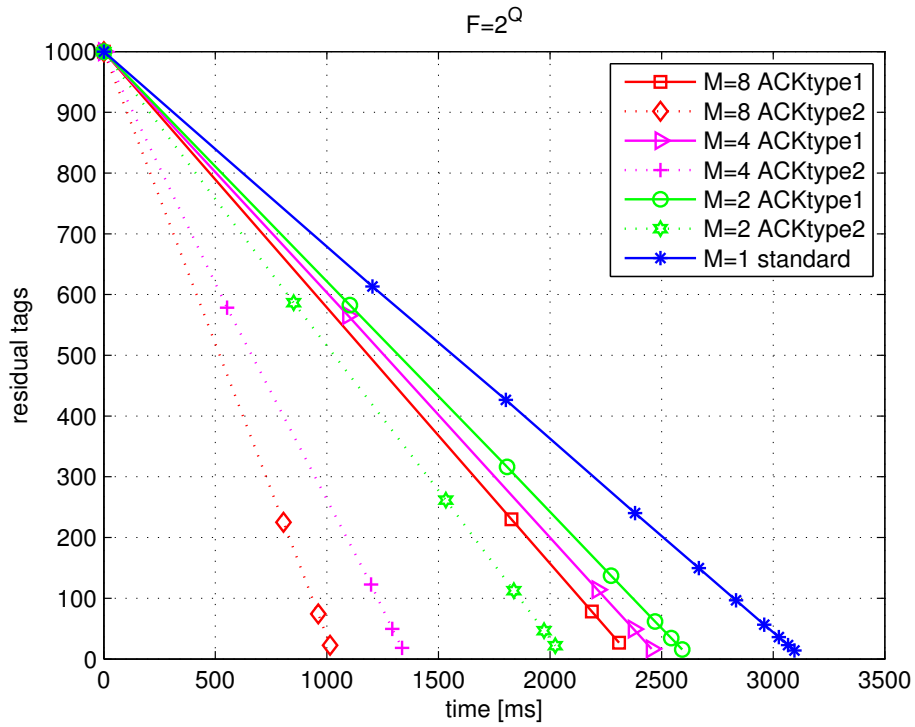
Time [ms]	95%	98%	99.5%
$M = 1$	2 980.9	3 075.1	3 122.1
$M = 2$	2 475.2 / 1 941.3	2 553.4 / 2 002.6	2 592.5 / 2 033.3
$M = 4$	2 350.3 / 1 261.4	2 424.5 / 1 301.2	2 461.7 / 1 321.2
$M = 8$	2 245.3 / 940.8	2 316.2 / 970.6	2 351.6 / 985.4

It can be observed that with ACK type 1, a reader with $M = 8$ shortens the identification time by 32%, while when ACK type 2 is employed the identification time decreases significantly and an improvement of more than 317% is achieved.

Furthermore, by comparing Figure 4.14 and Figure 4.21, it can be seen that the results of the Monte Carlo simulation are in accordance with the analytically calculated identification time and residual population. Even though the number of the identified tags in a frame varies due to the different frame sizes, F_{opt} from Equation (4.14) and F_{DSFA} from Equation (4.13), the total time, necessary to read the tag population, does not change significantly.

DFSA= 2^Q

A comparative overview of the performances with quantized frame sizes of $F_{2^Q} = 2^{\lceil \log_2(F) \rceil}$ is provided in Figure 4.22. Again, the reader with $M = 8$ and ACK type 2 is the most efficient. It is noticed from Table 4.18 that the readers with collision recovery capabilities are more sensitive to the changes in frame sizes. The suboptimal performances are observed and the identification time is increased since the frame size is quantized and can take one of the following values: $F = \{1, 2, 4, 8, 16, 32, 64, 128, 256, 512, 1024\}$ depending on the collision recovery factor of a reader and the residual tag population.

Figure 4.22: Residual tags vs. elapsed time in quantized 2^Q DFSA.Table 4.18: Identification time (ack type 1 vs. ack type 2) for reading out 95%, 98% and 99.5% of tags in quantized 2^Q DFSA.

Time [ms]	95%	98%	99.5%
$M = 1$	2 980.5	3 074.8	3 121.9
$M = 2$	2 503 / 1 966.7	2 581.9 / 2 028.9	2 621.4 / 2 060
$M = 4$	2 373.6 / 1 291.6	2 448.4 / 1 332.7	2 485.8 / 1 353.2
$M = 8$	2 254.3 / 986.6	2 325.5 / 1 017.8	2 361.1 / 1 033.4

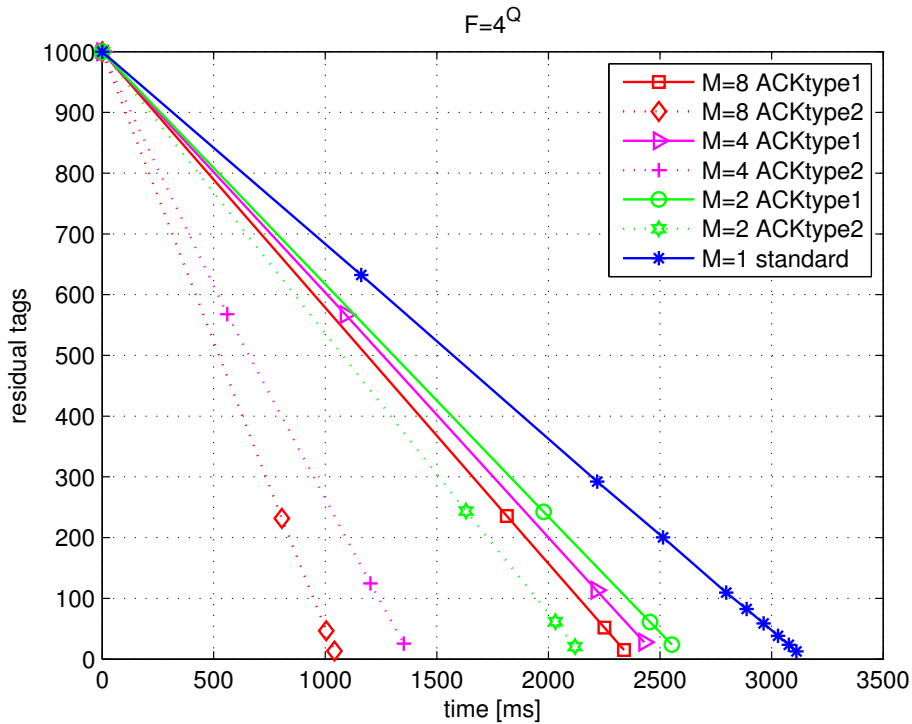


Figure 4.23: Residual tags vs. elapsed time in quantized 4^Q DFSA.

DFSA= 4^Q

The residual tags vs. the identification times for readers with $M = 1$, $M = 2$, $M = 4$ and $M = 8$ are plotted in Figure 4.23 for even higher quantization of frame sizes $F_{4^Q} = 4^{\lceil \log_4(F) \rceil}$. Now the frame sizes can take one of the following values: $F = \{1, 4, 16, 64, 256, 1024\}$; depending on the collision recovery factor and the residual tag population. Once more, it is observed that the readers with collision recovery capabilities are less robust to the quantization. However, Table 4.19 shows that in the case of a reader with a collision recovery factor $M = 2$ and ACK type 1, there is even a slight improvement when compared with the same setup with F_{2^Q} , even though the results for ACK type 2 are, as expected, a bit worse. This can be explained with the inefficient use of the acknowledgement scheme in ACK type 1. On the other hand, ACK type 2 saves time since all EPC codes of resolved tags are sent at the same time. Thus, a higher number of collisions, due to the suboptimal frame sizes dynamically adjusted for each frame, that could be partially resolved does not necessarily decrease reader performances.

Table 4.19: Identification time (ack type 1 vs. ack type 2) for reading out 95%, 98% and 99.5% of tags in quantized 4^Q DFSA.

Time [ms]	95%	98%	99.5%
$M = 1$	2 990.2	3 084.7	3 131.9
$M = 2$	2 484 / 2 054.4	2 562.5 / 2 119.3	2 601.7 / 2 151.7
$M = 4$	2 375.6 / 1 306.5	2 450.4 / 1 348.2	2 487.9 / 1 369.1
$M = 8$	2 255.5 / 1 000	2 326.8 / 1 031.6	2 362.4 / 1 047.5

4.6 Discussion and Conclusion

In this chapter, the theoretical throughput of an FSA RFID system is analysed and the influence of several parameters on the system throughput is studied. In addition to that, the maxima of the theoretically expected throughput for receivers with different collision recovery factors and for different receiver architectures are calculated.

Furthermore, I have investigated the benefits of an additional “postpreamble” to the throughput, and I observed that without taking into account the receiver structure and the channel estimation method, it is possible to increase the system throughput by more than 17 times. On the other hand, if the receiver structure is taken into account, then a throughput increase of more than 12 times can still be achieved for a reader capable of successfully reading and acknowledging up to eight tags per slot. In these calculations, it is assumed that the readers have perfect channel knowledge.

However, in order to recover from a collision, a reader needs to perform channel estimation. For the channel estimation procedure, the tags are augmented by “postpreambles”. Based on this, several collision scenarios can be differentiated, and if the probability of scenarios that can be resolved and the number of tags that can be successfully decoded are included, the maximal theoretical throughput is still about eight times the throughput of a conventional system at 30 dB SNR.

Moreover, the necessary time to read out a high tag population is investigated. It is shown that at the average SNR of 15 dB, a smart reader with collision recovery factor $M = 8$ successfully decodes all tags in the reader range, more than 13 times faster than a conventional reader, and performances are considerably enhanced.

In the first part of the performance analysis, the system performance was evaluated with respect to the given slots and the slot duration was not taken into account. The obtained results are compared by just looking at the first part of the identification process that was finished with the RN16 reception. The second phase, i.e., the acknowledgement, was not taken into account nor the necessary protocol changes. However, in order to obtain a fairer comparison of different collision recovery schemes, it is important to take into account the necessary protocol changes and to evaluate the complete read

out process. Thus, in this chapter, I have stated what the required changes are in the protocol in order to benefit from collision recovery. Besides, I have proposed two different acknowledgement schemes: ACK type 1 and ACK type 2 that can be used in collision scenarios and I have computed the modified slot durations. Furthermore, I have derived analytical formulas for calculating the expected number of identified tags in a frame and the expected frame duration. Additionally, I have determined new optimal frame sizes that minimize the identification time per tag. In the second part of the performance analysis, I have evaluated the total identification time of proposed schemes by means of Monte Carlo simulations.

The obtained results prove that the readers with collision recovery capabilities decrease the identification time, especially with ACK type 2. However, the order of the improvement is much lower than the observed improvement listed in Table 4.15 when only slots are counted and their durations were not taken into account. When all changes in the protocol are taken into account, an improvement of 3.17 times is observed for a reader with $M = 8$, while without taking into account the second part of the identification cycle and only considering slots and not their durations, the improvement was eight times, as shown in Table 4.15. Moreover, I have shown that suboptimal frame lengths have only little influence on the performance.

Furthermore, in order to analyse the behaviour of the proposed readers with collision recovery in a dense reader environment with time scheduling it would be convenient to know the mean number of identifications at any point of time. The analytical derivation of the mean number of tag identifications in collision scenarios is planned for the future work. Additionally, I plan to extend the mathematical model for calculating the number of identifications and to take into account spatial filtering. In that way, an additional factor that depends on the tag's position will be taken into account. That would allow more detailed analytical evaluation of the proposed postprocessing.

5 CONCLUSIONS

Nowadays, RFID has found its application in a variety of fields such as tracking of goods, access management, localization of animals and persons, contactless payment, timing sports events, etc. With the utilization of RFID, a lot of tedious jobs, e.g., counting of goods, can be achieved more efficiently and less people are required. Since RFID does not require direct line of sight, tags can be read even if they are placed within an object and items can be identified without directly accessing them.

The identification time directly depends on the number of tags that are within the read range of the reader. The transmission of tags is scheduled on the MAC layer with a collision avoidance protocol. If collision at the air interface occurs, the complete time slot is discarded and that prolongues the identification process.

In this thesis, I focus on a physical layer collision recovery with a multiantenna RFID reader. The main goal of the thesis is to increase the system throughput by resolving collisions, and to faster identify tags from the reader range. Thus, the thesis aims on the establishment and application of advanced algorithms to increase the performance of the system. Since my work is focused on passive UHF RFID systems that work with simple tags which are only capable of incomplex operations, almost all proposed changes and signal processing is performed on the reader side.

5.1 Open Issues and Outlook

Despite the effort invested in this dissertation, there are still some issues left that require further investigations. In the proposed system a perfect isolation of the transmit and received part of the reader is assumed. The influence of incomplete carrier compensation is left to be analysed. Furthermore, in order to perform successive interference cancellation, a perfect alignment of signals from collided tags is considered. However, currently available passive tags have a lot of synchronization issues and the duration of signals varies. Consequences of misalignment at the reception are left for future study. Additionally, for more detailed study of the performances of the reader with postprocessing, a more complex geometrical channel model is required. Moreover, practical assesment of the proposed work through measurements would be beneficial for a more complete evaluation.

5.2 Conclusion

The advanced RFID readers proposed in this thesis improve performances and shorten the read out time. They incorporate different signal processing methods in order to recover from a collision and in addition to that, acknowledge multiple resolved tags. They exploit multiantenna setups and perform spatial filtering in postprocessing and in that way further improve the system throughput.

Furthermore, in order to benefit from the proposed collision recovery, changes in protocol are recommended. Slot durations are adopted to the recommended tag signal modifications and two different acknowledge schemes are proposed for resolved tags from collision scenarios. Additionally, the evaluation of the complete read out process is performed and the obtained results prove that the proposed advanced RFID readers significantly decrease the identification time.

Moreover, I have investigated the performance of the proposed RFID readers in suboptimal circumstances, i.e., when the quantized frame lengths are announced. The obtained results show that the readers are quite robust and that suboptimally chosen parameters have only little influence on the performance.

APPENDICES

A LIST OF TERMS AND SYMBOLS

Variable	Description
Latin symbols	
$a(t)$	Modulation signal
$\mathbf{a}(t)$	$R \times 1$ vector of modulation signals $a_i(t)$
$\mathbf{a}_{\text{MMSE}}(t)$	resolved $R \times 1$ vector of modulation signals $a_i(t)$ after MMSE
$\mathbf{a}_{\text{ZF}}(t)$	resolved $R \times 1$ vector of modulation signals $a_i(t)$ after ZF
c	Speed of Light
C	Number of "postpreambles" in a set
C^a	Tag absorb state
C^r	Tag reflect state
D	Number of "colliding" colours
D_r	The largest dimension of the radiator
$d_{n/f}$	Near filed / far field limit
d_j^f	Distance from the readers transmit antenna and tag j
d_s	Antenna spacing
$E\{\cdot\}$	Expected value
E_b	Energy per bit
f	Operating frequency
F	Frame size in Framed Slotted Aloha protocol
$\mathbf{g}(\phi, \theta)$	Antenna pattern
h	Channel coefficient
h^b	Backward channel coefficient (tag-to-reader)
h^f	Forward channel coefficient (reader-to-tag)
$h_{i,j}$	Channel coefficient from tag j to receive antenna i
h_s	Hight of the substrate
\mathbf{H}	Channel matrix
$\hat{\mathbf{H}}$	Estimated channel matrix
$\hat{\mathbf{H}}_{\text{LS}}$	LS estimated channel matrix
i	Receive antenna index
j	Tag index
J	Number of tags a reader can acknowledge simultaneously
k_0	Wave number
\mathbf{l}	$N_{\text{RA}} \times 1$ vector of carrier leakages $l_j(t)$
L_{eff}	Effective wave length of the patch antenna
M	Collision recovery factor

$n(t)$	Noise term
$\mathbf{n}(t)$	$N_{\text{RA}} \times 1$ vector of noise terms $n_j(t)$
N	Number of tags in the read range of the reader
N_{RA}	Number of receive antennas
N_{TA}	Number of transmit antennas
N_0	Noise power spectral density
N_{iter}	Number of iterations
\mathbf{p}	“Postpreamble” sequence
\mathbf{p}_j	Position vector of tag j
Q	Speed factor
R	Number of colliding tags
R_d^{cc}	Number of tags with the same colour D
$r(t)$	Baseband receive signal
$\mathbf{r}^{pp}(t)$	part of the baseband received signal containing the postpreamble
$\mathbf{r}(t)$	$N_{\text{RA}} \times 1$ vector of receive signals $r_i(t)$
\mathbf{S}_M	Set of M “postpreamble” sequences
$S_l(R)$	Collision scenarios with R colliding tags
t_C	Duration of collision slot
t_E	Duration of empty slot
t_{pp}	“Postpreamble” duration
t_S	Duration of singleton slot
U	Number of “unique” colours
\mathbf{u}	Unit vector
$\mathbf{v}(\phi, \theta)$	Steering vector
\mathbf{w}	Sector weights

Greek symbols

γ	Expected number of acknowledged tags
$\delta(\theta)$	Normalized angular attenuation
ϵ_r	Relative permittivity of the dielectric
θ	Azimuth
λ	Wavelength
ϕ	Elevation
σ_i^2	Noise variance at antenna i

Operators

$E\{\cdot\}$	Expected value
$E\{\cdot\}_T$	Averaged value over time period T
h^*	Conjugate complex of h
\mathbf{H}^H	Hermitian transpose of matrix \mathbf{H}
$\Im\{\cdot\}$	Imaginary part
$\Re\{\cdot\}$	Real part

B LIST OF ACRONYMS

<i>ACK</i>	Acknowledge
<i>AMP</i>	Approximate Message Passing
<i>AWGN</i>	Additive White Gaussian Noise
<i>BER</i>	Bit Error Ratio
<i>CR</i>	Collision Recovery
<i>CRC</i>	16-bit cyclic redundancy check code
<i>EAN</i>	European Article Number
<i>EPC</i>	Electronic Product Code
<i>FFT</i>	Fast Fourier Transform
<i>FS</i>	Frame sync
<i>FSA</i>	Framed Slotted Aloha
<i>IQ</i>	In-phase/Quadrature
<i>ISI</i>	Inter-Symbol Interference
<i>ISIC</i>	Inter-frame Successive Interference Cancellation
<i>LMMSE</i>	Linear Minimum Mean Square Error
<i>LOS</i>	Line Of Sight
<i>MAC</i>	Medium Access Control
<i>MMSE</i>	Minimum Mean Square Error
<i>P</i>	Preamble
<i>PC</i>	Protocol Control
<i>PP</i>	"Postpreamble"
<i>QRep</i>	Query Repeat
<i>RFID</i>	Radio Frequency Identification
<i>RN16</i>	16-bit random number
<i>RX</i>	Receive, Receiver
<i>SIC</i>	Successive Interference Cancellation
<i>SNR</i>	Signal to Noise Ratio
<i>TX</i>	Transmit, Transmitter
<i>UCC</i>	Uniform Code Council
<i>UHF</i>	Ultra High Frequency
<i>ZF</i>	Zero Forcing

C APPROXIMATIONS

C.1 Approximation of Tps_M

The number of tags in the reader range N is much bigger than the number of colliding tags R that the reader is capable of resolving ($N \gg R$). Taking this into account the first part of Equation (4.4)

$$\binom{N}{R} = \frac{N \cdot (N-1) \cdot \dots \cdot (N-R+1)}{R!} \quad (\text{C.1})$$

can be approximated by:

$$\binom{N}{R} \approx \frac{N^R}{R!}. \quad (\text{C.2})$$

The part $\left(1 - \frac{1}{F}\right)^{N-R}$ for $F \gg 1$ can be approximated by

$$\left(1 - \frac{1}{F}\right)^{N-R} \approx \left(\left(1 - \frac{1}{F}\right)^F\right)^{\frac{N-R}{F}} = \underbrace{\left(\left(1 + \frac{1}{-F}\right)^{-F}\right)^{\frac{N-R}{F}}}_{\approx e^{-1}} \quad (\text{C.3})$$

$$\approx e^{-\frac{N-R}{F}}. \quad (\text{C.4})$$

Using that $N \gg R$, finally Equation (4.4) can be approximated by:

$$\text{Tps}_M \approx \sum_{R=1}^M \frac{N^R}{R!} \left(\frac{1}{F}\right)^R e^{-\frac{N}{F}} R \quad (\text{C.5})$$

$$\approx \sum_{R=1}^M \left(\frac{N}{F}\right)^R e^{-\frac{N}{F}} \frac{1}{(R-1)!} \quad (\text{C.6})$$

$$\approx \sum_{R=1}^M \left(\frac{F}{N}\right)^{-R} e^{-\frac{1}{F/N}} \frac{1}{(R-1)!}. \quad (\text{C.7})$$

Thus, the entire expression is a function of F/N .

If functions are now approximated as functions of $x = F/N$, they take on the form:

$$\text{Tps}_M \approx \sum_{R=1}^M x^{-R} e^{-\frac{1}{x}} \frac{1}{(R-1)!}, \quad (\text{C.8})$$

which offers them to differentiate with respect to x and to find the maxima for throughput and thus the optimal F/N ratio.

The obtained optimal ratios F/N for maximal throughput are:

[1; 0.618; 0.441; 0.340; 0.275; 0.230; 0.197; 0.172] for $R = 1, 2, \dots, 8$, respectively. When compared to simulation results, this approximation shows an almost perfect agreement.

C.2 Approximation of Tps_C

Following the approximations from Appendix C.1 now for $\frac{N}{C} \gg R_C$ and $F \gg 1$, Equation (4.5) can be approximated by:

$$\text{Tps}_C \approx C \sum_{R_C=1}^{J_C} \left(\frac{F}{N/C} \right)^{-R_C} e^{-\frac{1}{F/C/N}} \frac{1}{(R_C-1)!}. \quad (\text{C.9})$$

Furthermore, this term now can be approximated as a function of $x = F/N$:

$$\text{Tps}_C \approx C \sum_{R_C=1}^{J_C} (Cx)^{-R_C} e^{-Cx} \frac{1}{(R_C-1)!}. \quad (\text{C.10})$$

This allows to differentiate with respect to x and to find the maxima for throughput and thus the optimal F/N ratio. When compared to simulation results, this approximation shows an almost perfect agreement.

C.3 Approximation of Tps_f

Using the approximations from Appendix C.1, Equation (4.7) can be approximated by:

$$\text{Tps}_f \approx \sum_{R=1}^M \left(\frac{F}{N} \right)^{-R} e^{-\frac{1}{F/N}} \frac{1}{R!} \cdot \left(\sum_{l=1}^{S(R)} P_{s_l}(R) \cdot R_{s_l}^{\text{sol}}(R) \right). \quad (\text{C.11})$$

Thus, the entire expression can be written as a function of $x = F/N$.

$$\text{Tps}_f \approx \sum_{R=1}^M x^{-R} e^{-\frac{1}{x}} \frac{1}{R!} \cdot \left(\sum_{l=1}^{S(R)} P_{s_l}(R) \cdot R_{s_l}^{\text{sol}}(R) \right). \quad (\text{C.12})$$

Now, Equation (C.12) can be differentiated with respect to x and find the optimal F/N ratio that corresponds to the throughput maxima. When compared to simulation results, this approximation shows an almost perfect agreement.

BIBLIOGRAPHY

- [1] H. Stockman. Communication by Means of Reflected Power. In *Proc. IRE*, volume 36, pages 1196–1204, 1948.
- [2] M. Cardullo and W. Parks. Transponder apparatus and system, January 23 1973. US Patent 3,713,148.
- [3] C. A. Walton. Portable radio frequency emitting identifier, May 17 1983. US Patent 4,384,288.
- [4] GS1, 2015. [Online]. Available: <http://www.gs1.org/epcrfid/epc-rfid-uhf-air-interface-protocol/2-0-1>.
- [5] EPCGlobal. EPC Radio-Frequency Identity Protocols Class-1 Generation-2 UHF RFID. [Online]. Available: <http://www.gs1.org/sites/default/files/docs/epc>.
- [6] M. V. Bueno-Delgado, J. Vales-Alonso, and F. J. Gonzalez-Castao. Analysis of DFSA anti-collision protocols in passive RFID environments. In *Proc. of 35th Conf. IEEE Industrial Electronics Society (IECON)*, Nov. 2009.
- [7] R. S. Khasgiwale, R. U. Adyanthaya, and D. W. Engels. Extracting Information from Tag Collisions. In *Proc. of the IEEE International Conference on RFID*, Orlando, USA, April 2009.
- [8] D. Shen, G. Woo, D. P. Reed, A. B. Lippman, and J. Wang. Separation of Multiple Passive RFID Signals Using Software Defined Radio. In *Proc. of the IEEE International Conference on RFID*, Orlando, USA, April 2009.
- [9] A. F. Mindikoglu and A.-J. van der Veen. Separation of overlapping RFID signals by antenna arrays. In *Proc. of IEEE International Conference on Acoustics, Speech and Signal Processing, ICASSP 2008*, pages 2737–2740, April 2008.
- [10] B. Knerr, M. Holzer, C. Angerer, and M. Rupp. Slot-wise maximum likelihood estimation of the tag population size in FSA protocols. *IEEE Trans. Commun.*, 58(2):578–585, 2010.
- [11] M. Holzer, B. Knerr, C. Angerer, and M. Rupp. Early frame restart in RFID systems. In *Proc. of the Second International EURASIP Workshop on RFID Technology*, Budapest, July 2008.

- [12] M. V. Bueno-Delgado, C. Angerer, J. Vales-Alonso, and M. Rupp. Estimation of the Tag Population with Physical Layer Collision Recovery. In *Proc. of the Third International EURASIP Workshop on RFID Technology*, La Manga del Mar Menor, Cartagena, Spain, Sep. 2010.
- [13] J. Yu, K. H. Liu, X. Huang, and G. Yan. An anti-collision algorithm based on smart antenna in RFID system. In *Proc. of International Conference on Microwave and Millimeter Wave Technology, 2008. ICMWT 2008*, volume 3, pages 1149–1152, April 2008.
- [14] K. Fyhn, R. M. Jacobsen, P. Popovski, A. Scaglione, and T. Larsen. Multipacket Reception of Passive UHF RFID Tags: A Communication Theoretic Approach. *IEEE Transactions on Signal Processing*, 59(9):4225 – 4237, Sep. 2011.
- [15] F. Ricciato and P. Castiglione. Pseudo-random Aloha for Enhanced Collision-recovery in RFID. *IEEE Communications Letters*, 17, March 2013.
- [16] J. Myung, W. Lee, and J. Srivastava. Adaptive Binary Splitting for Efficient RFID Tag Anti-Collision. *IEEE Communications Letters*, 10(3):144–146, March 2006.
- [17] Y. Cui. System Efficiency of Collision Recover Binary Tree Algorithm in RFID. In *Proc. of IEEE International Conference on RFID-Technologies and Applications (RFID-TA)*, Nice, France, Nov. 2012.
- [18] C. Angerer, G. Maier, M. V. Bueno-Delgado, M. Rupp, and J. Vales-Alonso. Single Antenna Physical Layer Collision Recovery Receivers for RFID Readers. In *Proc. of the IEEE International Conference on Industrial Technology*, pages 1386–1391, March 2010.
- [19] A. Bletsas, J. Kimionis, A. G. Dimitriou, and G. N. Karystinos. Single-Antenna Coherent Detection of Collided FM0 RFID Signals. *IEEE Transactions on Communications*, 60(3):756 – 766, March 2012.
- [20] J. Kimionis, A. Bletsas, A. G. Dimitriou, and G. N. Karystinos. Inventory Time Reduction in Gen2 with Single-Antenna Separation of FM0 RFID Signals. In *Proc. of IEEE International Conference on RFID-Technologies and Applications (RFID-TA)*, Sitges, Spain, Sep. 2011.
- [21] D. De Donno, V. Lakafosis, L. Tarricone, and M. M. Tentzeris. Increasing performance of SDR-based collision-free RFID systems. In *Proc. of IEEE MTT-S Int. Microwave Symp. Digest (MTT)*, pages 1–3, June 2012.
- [22] S. Kim, S. Kwack, S. Choi, and B. Gi Lee. Enhanced collision arbitration protocol utilizing multiple antennas in RFID systems. In *Proc. of 17th Asia-Pacific Conf. Communications (APCC)*, pages 925–929, Oct. 2011.
- [23] C. Angerer, R. Langwieser, and M. Rupp. RFID Reader Receivers for Physical Layer Collision Recovery. *IEEE Trans. Commun.*, 58(12):3526–3537, Dec. 2010.

- [24] M. Mayer, N. Görtz, and J. Kaitovic. RFID tag acquisition via compressed sensing. In *Proc. of 2014 IEEE RFID Technology and Applications (RFID-TA) Conference*, Tampere, Finland, September 2014.
- [25] M. F. Khelladi, A. Metref, and B. Fergani. Request Efficient Channel Estimation Method for MIMO Passive RFID Systems. In *Proc. of 2015 IEEE International Conference on RFID (RFID)*, San Diego, CA, USA, April 2015.
- [26] J. Vales-Alonso, F. J. Parrado-Garcia, and J. J. Alcaraz. Analytical Computation of the Mean Number of Tag Identifications During a Time Interval in FSA. *IEEE Communications Letters*, 18(11):1923–1926, 2014.
- [27] J. Kaitovic, R. Langwieser, and M. Rupp. RFID reader with multi antenna physical layer collision recovery receivers. In *Proc. of IEEE International Conference on RFID-Technologies and Applications (RFID-TA)*, Sitges, Spain, Sep. 2011.
- [28] J. Kaitovic, M. Šimko, R. Langwieser, and M. Rupp. Channel estimation in tag collision scenarios. In *Proc. of 2012 IEEE International Conference on RFID (RFID)*, Orlando, Florida, April 2012.
- [29] J. Kaitovic, R. Langwieser, and M. Rupp. Advanced Collision Recovery Receiver for RFID. In *Proc. of the 4th International EURASIP Workshop on RFID Technology*, Torino, Italy, Sep. 2012.
- [30] J. Kaitovic, R. Langwieser, and M. Rupp. A smart collision recovery receiver for RFIDs. *EURASIP Journal on Embedded Systems*, 7:1–19, 2013.
- [31] J. Kaitovic and M. Rupp. Improved Physical Layer Collision Recovery Receivers for RFID Readers. In *Proc. of IEEE International Conference on RFID*, pages 103–109, Orlando, April 2014.
- [32] J. Kaitovic and M. Rupp. RFID Physical Layer Collision Recovery Receivers with Spatial Filtering. In *Proc. of IEEE International Conference on RFID-Technologies and Applications (RFID-TA)*, Tokyo, Japan, Sep. 2015.
- [33] J. Kaitovic and M. Rupp. Tag Identification Time in Multiantenna Collision Scenarios. In *Proc. of the 5th International EURASIP Workshop on RFID Technology*, Rosenheim, Germany, Oct. 2015.
- [34] J. D. Griffin and G. D. Durgin. Complete Link Budgets for Backscatter-Radio and RFID Systems. *IEEE Antennas and Propagation Magazine*, 51(2):11–25, 2009.
- [35] A. Lazaro, D. Girbau, and D. Salinas. Radio Link Budgets for UHF RFID on Multipath Environments. *IEEE Trans. Antennas Propag.*, 57(4):1241–1251, April 2009.
- [36] D. Kim, M. A. Ingram, and W. W. Smith. Measurements of small-scale fading and path loss for long range RF tags. *IEEE Trans. Antennas Propag.*, 51(8):1740–1749, Aug. 2003.

- [37] J. D. Griffin and G. D. Durgin. Gains For RF Tags Using Multiple Antennas. *IEEE Trans. Antennas Propag.*, 56(2):563–570, 2008.
- [38] A. Paulraj, R. Nabar, and D. Gore. *Introduction to Space-Time Wireless Communication*. Cambridge University Press, 2003.
- [39] G. Durgin. Balance Codes for More Throughput in RFID and Backscatter Links. In *Proc. of IEEE International Conference on RFID-Technologies and Applications (RFID-TA)*, Tokyo, Japan, Sep. 2015.
- [40] J. Balakrishnan, M. Rupp, and H. Viswanathan. Optimal Channel Training for Multiple Antenna Systems. In *Proc. of Conference on Multiaccess, Mobility and Teletraffic for Wireless Communications*, Florida, USA, Dec. 2000.
- [41] M. Šimko, C. Mehlführer, T. Zemen, and M. Rupp. Inter-Carrier Interference Estimation in MIMO OFDM Systems with Arbitrary Pilot Structure. In *Proc. of 73rd IEEE Vehicular Technology Conference (VTC2011-Spring)*, Budapest, Hungary, May 2011.
- [42] M. Loncar, C. F. Mecklenbräuker and R. R. Müller. Co-channel interference mitigation in GSM networks by iterative estimation of channel and data. *European Transactions on Telecommunications*, 14(1):71–80, 2003.
- [43] G. Lasser, R. Langwieser, and C. Mecklenbräuker. Automatic leaking carrier canceller adjustment techniques. *EURASIP Journal on Embedded Systems, RFID and near field communications in embedded systems*(8):1–15, 2013.
- [44] R. Langwieser and G. Lasser. Measurement and Simulation of Crosstalk and Crosstalk Compensation in UHF RFID. In *Fourth International EURASIP Workshop on RFID Technology*, Torino, Italy, September 2012.
- [45] G. Lasser, W. Gartner, R. Langwieser, and C. Mecklenbräuker. Fast Algorithm for Leaking Carrier Cancellation Adjustment. In *Fourth International EURASIP Workshop on RFID Technology*, Torino, Italy, September 2012.
- [46] G. Lasser, R. Langwieser, R. Dallinger, and C. Mecklenbräuker. Broadband Leaking Carrier Cancellation for RFID Systems. In *IEEE MTT-S International Microwave Symposium*, Montreal, June 2012. IEEE.
- [47] R. Langwieser, C. Angerer, A.L. Scholtz, and M. Rupp. Crosstalk and SNR Measurements using a Multi-Antenna RFID Reader with Active Carrier Compensation. In *Third International EURASIP Workshop on RFID Technology*, pages 66–69, La Manga del Mar Menor, Cartagena, Spain, September 2010.
- [48] R. Langwieser, G. Lasser, C. Angerer, M. Fischer, and A.L. Scholtz. Active Carrier Compensation for a Multi-Antenna RFID Reader Frontend. In *2010 IEEE MTT-S International Microwave Symposium Digest*, pages 1532–1535, Anaheim, CA, May 2010.

- [49] L.W. Mayer, R. Langwieser, and A.L. Scholtz. Evaluation of Passive Carrier-Suppression Techniques for UHF RFID Systems. In *2009 IEEE MTT-S International Microwave Workshop on Wireless Sensing, Local Positioning and RFID*, Cavtat, Croatia, September 2009.
- [50] H. A. Ahmed, H. Salah, J. Robert, and A. Heuberger. Backwards Compatible Improvement of the EPCglobal Class 1 Gen 2 Standard. In *Proc. of IEEE International Conference on RFID-Technologies and Applications (RFID-TA)*, Tokyo, Japan, Sep. 2015.
- [51] C. Mehlführer and M. Rupp. Novel Tap-wise LMMSE Channel Estimation for MIMO W-CDMA. In *Proc. 51st Annual IEEE Globecom Conference, 2008*, New Orleans, LA, USA, November 2008.
- [52] S. Caban, C. Mehlführer, M. Rupp, and M. Wrulich. *Evaluation of HSDPA and LTE: From Testbed Measurements to System Level Performance*. John Wiley & Sons, UK, 2012.
- [53] S. H. Han and J. H. Lee. Objective function based group-wise successive interference cancellation receiver for dual-rate DS-CDMA system. In *Vehicular Technology Conference, 2002. VTC Spring 2002. IEEE 55th*, volume 4, pages 1685–1688 vol.4, 2002.
- [54] X. Zhang and M. Haenggi. The Performance of Successive Interference Cancellation in Random Wireless Networks. *IEEE Transactions on Information Theory*, 60(10):6368–6388, 2014.
- [55] C. A. Balanis. *Antenna Theory: Analysis and Design*. Wiley-Interscience, 2005.
- [56] H. L. Van Trees. *Detection, Estimation, and Modulation Theory, part IV: Optimum Array Processing*. J. Wiley & Sons, 2002.
- [57] J. Yu, K. Liu, and G. Yan. A novel RFID anti-collision algorithm based on SDMA. In *Proc. of the 4th International Conference on Wireless Communications, Networking and Mobile Computing*, 2008.
- [58] A. Tkacenko, P. P. Vaidyanathan, and T. Q. Nguyen. On the Eigenfilter Design Method and its Applications: A Tutorial. *IEEE Trans. Circuits Syst. II*, 50:497–517, 2003.
- [59] T. Chen. Unified eigenfilter approach: with applications to spectral/spatial filtering. In *Proc. of IEEE Intl. Symp. on Circuits and Systems*, 1993.
- [60] R. A. Horn and C. R. Johnson. *Matrix Analysis*. Cambridge University Press, 1985.
- [61] S. Doclo and M. Moonen. Comparison of least-squares and eigenfilter techniques for broadband beamforming. In *Proc. of 3rd IEEE Benelux Signal Processing Symposium*, March 2002.

- [62] M. Haardt, C.F. Mecklenbräuker, M. Vollmer, and P. Slanina. Smart antennas for UTRA TDD. *European Transactions on Telecom. (ETT)*, 12:393 – 406, 2001.
- [63] B. Knerr, M. Holzer, C. Angerer, and M. Rupp. Slot-by-slot Minimum Squared Error Estimator for Tag Populations in FSA Protocols. In *The 2nd Int. EURASIP Workshop on RFID Technology*, pages 1–13, Budapest, July 2008.
- [64] J. Vales-Alonso, M. V. Bueno-Delgado, E. Egea-Lopez, F. J. Gonzalez-Castao, and J. Alcaraz. Multiframe Maximum-Likelihood Tag Estimation for RFID Anticollision Protocols. *IEEE Transactions on Industrial Informatics*, 7(3):487–496, August 2011.
- [65] C. Qian, Y. Liu H. Ngan, and L. M. Ni. Cardinality Estimation for Large-scale RFID Systems. *IEEE Transactions on Parallel and Distributed Systems*, pages 1441 – 1454, 2011.
- [66] H. Han, B. Sheng, C. C. Tan, Q. Li, W. Mao, and S. Lu. Counting RFID Tags Efficiently and Anonymously. In *Proc. of IEEE INFOCOM*, 2010.
- [67] X. Yang, H. Wu, Y. Zeng, and F. Gao. Capture-Aware Estimation for the Number of RFID Tags with Lower Complexity. *IEEE Communications Letters*, 17(10):1873–1876, 2013.
- [68] M. Rupp, M. V. Bueno-Delgado, C. Angerer, and S. Schwarz. ML estimation of population size when observing multiple fill levels in slotted aloha. In *Proc. of 40th IEEE International Conference on Acoustics, Speech and Signal Processing (ICASSP) 2015*, Brisbane, Australia, April 2015.
- [69] N. Khanna and I. Uysal. Q-frame-collision-counter: a novel and dynamic approach to RFID Gen 2s Q algorithm. In *Proc. of IEEE International Conference on RFID-Technologies and Applications (RFID-TA)*, Tokyo, Japan, Sep. 2015.
- [70] C. Floerkemeier and S. Sarma. RFIDSim—A Physical and Logical Layer Simulation Engine for Passive RFID. *IEEE Transactions on Automation Science and Engineering*, 6(1):33–43, January 2009.